MOBILITY AND CHEMICAL FATE OF ANTIMONY AND ARSENIC IN HISTORIC MINING ENVIRONMENTS OF KANTISHNA HILLS, DENALI NATIONAL PARK AND PRESERVE, ALASKA

By

Vanessa J. Ritchie

RECOMMENDED:

Advisory Committee Chair

Chair, Department of Chemistry and Biochemistry

APPROVED:

Dean, College of Natural Science and Mathematics

Dean of the Graduate School

Apr 5, 2011

Date

MOBILITY AND CHEMICAL FATE OF ANTIMONY AND ARSENIC IN HISTORIC MINING ENVIRONMENTS OF KANTISHNA HILLS, DENALI NATIONAL PARK AND PRESERVE, ALASKA

A

THESIS

Presented to the Faculty

of the University of Alaska Fairbanks

in Partial Fulfillment of the Requirements

for the Degree of

MASTER OF SCIENCE

By

Vanessa J. Ritchie, B.S.

Fairbanks, Alaska

May 2011

Abstract

Oxidative weathering processes of acid-forming sulfide minerals, such as pyrite (FeS_2), and associated arsenopyrite (FeAsS) and stibnite (Sb_2S_3), can have a significant impact on water quality associated with current and legacy mining operations. Concentrations of toxic metals and metalloids, such as antimony (Sb) and arsenic (As), in acid mine drainage can exceed drinking water quality standards by orders of magnitude. This study provides a detailed hydrogeochemical assessment of the mobility and chemical fate of antimony and arsenic in streams draining from historic antimony mines within Denali National Park and Preserve, Alaska. Antimony and arsenic concentrations in stream water reach up to 720 parts per billion (ppb) and 239 ppb, respectively. Aqueous phase antimony and arsenic speciation was determined using liquid chromatography coupled to an inductively coupled plasma - mass spectrometer. Antimony in all water samples is predominantly found as Sb^{5+}, whereas arsenic was detected as mixtures of As^{3+}/As^{5+}. Elevated antimony concentrations extend over 8 km downstream from the source, whereas arsenic quickly attenuates within 1.5 km. High correlation between antimony/arsenic and iron concentrations in fine-fraction streambed sediment indicates that sorption and (co)precipitation with iron (hydr)oxides is an important pathway for the attenuation of antimony and arsenic in natural waters.

Table of Contents

Page

List of Figures

Page

Page

List of Tables

Page

List of Appendices

Acknowledgements

There are several people who deserve a great deal of credit for helping this project come together and to whom I owe many thanks. First, I would like to thank my thesis advisor, Tom Trainor, for welcoming me into his group and providing me with guidance throughout my studies and research. Tom's invested enthusiasm for this project and optimistic view point has helped me through several periods of frustration and exhaustion (in particular, his optimism has stopped me from setting fire to the LC-ICP-MS, despite my strong desire to do so). I also have to acknowledge Tom's patience with me for running off and finding full-time employment before graduating, for at times I'm sure it seemed like I would never finish. I would like to extend gratitude to my other advisory committee members, Bill Simpson and Cathy Cahill, for providing valuable comments throughout my research endeavors and thesis writing process. Thanks!

I thank National Park Service personnel, Lucy Tyrrell and the late Phil Brease, for access to the study sites in the Denali National Park and Preserve and for logistical support. Lucy Tyrrell also provided helpful suggestions in producing public outreach literature about my project for the Murie Science and Learning Center located in the park. I also thank field work participants Kunaljeet Tanwar, Anastasia Ilgen, and Sarah Petitto who willingly spent several days soaked to the bone from stomping through streams and climbing hills with heavy packs. A special thanks to Sarah for planning an awesome field food menu and for providing homemade snacks! You rock. Thanks to Seth Mueller, our collaborator (formally with USGS), for being open to the idea of me jumping in on the project (and for providing an undeniable level of entertainment).

I thank my friends Sarah Petitto, Chris Iceman, and Emily Reiter for their endless moral support and acting as sounding boards when I needed it. Fellow laboratory mate, Anastasia Ilgen, deserves a lot of thanks for analytical consultation and advice. Anastasia and I performed many of the same analytical methods in our research and I appreciate the opportunity and her willingness to collaborate.

I thank my sister, Nadine Ritchie-Wheeler, for being crazy enough (or kind enough) to assist me with the many details of thesis formatting. You are a star and I love

you! Most of all, I would like to thank my husband, Seth Branson, for his love, support, and friendship. Without his patience and understanding, my success would not have been possible.

Chapter 1: Introduction and Objectives

1.1 Sources and impacts of antimony and arsenic contamination

A great deal of research effort has been devoted to understanding the geochemical and biogeochemical processes in natural waters that controls the fate of toxic trace elements, predominantly transition metals. Comparatively, less attention has been focused on metalloid elements, such as arsenic (As) and, in particular, antimony (Sb). The speciation of potentially toxic trace metal(loids) in aqueous geochemical systems is a topic of critical interest to modeling and assessment of water quality. In particular, the ability to predict trace metal source lability, mobility and bioavailability is essential to understanding potential impacts to both humans and the ecosystem. This research advances the fundamental understanding of the aqueous geochemical reactions affecting the transformation, retention, and transport of the metalloid elements antimony (Sb) and arsenic (As) in natural aquatic environments.

Antimony and arsenic are widespread in the environment as a result of natural processes (e.g., oxidative weathering of geologic materials and volcanic outgassing), as well as through a range of anthropogenic activities (Filella et al., 2002a). Antimony and arsenic occur in association with minerals commonly exploited for their metals (e.g., copper, nickel, lead, silver, and gold), and as such are often produced as by-products of current and legacy mining (Plumlee et al., 1999; Filella et al., 2002a).

Antimony has an average crustal abundance of 0.2 mg/kg and a typical concentration of dissolved Sb in unpolluted waters of less than 1 µg/L (Filella et al., 2002a). However, in proximity to large Sb-rich mineral deposits or anthropogenic sources, concentrations can exceed the typical background levels by up to several 100 times. Estimated world reserves of Sb are in excess of two million metric tons and are located primarily in China, Russia, Bolivia, South Africa, and Mexico (Carlin, 2010). United States (U.S.) Sb reserves are estimated to be 80,000 metric tons, located principally in Alaska, Idaho, Montana, and Nevada. Although global production is in decline due to increased awareness of the toxicity of Sb, production reaches over 100,000 metric tons annually (Carlin, 2010). Common uses of Sb include flame retardant additive

for textiles and plastics, lead alloy hardener, paint pigment, ceramic and glass clarifier, semiconductor production, and a catalyst in the manufacturing of plastics (Filella et al., 2002a; Carlin, 2010).

Arsenic has an average crustal abundance of 1.5 mg/kg and common background concentrations less than 1 μg/L in unpolluted waters (Vaughan, 2006). Much greater concentrations are found in areas of anthropogenic sources and in geothermal systems, enhancing concentrations by factors of 100 to 1000, or more. Global production of As (generally as the oxidized form As_2O_3) is approximately 50,000 metric tons (Brooks, 2006). The dominant use for As has been for the manufacture of chemicals such as chromated copper arsenate (CCA) used as a wood preservative, and in herbicides and insecticides. Much smaller amounts have been used in the manufacture of products such as glass and semiconductors (Brooks, 2006; Vaughan, 2006).

Antimony and arsenic are highly toxic and elevated concentrations in drinking water have resulted in severe health and environmental problems (Bencze, 1994; Vaughan, 2006). Although As-contaminated drinking water is more widespread, mining activities of Sb-rich mineral deposits and smelting operations have created concern for drinking water contamination on a local scale (Wilson et al., 2010). It is debatable whether or not As is essential to human health, but there is no known biological function for Sb (Bhattacharya et al., 2002; Bencze, 1994). The carcinogenic properties of As have long been documented (Goering et al., 1999; Vaughan, 2006). Although studies have shown Sb to cause cancer in rats by inhalation of Sb_2O_3 (Newton et al., 1994) and is a suspected human carcinogen, the topic is currently debated (Wilson et al., 2010). The most common route of exposure to As and Sb is contaminated drinking water. Based on recommendations from several ecotoxicological and risk assessment studies, the U.S. Environmental Protection Agency (EPA) established maximum concentration levels for Sb and As in drinking water at 6 μg/L and 10 μg/L, respectively. These stringent EPA standards emphasize the need to improve the capability of current environmental models to accurately predict the long term mobility and potential bioavailability of Sb and As in aqueous and soil ecosystems.

1.2 Geochemistry of acid mine drainage from sulfidic mine tailings

1.2.1 Acidic water formation

A major hydrogeochemical process that controls the chemical composition of natural waters is the formation of acidic water. The oxidation of iron sulfides, such as pyrite (FeS_2) - a globally abundant sulfide mineral (Nordstrom and Alpers, 1999) - is fundamental to the alteration of mineral deposits and development of acid rock drainage (ARD) or, if from a mined area, acid mine drainage (AMD). Acid mine waters often have pH values in the range of 2-4 and can accelerate the release of metal(loid)s to concentrations known to be toxic to living organisms. Although pyrite oxidation occurs in the absence of mining, mining activities lead to more rapid physical and chemical weathering processes by increasing surface areas of sulfides, as well as other minerals, in mine workings, wastes, and tailings (Nordstrom and Alpers, 1999; Lambeth, 1999).

When pyrite is exposed to air and oxygen-charged waters, a simplified chemical reaction responsible for the oxidation-induced dissolution of pyrite, and subsequent formation of AMD, may be written as:

$$2FeS_2(s) + 7O_2(g) + 2H_2O(l) \rightarrow 2Fe^{2+}(aq) + 4SO_4^{2-}(aq) + 4H^+(aq) \qquad [1]$$

In reaction [1] (Nordstrom and Munoz, 1986), for every mole of pyrite, one mole of ferrous iron (Fe^{2+}) and two moles of acid are released. The acidic waters are neutralized by the surrounding carbonate and silicate minerals and ions and aqueous complexes of major and minor mineral-forming elements, such as aluminum (Al), calcium (Ca), potassium (K), magnesium (Mg), iron (Fe), silica (SiO_2), carbonate (CO_3), are released.

If the waters are sufficiently oxidized, much of the Fe^{2+} will undergo oxidation to ferric iron (Fe^{3+}) (reaction [2]; Moses et al., 1987).

$$4Fe^{2+}(aq) + O_2(g) + 4H^+(aq) \rightarrow 4Fe^{3+}(aq) + 2H_2O(l) \qquad [2]$$

In mildly acidic to circumneutral pH waters, ferric iron hydrolyzes to form poorly crystalline to amorphous iron (hydr)oxide phases, such as ferrihydrite ($Fe(OH)_3$) (reaction [3]; Moses et al., 1987).

$$Fe^{3+}(aq) + 3H_2O(l) \rightarrow Fe(OH)_3(am) + 3H^+(aq) \qquad [3]$$

Through this reaction, acid is released and ferrihydrite develops, generally forming colloids within the water column and may settle to the streambed. In more acidic waters (in which Fe^{3+} is stable), dissolved ferric iron readily oxidizes pyrite and releases more acid and additional ferrous iron (reaction [4]), which may reenter the redox reaction cycle via reaction [2].

$$FeS_2(s) + 14Fe^{3+}(aq) + 8H_2O(l) \rightarrow 15Fe^{2+}(aq) + 2SO_4^{2-}(aq) + 16H^+(aq) \qquad [4]$$

Several studies have determined that the abiotic oxidation of pyrite by aqueous ferric ions is considerably faster than by dissolved oxygen. However, under acidic conditions at pH values below approximately 4, the oxidation rate for ferrous to ferric iron according to reaction [2] is significantly slower than the rate of oxidation of pyrite by ferric iron; hence, reaction [2] is the rate-limiting step under abiotic conditions (Singer and Stumm, 1970). However, rapid ferrous iron oxidation rates have been observed in nature. Most researchers attribute the rapid rates of ferrous iron oxidation to the catalyzing properties of some clays and metals, including Al, Fe, Co, and Mn, but more notably to the enzymatic oxidation by bacteria (e.g., *Thiobacillus ferrooxidans).* As most iron-oxidizing bacteria are aerobic, the oxidation rates in anoxic waters are generally much slower (Nordstrom, 1982; Singer and Stumm, 1970).

1.2.2 Controls on drainage chemical composition

The chemical composition of acid drainage waters is a function of a variety of processes, including acid neutralization, precipitation, aqueous complexation, and sorption onto particles and colloids within the water column. With the oxidation and

dissolution of FeS_2 other commonly associated metal (Cu, Mn, Pb, and Zn) and metalloid (Sb and As) sulfides can be exposed to the oxidizing conditions. Similar to FeS_2, these associated metal(loid)-bearing sulfides are only stable under reducing conditions and readily oxidize when exposed to air and meteoric water. Dissolution of these sulfides releases large concentrations of metal(loids) into aquatic ecosystems. Stibnite (Sb_2S_3) and arsenopyrite (FeAsS) are the most common sulfide minerals and are leading contributors to Sb and As pollution (Filella et al., 2002a; Corkhill and Vaughan, 2009).

The neutralization of the acidic water occurs by reaction with acid neutralizing minerals present in the deposit or host rocks, such as carbonates or aluminosilicates, or by dilution with non-acidic ground or surface water. When the pH of acidic waters is increased, the solubility of some metal ions, such as Al^{3+} and Fe^{3+}, is greatly reduced; causing formation of precipitates (Stumm and Morgan, 1996). Previous studies have shown that, at pH values above approximately 2-3, poorly crystalline to amorphous iron (hydr)oxide phases, such as ferrihydrite, precipitate and form into colloids within the water column and may coat materials with orange to reddish-brown precipitates lining streambeds. Similarly, studies have shown that, at pH values above 4.5-5, aluminum concentrations are limited by the formation of aluminum oxyhydroxsulfates, such as basaluminite ($Al_4(SO_4)(OH)_{10}$), which are typically seen as white coatings on streambeds (Nordstrom and Alpers, 1999).

The concentrations of metals such as lead (Pb), copper (Cu), zinc (Zn), cadmium (Cd), and nickel (Ni), and metalloids such as Sb and As, are variably controlled by aqueous complexation, coupled with sorption onto particulates and colloids (most commonly the ferrihydrite ($Fe(OH)_3$) or hydrous aluminum oxides (Smith, 1999)). Colloidal Al and Fe precipitates and other metal(loid)s that (co)precipitate can be transported long distances before settling to the streambed (Plumlee et al., 1999).

The extent of sorption onto particulates is a function of the pH of the waters, the identity of adsorbing metal, the concentrations of aqueous complexing ligands, and the concentration of the metals relative to the amounts of particulates. Smith et al. (1992, 1993) demonstrated that sorption is largely mediated by particulates suspended in the

water column and not by bed sediments. Arsenic is effectively sorbed at quite acidic pH values, whereas Pb, Zn, Cd, and Ni are more strongly sorbed at near-neutral pH values. Some elements, such as As, primarily exists in water as oxyanion and therefore tend to desorb at near-neutral pH values. Metals such as Cu and Pb also tend to desorb at near neutral pH values due to competition from complexing ligands, such as aqueous carbonates (Plumlee et al., 1999).

Other geochemical processes that affect drainage composition include evaporation and, should sufficient evaporation occur, precipitation of secondary sulfate salts (Nordstrom and Alpers, 1999). Evaporation can be important in open-pit mines, mine dumps, tailings, and underground mine workings. These metal salts can store acid and metals in the solid form, and dissolve readily during the next wet period such as snow-melt or rainstorm runoff, resulting in a high influx of acid and metal(loid)s into the drainage system (Plumlee et al., 1999).

There are a variety of geological features of mineral deposits that control the composition of natural- and mine-drainage waters, including: the content of acid-generating sulfides in the deposit; the content of carbonates and other acid-consuming minerals in the deposit; the rock types hosting the deposit; the types of alteration present in the deposit and host rocks; the nature of the ore (vein, disseminated, massive); and, the reactivity of both the acid-generating and acid-consuming minerals (a function of grain size and trace-element content of the minerals). In general, the trend of increasing metal content with decreasing pH reflects greater amounts of pyrite and other sulfide minerals associated with the deposit and a smaller content of carbonates and other minerals that consume acid. However, some deposits can be carbonate-rich and can still generate acidic waters if the acid-buffering carbonates are physically separate from the acid-generating sulfides, or if a reaction barrier of iron hydroxides or other minerals protects the carbonates from reaction with the acid waters (Plumlee et al., 1999).

1.3 Antimony and arsenic in natural waters

The aqueous concentration, mobility, and bioavailability of Sb and As are generally limited by (co)precipitation and partitioning reactions. Iron, aluminum, and manganese oxides, along with clay minerals, are capable of serving as effective sinks for both Sb and As. The major factors affecting Sb and As partitioning between aqueous and solid phases are Sb and As speciation, the nature of the surface moieties on the adsorbing substrate, the presence of competing ions or complexing ligands, pH, and, to a lesser extent, ionic strength. The reversibility of adsorption depends on the bonding between the adsorbed species and the mineral surface.

Antimony and arsenic are chalcophylic elements that are commonly found together in nature. Both can occur in a variety of oxidation states (-3, 0, +3, +5); however, they are mainly found in the III and V oxidations states in aqueous, biological and geological systems. Antimony and arsenic in their oxidized forms (III/V) form oxyanions that hydrolyze easily in aqueous solutions. Redox potential (E_H) and pH are the most important factors controlling Sb and As speciation. The trivalent forms of Sb (Bencze, 1994) and As (ATSDR, 2010) are more toxic than the pentavalent forms due to the cellular uptake efficiency of the trivalent species and the subsequent intracellular stress caused by oxidative processes. Therefore, controls on Sb and As oxidation state play an important role in both environmental impact and transport properties of these toxic metalloids.

1.4 Antimony aqueous geochemistry

1.4.1 Thermodynamic equilibrium predictions for antimony

Antimony primarily occurs in inorganic form as oxyanions of antimonite (Sb^{3+}) and antimonate (Sb^{5+}) in the natural environment. According to thermodynamic equilibrium predictions and as illustrated in a simplified E_H-pH diagram (Figure 1.1), $Sb(OH)_6^-$ is dominant under oxidizing conditions over a broad E_H-pH range. Under reducing conditions, within a typical environmental pH range, the uncharged antimonite species $Sb(OH)_3$ will dominate. In the presence of sulfur in an anoxic environment,

stibnite is formed in low to intermediate pH values. As pH increases, stibnite is replaced by the aqueous SbS_2^- species (Pitman et al., 1957; Vink, 1996; Takayanagi and Cossa, 1997). Thermodynamic data used in plotting Sb species theoretical stability fields in Figure 1.1 was obtained from Wagman et al. (1982) and Brookins (1988).

1.4.2 Kinetic influences on antimony speciation

In contrast to thermodynamic equilibrium predictions, significant concentrations of Sb^{3+} species have been detected in oxic waters and Sb^{5+} species in anoxic waters (Sun et al., 1993; Takayanagi and Cossa, 1997; Hou and Narasaki, 1998; Deng et al., 2001). This discrepancy can be explained by either slow kinetics of the redox reaction or by stabilization of the thermodynamically unstable species via complexation. A variety of mechanisms have been postulated to explain the stabilization, but few systematic studies exist under natural aquatic conditions.

Several authors invoke biological activity as the cause for Sb^{3+} presence in oxic waters (Sun et al., 1982; de la Calle-Guntinas et al., 1992; Cutter, 1992). In contrast, enriched Sb^{3+} concentrations in shallow ocean depths were attributed to possible photochemical reduction (rather than reduction by phytoplankton), due to the lack of correlation with bio-indicators (e.g., chlorophyll) (Cutter and Cutter, 2005). Other studies have shown that the rate of oxidation of Sb^{3+} to Sb^{5+} decreases with increasing acidity of water samples (Sun et al., 1982; Sherman et al., 2000; Belzile et al., 2001). This effect may be related to complex hydrolytic processes taking place simultaneously with the redox reaction (Filella et al., 2002b). The presence of Sb^{5+} in anoxic environments has also been observed (Cutter, 1991). One study reported the formation Sb^{5+} thioanions (and $H_2(g)$) upon dissolution of stibnite in deoxygenated aqueous NaHS solutions (Mosselmans et al., 2000), which may account for the presence of Sb^{5+} in some anoxic environmental systems.

In a recent study focused on the Fe-mediated oxidation kinetics of Sb^{3+} in the presence of O_2 and H_2O_2 (Leuz et al., 2006a) it was shown that the pseudo-first-order oxidation rate coefficients of Sb^{3+} in the presence of Fe^{2+} and O_2 or H_2O_2 increased with

increasing pH. Half-lives of Sb^{3+} in reaction with Fe^{2+} and O_2 were 35 and 1.4 hours at pH 5.0 and pH 6.2, respectively. The co-oxidation with Fe^{2+} and H_2O_2 was tens to thousands of times faster than the Fe-mediated reaction with O_2. A key role is played by the Fenton reaction, in which differently protonated Fe^{2+} species exchange H_2O with H_2O_2 via an inner-sphere electron-transfer. Although there is uncertainty about the exact intermediate species, a reaction scheme has been proposed in which hydroxyl radials are formed at low pH and a different oxidant (possibly an Fe^{4+} species) at intermediate pH (Hug and Leupin, 2003; Leuz et al., 2006a). The oxidation of Sb^{3+} by amorphous Fe and Mn (hydr)oxides was also investigated (Belzile et al., 2001). The oxidation of Sb^{3+} to Sb^{5+} was rapid and completed after a few days. A slightly slower oxidation rate was observed at low pH and was attributed to the lower stability of the (hydr)oxide compounds under more acidic conditions.

The increased rate of Sb^{3+} oxidation in the presence of Fe and Mn (hydr)oxide is apparent when comparing studies of Sb^{3+} homogeneous oxidation by aqueous O_2 and H_2O_2 (Quentel et al., 2004; Leuz and Johnson, 2005). The oxidation of Sb^{3+} to Sb^{5+} by aqueous O_2 appeared to be extremely slow, with an estimated half-life of 170 years at pH 8.5. The estimated half-lives of Sb^{3+} oxidation by H_2O_2, over a range of environmentally relevant pH values and reactant concentrations, ranged from 11 days to over 330 years (Leuz and Johnson, 2005). Quentel et al. (2004) estimated the half-life of Sb^{3+} oxidation by H_2O_2 at similar reactant concentrations at pH 7.5 to be approximately 9 years.

Limited information is available on Sb^{5+} reduction kinetics in anoxic media. In a recent study, Sb^{5+} was reduced to Sb^{3+} by dissolved sulfide under a wide range of environmentally relevant concentrations and pH values. Furthermore, under acidic conditions, metastibnite (Sb_2S_3) was found to precipitate after the reduction of $Sb(OH)_6^-$ by dissolved sulfide (Polack et al., 2009). Previous studies resulting in the reduction of Sb^{5+} to Sb^{3+} in the presence of natural sulfidic waters were also conducted (Bertine and Lee, 1983).

1.4.3 Antimony mobility

Antimony(V) has a lower affinity for mineral surfaces and is found to be more mobile in aquatic systems than Sb^{3+}. Fractionation of the dissolved phase into several classes by ultrafiltration suggested that most of the "dissolved" Sb (≥70%) is present as $Sb(OH)_6^-$ in pseudo-neutral pH ranges (Tanizaki, 1992a,b). Antimony(III) adsorbs strongly to Fe and Mn (hydr)oxides over a wide pH range (Belzile et al., 2001; Filella et al., 2002b; Leuz et al., 2006b; Casiot et al., 2007; Wilson et al., 2010), which results in the oxidation and ultimate release of the Sb^{5+} species (Leuz et al., 2006b).

Antimony(V) has also been found to adsorb to Fe (hydr)oxides, however, there is a lack of understanding of its sorption behavior in the natural environment. Tighe et al. (2005) investigated Sb^{5+} sorption by amorphous $Fe(OH)_3$ and floodplain soils across a pH range of 2.5-7. Adsorption was found to decrease with increasing pH, with maximum sorption occurring at approximately pH 4. Similar results were observed with Sb^{5+} adsorption to goethite, whereas Sb^{3+} strongly adsorbed over a pH range of 3-12 (Leuz et al., 2006b).

1.5 Arsenic aqueous geochemistry

1.5.1 Thermodynamic equilibrium predictions for arsenic

Arsenic primarily occurs in inorganic form as oxyanions of arsenite (As^{3+}) and arsenate (As^{5+}) in the natural aqueous environments. According to thermodynamic equilibrium predictions and as illustrated in a simplified E_H-pH diagram (Figure 1.2), H_3AsO_4 is dominant under oxidizing conditions at pH values below 2. In the pH range from approximately 2-11, H_3AsO_4 dissociates to $H_2AsO_4^-$, $HAsO_4^{2-}$, and AsO_4^{3-}, respectively. Under reducing conditions As is stable as H_3AsO_3, and up to pH 9 does not dissociate. At higher pH values $H_2AsO_3^-$, $HAsO_3^{2-}$, and AsO_3^{3-} species form. In the presence of sulfur or H_2S in an anoxic environment, various As-sulfide species can form (Brookins, 1988; Yan et al., 2000; Smedley and Kinniburgh, 2002; Bissen and Frimmel, 2003). Thermodynamic data used in plotting As species theoretical stability fields in Figure 1.2 was obtained from Ferguson and Gavis (1972) and Vink (1996).

1.5.2 Kinetic influences on arsenic speciation

Due to commonly observed thermodynamic disequilibrium in natural environments, significant concentrations of As^{3+} have been detected in oxic waters and As^{5+} in anoxic waters. Similarly to Sb, homogeneous oxidation of As^{3+} in solutions by dissolved O_2 is a particularly slow reaction, with half-lives estimated to range between several months to years (Smedley and Kinniburgh, 2002). Laboratory studies have shown that As^{3+} oxidation kinetics is slowest in the slightly acidic pH range, with estimated half-lives of 1-3 years (Eary and Schramke, 1990).

There is considerable evidence that the faster kinetic rates observed in nature are attributed to biological activity (Smedley and Kinniburgh, 2002), and are temperature dependent (Casiot et al., 2005; Andrade et al., 2010). Andrade et al. (2010) reported late summer pore waters containing equal concentrations of As^{3+} and As^{5+} (16-415 μg/L), whereas late winter pore waters were dominated by As^{3+} (284-947 μg/L). The increase in As^{3+} was attributed to As^{3+} desorption associated with the conversion of FeS to FeS_2 and the reduction of As^{5+} to As^{3+} through oxidation of dissolved sulfide, both microbially-mediated processes. Manganese oxides have been reported to increase the rate of As^{3+} oxidation compared to the homogeneous reaction, with half-lives being reduced to 10-20 minutes (Scott and Morgan, 1995). Rapid As^{3+} oxidation rates have also been observed upon sorption to Fe (hydr)oxides (Leuz et al., 2006a; Ona-Nguema et al., 2010). Photochemical reactions may also affect oxidation and reduction in surface waters (Foster et al., 1998).

1.5.3 Arsenic mobility

Arsenic(III) has lower affinity for mineral surfaces and is found to be more mobile in aquatic systems compared to As^{5+}. At acidic to pseudoneutral pH and aerobic conditions, As^{5+} is effectively immobilized by sorption and (co)precipitation with metal (hydr)oxides. As pH increases, especially above pH 8.5, As desorbs from oxide surfaces, thereby increasing the concentration of As in solution (Smedley and Kinniburgh, 2002; Bissen and Frimmel, 2003).

Arsenic can also be released from metal (hydr)oxides on the onset of strongly reducing conditions due to reductive dissolution of the sorbent (Guo et al., 1997; Smedley and Kinniburgh, 2002). Both As^{5+} and As^{3+} can be released from metal oxides, eventually leading to the reduction of As^{5+} to As^{3+} (Rochette et al., 1998). Under strongly reducing conditions in the presence of sulfide, As concentration in the aqueous phase is controlled by the formation of insoluble As-sulfide species (Harvey et al., 2002; Ryu et al., 2002).

1.6 Research objectives

This research addresses the mobility and chemical fate of Sb and As in streams draining historic Sb mines within the Kantishna Hills, Denali National Park and Preserve, Alaska. The presences of large quantities of stibnite (Sb_2S_3) and its weathering product stibiconite ($Sb_3O_6(OH)$), among many other Sb bearing phases associated with mineral deposits throughout Kantishna Hills, affords an opportunity to directly investigate Sb speciation and mobility in sub-arctic aquatic environments.

The specific objectives of this study were: 1) to characterize the chemical composition of surface waters draining mine tailings and waste-rock to determine overall water quality over a broad range of E_H and pH; 2) to examine the fine-fraction bed-sediments in these streams to determine the association with metals (e.g., Fe and Mn) in secondary precipitates; 3) to provide a detailed analysis of Sb and As speciation in the surface water and sediment to correlate chemical form with transport characteristics along a downstream profile; and 4) to compare the geochemical behavior of Sb and As between various sampling locations within the Kantishna Hills.

To develop robust predictive geoenvironmental models it is critical to provide results on the elemental speciation in addition to elemental abundances. Therefore, the conventional water chemical characterization is coupled with detailed analysis of Sb and As speciation in the aqueous phase.

1.7 Outline of presented work

The presented work is a compilation of data collected from three sampling events within the Kantishna Hills, Denali National Park and Preserve. The Slate Creek drainage was extensively sampled in 2005 and (to a lesser extent) in 2007. Distinct chemical differences were observed between the 2005 and 2007 Slate Creek data and are compared and discussed. In addition, minor sampling of the Eureka and Friday creeks (drainages in the vicinity of Slate Creek) occurred in 2007. The Stampede Creek was sampled in 2006.

Chapter 2 is written as a manuscript for submission to a peer reviewed journal, which details the field study described above. Various types of water and sediment samples (collected from streams, springs, a pond, and tailings seeps) were analyzed using analytical wet chemistry methods to correlate the redox and adsorption behavior of Sb and As with the geochemical characteristics of the system. The results indicate that streams draining these legacy mines have elevated Sb and As concentrations that can be traced several kilometers downstream of the mine workings and, in some cases, the concentrations exceed USEPA maximum contamination levels up to two orders of magnitude. The results also show that the different water types are distinguished based on their ion composition, and that significant dissolved metals can be transported in both acidic and pseudoneutral pH waters. Dissolved Sb and As speciation analysis indicates that the predominant form of Sb in these waters is Sb(V), whereas As is present in mixed As(III)/As(V) oxidation states. The correlations between the aqueous phase oxidation state and the mobility/attenuation of Sb and As are discussed.

In Chapter 3, the current research findings and their relevance to the natural environment are summarized. Possibilities for future work building from these results are presented.

The analytical methods that are discussed within the methods section of Chapter 2 are described in further detail in Appendices A.1 through A.6. In addition to analytical instruction, any analytical problems or noteworthy observations encountered during analysis that would aid future analytical endeavors are discussed. Lastly, complete tables

of analytical data (unless presented in Chapter 2) are provided in Appendix A.7 for reference.

References

Agency for Toxic Substance and Disease Registry (ATSDR). Arsenic. 1 September 2010. Retrieved from http://www.atsdr.cdc.gov/substances/toxsubstance.asp?toxid=3. Accessed on 6 December 2010.

Andrade, C.F., Jamieson, H.E., Kyser, T.K., Praharaj, T., Fortin, D., 2010. Biogeochemical redox cycling of arsenic in mine-impacted lake sediments and co-existing pore waters near Giant Mine, Yellowknife Bay, Canada. Appl. Geochem. 25(2), 199-211.

Belzile, N., Chen, Y.-W., Wang, Z., 2001. Oxidation of antimony(III) by amorphous iron and manganese oxyhydroxides. Chem. Geol. 174(4), 379-387.

Bencze, K., 1994. Antimony. in: Seiler, H.G., Sigel, A., Sigel, H. (Eds.), Handbook on Metals in Clinical and Analytical Chemistry. Marcel Dekker, New York, pp. 227-236.

Bertine, K.K., Lee, D.S., 1983. Antimony content and speciation in the water column and interstitial waters of Saanich Inlet, in: Trace Metals in Sea Water NATO Adv. Res. Inst. Plenum Press, New York, pp. 21-38.

Bhattacharya, P., Jacks, G., Frisbie, S.H., Naidu, R., Smith, E., Sarkar, B., 2002. Arsenic in the environment: a global perspective, in: Sarkar, B. (Ed.), Heavy Metals in the Environment. Marcel Dekker, New York, pp. 147–215.

Bissen, M., Frimmel, F.H., 2003. Arsenic – A review. Part I: Occurrence, toxicity, speciation, mobility. Acta Hydroch. Hydrob. 31(1), 9-18.

Brookins, D.G., 1988. Eh-pH Diagrams for Geochemistry. Springer-Verlag, Berlin, New York, pp. 30-31.

Brooks, W.E., 2006. Arsenic. U.S. Geological Survey, 2006, Mineral Commodity Summaries, 2006: U.S. Geological Survey, pp. 26-27.

Carlin Jr, J., 2010. Antimony. U.S. Geological Survey, 2010, Mineral Commodity Summaries, 2010: U.S. Geological Survey, pp. 18-19.

Casiot, C., Lebrun, S., Morin, G., Bruneel, O., Personne, J.C., Elbaz-Poulichet, F., 2005. Sorption and redox processes controlling arsenic fate and transport in a stream impacted by acid mine drainage. Sci. Total Environ. 347(1-3), 122-130.

Casiot, C., Ujevic, M., Munoz, M., Seidel, J.L., Elbaz-Poulichet, F., 2007. Antimony and arsenic mobility in a creek draining an antimony mine abandoned 85 years ago (upper Orb basin, France). Appl. Geochem. 22(4), 788-798.

Corkhill, C.L., Vaughan, D.J., 2009. Arsenopyrite oxidation – A review. Appl. Geochem. 24(12), 2342-2361.

Cutter, G.A., 1991. Dissolved arsenic and antimony in the Black Sea. Deep Sea Res. Part A. 38(Suppl.), S825-S843.

Cutter, G.A., 1992. Kinetic controls on metalloid speciation in seawater. Mar. Chem. 40(1-2), 65-80.

Cutter, G.A., Cutter, L.S., 2005. Surprising findings on the marine biogeochemistry of antimony, in: Shotyk, W., Krachler, M., Chen, B. (Eds.), 1st International Workshop on Antimony in the Environment. Institute of Environmental Geochemistry, University of Heidelberg, Heidelberg, Germany.

de la Calle-Guntinas, M.B., Madrid, Y., Camara, C., 1992. Stability study of total antimony, Sb(III) and Sb(V) at the trace level. Fresenius J. Anal. Chem. 344(1-2), 27-29.

Deng, T.-L., Chen, Y.-W., Belzile, N., 2001. Antimony speciation at ultra trace levels using hydride generation atomic fluorescence spectrometry and 8-hydroxyquinoline as an efficient masking agent. Anal. Chim. Acta 432(2), 293-302.

Eary, L.E., Schramke, J.A., 1990. Rates of inorganic oxidation reactions involving dissolved oxygen, in: Melchior, D.C., Bassett, R.L., (Eds.), Chemical Modeling of Aqueous Systems, II, Chapter 30. Am. Chem. Soc., Washington, D.C., pp. 379-396.

Ferguson, J.F., Gavis, J., 1972. A review of the arsenic cycle in natural waters. Water Res. 6(11), 1259-1274.

Filella, M., Belzile, N., Chen, Y.-W., 2002a. Antimony in the environment: a review focused on natural waters: I. Occurrence. Earth Sci. Rev. 57(1-2), 125-176.

Filella, M., Belzile, N., Chen, Y.-W., 2002b. Antimony in the environment: a review focused on natural waters: II. Relevant solution chemistry. Earth Sci. Rev. 59(1-4), 265-285.

Foster, A.L., Brown Jr., G.E., Tingle, T.N., Parks, G.A., 1998. Quantitative arsenic speciation in mine tailings using X-ray absorption spectroscopy. Am. Mineral. 83(5-6), 553-568.

Goering, P.L., Aposhian, H.V., Mass, M.J., Cebrian, M., Beck, B.D., Waalkes, M.P., 1999. The Enigma of arsenic carcinogenesis: role of metabolism. Toxicol. Sci. 49(1), 5-14.

Guo, T., DeLaune, R.D., Patrick Jr., W.H., 1997. The influence of sediment redox chemistry on chemically active forms of arsenic, cadmium, chromium, and zinc in estuarine sediment. Environ. Int. 23(3), 305-316.

Harvey, C.F., Swartz, C.H., Badruzzaman, A.B.M., Keon-Blute, N., Yu, W., Ali, M.A., Jay, J., Beckie, R., Niedan, V., Brabander, D., Oates, P.M., Ashfaque, K.N., Islam, S., Hemond, H.F., Ahmed, M.F., 2002. Arsenic mobility and groundwater extraction in Bangladesh. Science 298(5598), 1602-1606.

Hou, H.-B., Narasaki, H., 1998. Differential determination of antimony(III) and antimony(V) by inductively coupled plasma atomic emission spectrometry with hydride generation. Anal. Sci. 14(6), 1161-1164.

Hug, S.J., Leupin, O., 2003. Iron-catalyzed oxidation of arsenic(III) by oxygen and by hydrogen peroxide: pH-dependent formation of oxidants in the Fenton reaction. Environ. Sci. Technol. 37(12), 2734-2742.

Lambeth, R.H., 1999. Natural attenuation of acidic drainage from sulfidic tailings at a site in Washington state, in: Filipek, L.H., and Plumlee, G.S., (Eds.), The Environmental Geochemistry of Mineral Deposits, Part B: Case Studies and Research Topics. Soc. Econ. Geol., Reviews in Econ. Geol. 6B, 479-491.

Leuz, A.-K., Johnson, C.A., 2005. Oxidation of Sb(III) to Sb(V) by O_2 and H_2O_2 in aqueous solutions. Geochim. Cosmochim. Acta 69(5) 1165-1172.

Leuz, A.-K., Hug, S.J., Wehrli, B., Johnson, C.A., 2006a. Iron-mediated oxidation of antimony(III) by oxygen and hydrogen peroxide compared to arsenic(III) oxidation. Environ. Sci. Technol. 40(8), 2565-2571.

Leuz, A.-K., Monch, H., Johnson, C.A., 2006b. Sorption of Sb(III) and Sb(V) to goethite: influence on Sb(III) oxidation and mobilization. Environ. Sci. Technol. 40(23), 7277-7282.

Moses, C.O., Nordstrom, D.K., Herman, J.S., Mills, A.L., 1987. Aqueous pyrite oxidation by dissolved oxygen and by ferric iron. Geochim. Cosmochim. Acta 51(6), 1561-1571.

Mosselmans, J.F.W., Helz, G.R., Pattrick, R.A.D., Charnock, J.M., Vaughan, D.J., 2000. A study of speciation of Sb in bisulfide solutions by X-ray absorption spectroscopy. Appl. Geochem. 15(6), 879-889.

Newton, P.E., Bolte, H.F., Daly, I.W., Pillsbury, B.D., Terrill, J.B., Drew, R.T., Ben-Dyke, R., Sheldon, A.W., Rubin, L.F., 1994. Subchronic and chronic inhalation toxicity of antimony trioxide in the rat. Fundam. Appl. Toxicol. 22(4), 561-576.

Nordstrom, D.K., 1982. Aqueous pyrite oxidation and the consequent formation of secondary iron minerals, in: Kittrick, J.A., Fanning, D.S., Hossner, L.R. (Eds.), Acid Sulfate Weathering. Soil Sci. Soc. Am., Special Publication 10, 37-56.

Nordstrom, D.K., Munoz, J.L., 1986. Geochemical Thermodynamics. Blackwell Scientific Publications, Palo Alto, Calif., pp. 477.

Nordstrom, D., Alpers, C.N., 1999. Geochemistry of acid mine waters, in: Plumlee G.S., Logsdon, M.J. (Eds.), The Environmental Geochemistry of Mineral Deposits, Part A: Processes, Methods, and Health Issues. Society of Economic Geologists, Reviews in Econ. Geol. 6A, 133-160.

Ona-Nguema, G., Morin, G., Wang, Y., Foster, A.L., Juillot, F., Calas, G., Brown, G.E., 2010. XANES evidence for rapid arsenic(III) oxidation at magnetite and ferrihydrite surfaces by dissolved O_2 via Fe^{2+}-mediated reactions. Environ. Sci. Technol. 44(14), 5416-5422.

Pitman, A.L., Pourbaix, M., de Zoubov, N., 1957. Potential-pH diagram of the antimony-water system. Its applications to properties of the metal, its compounds, its corrosion, and antimony electrodes. J. Electrochem. Soc. 104(10), 594-600.

Plumlee, G.S., Smith, K.S., Montour, W.R, Ficklin, W.H., Mosier, E.L., 1999. Geologic controls on the composition of natural waters and mine waters draining diverse mineral-deposit types, in: Filipek L.H., Plumlee, G.S. (Eds.), The Environmental Geochemistry of Mineral Deposits, Part B: Case Studies and Research Topics. Society of Economic Geologists, Reviews in Econ. Geol. 6B, 373-407.

Polack, R., Chen, Y.-W., Belzile, N., 2009. Behavior of Sb(V) in the presence of dissolved sulfide under controlled anoxic aqueous conditions. Chem. Geol. 262(3-4), 179-185.

Quentel, F., Filella, M., Elleouet, C., Madec, C.-L., 2004. Kinetic studies on Sb(III) oxidation by hydrogen peroxide in aqueous solution. Environ. Sci. Technol. 38(10), 2843-2848.

Rochette, E.A., Li, G.C., Fendorf, S.E., 1998. Stability of arsenate minerals in soil under biotically generated reducing conditions. Soil Sci. Soc. Am. J. 62(6), 1530-1537.

Ryu, J.-H., Gao, S., Dahlgren, R.A., Zierenberg, R.A., 2002. Arsenic distribution, speciation and solubility in shallow groundwater of Owens Dry Lake, California. Geochim. Cosmochim. Acta 66(17), 2981-2994.

Scott, M.J., Morgan, J.J., 1995. Reactions at oxide surfaces. 1. Oxidation of As(III) by synthetic birnessite. Environ. Sci. Technol. 29(8), 1898-1905.

Sherman, D.M., Ragnarsdottir, K.V., Oelkers, E.H., 2000. Antimony transport in hydrothermal solutions: an EXAFS study of antimony(V) complexation in alkaline sulfide and sulfide-chloride brines at temperatures from 25 °C to 300 °C at P_{sat}. Chem. Geol. 167(1-2), 161-167.

Singer, P.C., Stumm, W., 1970. Acidic mine drainage: the rate-determining step. Science 167(3921), 1121-1123.

Smedley, P.L., Kinniburgh, D.G., 2002. A review of the source, behaviour and distribution of arsenic in natural waters. Appl. Geochem. 17(5), 517-568.

Smith, K.S., Ficklin, W.H., Plumlee, G.S., Meier, A.L., 1992. Metal and arsenic partitioning between water and suspended sediment at mine-drainage sites in diverse geologic settings, in: Kharaka, Y.K., Maest, A.S., (Eds.), Low temperature environments, v. 1 of Water-rock interaction, Proceedings of the 7th International Symposium on Water-Rock Interaction, Park City, Utah, July 13-18, 1992: Rotterdam, A.A. Balkema, 1, 443-447.

Smith, K.S., Ficklin, W.H., Plumlee, G.S., Meier, A.L., 1993. Computer simulations of the influence of suspended iron-rich particulates on trace metal-removal from mine-drainage waters., in: Proceedings of the Mined Land Reclamation Symposium, Billings, Montana., March 21-27, 1993. 2, 107-115.

Smith, K.S., 1999. Metal sorption on mineral surfaces: an overview with examples relating to mineral deposits, in Plumlee, G.S., Logsdon, M.J. (Eds.), The Environmental Geochemistry of Mineral Deposits, Part A: Processes, Techniques, and Health Issues. Society of Economic Geologists, Reviews in Econ. Geol. 6A, 161-182.

Stumm, W., Morgan, J.J., 1996. Aquatic Chemistry, 3rd edition. John Wiley and Sons, Inc., New York.

Sun, H.-W., Shan, X.-Q., Ni, Z.-M., 1982. Selective separation and differential determination of antimony(III) and antimony(V) by solvent extraction with *N*-benzoyl-*N*-phenylhydroxylamine and graphite-furnace atomic-absorption spectrometry using a matrix-modification technique. Talanta 29(7), 589-593.

Sun, Y.C., Yang, J.Y., Lin, Y.F., Yang, M.H., Alfassi, Z.B., 1993. Determination of antimony(III,V) in natural water by coprecipitation and neutron activation analysis. Anal. Chim. Acta 276(1), 33-37.

Takayanagi, K., Cossa, D., 1997. Vertical distributions of Sb(III) and Sb(V) in Pavin Lake, France. Water Res. 31(3), 671-674.

Tanizaki, Y., Shimokawa, T., Nakamura, M., 1992a. Physicochemical speciation of trace elements in river water by size fractionation. Environ. Sci. Technol. 26(7), 1433-1444.

Tanizaki, Y., Shimokawa, T., Yamazaki, M., 1992b. Physicochemical speciation of trace elements in urban streams by size fractionation. Water Res. 26(1), 55-63.

Tighe, M., Lockwood, P., Wilson, S., 2005. Adsorption of antimony(V) by floodplain soils, amorphous iron(III) hydroxide and humic acid. J. Environ. Monit. 7, 1177-1185.

Vaughan, D.J., 2006. Arsenic. Elements 2(2), 71-75.

Vink, B.W., 1996. Stability relations of antimony and arsenic compounds in the light of revised and extended Eh-pH diagrams. Chem. Geol. 130(1-2), 21-30.

Wagman, D.D., Evans, W.H., Parker, V.B., Schumm, R.H., Halow, I., Bailey, S.M., Churney, K.L., Nuttall, R.L., 1982. The NBS Tables of Chemical Thermodynamic Properties: Selected Values for Inorganic and C1 and C2 Organic Substances in SI units. J. Phys. Chem. Ref. Data, 11 (Suppl. 2), 2-79, 2-80.

Wilson, S.C., Lockwood, P.V., Ashley, P.M., Tighe, M., 2010. The chemistry and behaviour of antimony in the soil environment with comparisons to arsenic: a critical review. Environ. Pollut. 158(5), 1169-1181.

Yan, X.-P., Kerrich, R., Hendry, M.J., 2000. Distribution of arsenic(III), arsenic(V) and total inorganic arsenic in porewaters from thick till and clay-rich aquitard sequence, Saskatchewan, Canada. Geochim. Cosmochim. Acta 64(15), 2637-2648.

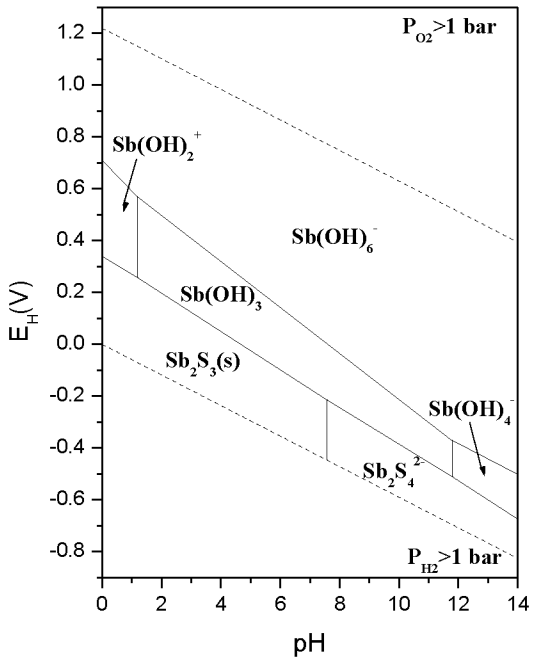

Figure 1.1 E_H-pH diagram of antimony in the Sb-S-H_2O system at dissolved concentrations of 10^{-8} M antimony and 10^{-3} M sulfur at 25 °C and 1 bar. Thermodynamic data obtained from Wagman et al. (1982) and Brookins (1988).

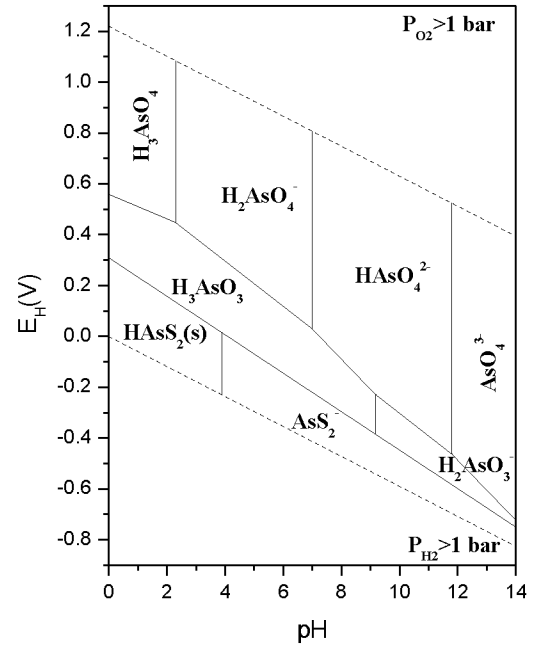

Figure 1.2 E_H-pH diagram of arsenic in the As-S-H_2O system at dissolved concentrations of 10^{-6} M arsenic and 10^{-2} M sulfur at 25 °C and 1 bar. Thermodynamic data obtained from Ferguson and Gavis (1972) and Vink (1996).

Chapter 2: Field study – site description, experimental methods, results and discussion[1]

Abstract

Mining activities can expedite oxidative weathering processes of acid-forming sulfide minerals, such as pyrite (FeS_2), and associated arsenopyrite (FeAsS) and stibnite (Sb_2S_3). The water quality of waters draining these mineralized areas can be adversely impacted for several kilometers downstream of the source. In this study we assess the mobility and chemical fate of antimony and arsenic in streams draining from historic antimony mines within Denali National Park and Preserve, Alaska. Antimony and arsenic concentrations in stream water reach up to 720 ppb and 239 ppb, respectively. The aqueous phase antimony and arsenic speciation was determined using liquid chromatography (LC) coupled to an inductively coupled plasma-mass spectrometer (ICP-MS). Antimony in all water samples is predominantly found as Sb^{5+}, whereas arsenic was detected as mixtures of As^{3+}/As^{5+} oxidation states. Elevated antimony concentrations extend over 8 km downstream from the source, whereas arsenic quickly attenuates within 1.5 km. The behavioral difference between antimony and arsenic is attributed to differences in aqueous speciation and affinities to mineral surfaces. A strong correlation between redox potentials calculated from iron (Fe^{2+}/Fe^{3+}) and arsenic (As^{3+}/As^{5+}) redox couples is observed; however, an obvious offset between the potentials suggests a disequilibrium between the redox pairs. High correlation was found in downstream dispersion between antimony/arsenic and iron concentrations in fine-fraction streambed sediment, indicating that sorption and (co)precipitation with iron (hydr)oxides is an important pathway for the attenuation of antimony and arsenic in natural waters.

[1] Ritchie, V.J., Trainor, T.P., Mueller, S.H., 2011. Mobility and chemical fate of antimony and arsenic in historic mining environments of the Kantishna Hills, Denali National Park and Preserve, Alaska. Prepared for submission to Chemical Geology.

2.1 Introduction

Oxidative weathering processes of acid-forming sulfide minerals, such as pyrite (FeS_2), and associated arsenopyrite (FeAsS) and stibnite (Sb_2S_3), can have a significant impact on water quality associated with current and legacy mineral extraction operations. Consequently, concentrations of As and Sb in acid mine drainage can reach hundreds of mg/L. These elevated concentrations are potentially harmful to the aquatic ecosystem located downstream from mining sites (Nam et al., 2009; Vaughan, 2006). Due to their high toxicity, the USEPA has listed As and Sb as priority pollutants with maximum concentration levels (MCLs) in drinking water of 10 and 6 ppb, respectively. The two elements are primarily present in the form of oxyanions with +V and +III oxidation states in natural waters.

The chemical composition of acid drainage waters is a function of a variety of processes, including acid neutralization, precipitation, aqueous complexation, and sorption onto particles and colloids within the water column or streambed sediments. The neutralization of the acidic water occurs by reaction with acid-neutralizing minerals present in the deposit or host rocks, such as carbonates or aluminosilicates, or by dilution with ground or surface water. When the pH of acidic waters is increased, the solubility of some metal ions, such as Fe^{3+}, is greatly reduced causing formation of precipitates (Nordstrom and Alpers, 1999; Stumm and Morgan, 1996). The concentrations of metals such as Pb, Cu, Zn, Cd, and Ni, and metalloids such as Sb and As, are variably controlled by aqueous complexation, coupled with sorption onto particulates and colloids (e.g., amorphous ferric-hydroxide or ferrihydrite, $Fe(OH)_3$ (Smith, 1999)). Colloidal Fe precipitates and other metal(loid)s that (co)precipitate can be transported long distances before settling to the streambed (Plumlee et al., 1999; Smith et al., 1992, 1993).

Comparing the oxidized forms of arsenic, it has generally been observed that As^{3+} has lower affinity for binding to mineral surfaces and is found to be more mobile in aquatic systems than As^{5+} (Herbel and Fendorf, 2006; Smedley and Kinniburgh, 2002; Zobrist et al., 2000). At acidic to pseudoneutral pH, As^{5+} is effectively immobilized by sorption and (co)precipitation with metal (hydr)oxides. As pH increases, especially

above pH 8.5, As desorbs from oxide surfaces, thereby increasing the concentration of As in solution (Bissen and Frimmel, 2003; Smedley and Kinniburgh, 2002). Both As^{5+} and As^{3+} can be released from metal (hydr)oxides during the onset of strongly reducing conditions due to the reductive dissolution of the sorbent (Guo et al., 1997; Herbel and Fendorf, 2006; Langner and Inskeep, 2000; Smedley and Kinniburgh, 2002; Takahashi et al., 2004). Microbial reduction of sorbed As has also been suggested to trigger release of As into the aquatic environment (Herbel and Fendorf, 2006; Tufano et al., 2008). Under strongly reducing conditions in the presence of sulfide, As concentration in the aqueous phase is controlled by the formation of insoluble As-sulfide species (Harvey et al., 2002; Ryu et al., 2002).

The behavior of Sb in natural waters has been less investigated than that of As (Filella et al., 2002; Wilson et al., 2010). In oxidizing conditions, Sb^{5+} has a lower affinity for mineral surfaces and is generally thought to be more mobile in aquatic systems than Sb^{3+}. The Sb^{3+} species adsorbs strongly to Fe and Mn (hydr)oxides over a wide pH range (Belzile et al., 2001; Casiot et al., 2007; Filella et al., 2002; Leuz et al., 2006a; Wilson et al., 2010), which results in the oxidation and ultimate release of the Sb^{5+} species (Leuz et al., 2006a). The Sb^{5+} species has also been found to adsorb to Fe (hydr)oxides; however, there is a lack of understanding of its sorption behavior in the natural environment. Tighe et al. (2005) investigated Sb^{5+} sorption by amorphous $Fe(OH)_3$ and floodplain soils across a pH range of 2.5 – 7. Adsorption was found to decrease with increasing pH, with maximum sorption occurring at approximately pH 4. Similar results were observed with Sb^{5+} adsorption to goethite, whereas Sb^{3+} strongly adsorbed over a pH range of 3 – 12 (Leuz et al., 2006a). Other studies have also supported the findings that iron (hydr)oxides are important sorbents for Sb^{5+} (Ackermann et al., 2009; Mitsunobu et al., 2006; Scheinost et al., 2006).

The aim of the present study was to assess the mobility and chemical fate of Sb and As in streams draining from historic Sb mines within Denali National Park and Preserve, Alaska. The specific objectives of this study were to characterize the chemical composition of surface waters draining mine tailings and waste-rock to determine overall

water quality, and to examine the fine-fraction bed-sediments in these streams to determine the association of As and Sb with secondary precipitates. Analysis of Sb and As speciation in the surface water was conducted to correlate oxidation state with transport characteristics along a downstream profile, and to directly compare the geochemical behavior of Sb and As within these drainage systems.

2.2 Study area

Numerous orogenic, intrusion-related gold deposits throughout Alaska and Yukon Territory contain massive, late stage, stibnite (Sb_2S_3) veining and pods (Bundtzen, 1978). Such deposits are particularly common within the Tintina Gold Province (TGP) of interior Alaska and Yukon, several of which served as a primary source of antimony ore throughout World Wars I and II (Bundtzen, 1978; Ebbley and Wright, 1948). In the current study, the Kantishna Hills Au and Sb mining district, located within the northwestern portion of Denali National Park and Preserve, was investigated (Figure 2.1). This district contains a number of Sb lode deposits including Alaska's historically largest Sb producer, the Stampede mine, as well as occurrences along Slate Creek. Hydrogeochemical characterization of both the Slate and Stampede creeks are presented.

The Kantishna district is made up of a number of polymetallic vein deposits that trend toward the northeast extending over a linear distance of 65 km from Slate Creek in the southwest to Stampede Creek in the northeast. The host rocks consist of Precambrian to Paleozoic metamorphic rocks of the Birch Creek Schist, the Spruce Creek sequence, and Keevey Peak and Totatlanika Schist formations (Bundtzen, 1978, 1983, 1994, and unpublished results; Bundtzen and Turner, 1979; Davis, 1922; Moffit, 1933). The veins that make up the bulk of the orebodies in the area are structurally controlled along faults and range in width from 8 cm to > 9 m and range in length from 30 m to > 500 m (Bundtzen, 1981; Capps, 1918; Lingren, 1933 Zobrist). The orebodies at both Stampede and Slate creeks are predominately composed of massive Sb_2S_3 (Bundtzen and Turner, 1979; Capps, 1918; Ebbley and Wright, 1948).

Although no hydrogeochemcial study of Stampede Creek is available, Eppinger et al. (2000) conducted a reconnaissance level environmental geochemical study of the Slate Creek deposit. They sampled naturally mineralized springs and streams, streams and pools that had contacted waste-rock and mine tailings, and streams outside of the mined zone. They found the pH in the waters ranged from 3 – 8, specific conductance ranged from 130-1700 μS/cm, and Sb concentrations ranged from < 1 μg/L to 190 μg/L. The highest Sb concentrations were found in water within the mine site; however, naturally mineralized samples also contained as much as 14 μg/L dissolved Sb. Stream sediments were also sampled and revealed a wide range of relatively high Sb concentrations from 43-6000 ppm.

2.3 Methods

2.3.1 Field sampling and in situ measurements

Field sampling was conducted twice at the Slate Creek site; August 2005 and July 2007. The sampling locations are shown in Figures 2.2 and 2.3, respectively, and sample descriptions are summarized in Table 2.1. In 2005, water and bed-sediment samples were collected, whereas only water samples were collected in 2007. Slate Creek merges with Eldorado Creek and in turn merges with Moose Creek. For simplicity, all waters containing Slate Creek mine-effected waters are referred to as the "main drainage". In 2005, a sample was collected upstream of any obvious mine disturbance (regional background), within and downstream of the mine workings, as well as from a tailings seep and other minor tributaries. A pond immediately adjacent to the main drainage and two springs flowing from the embankment into the main drainage were sampled. One sample was collected from Moose Creek (05SC21) downstream of the confluence with Slate Creek to further investigate the dilution profile of the mine-effected waters. The 2007 Slate Creek sampling was less extensive than 2005. Although the exact 2005 main drainage locations were not re-sampled in 2007, the same pond (05SC16, 07SC08) and tailings seep near headwater (05SC02, 07SC03) were re-sampled and are directly compared (Figure 2.2).

In 2007, additional samples were collected from Friday and Eureka creeks (not shown), which are tributaries to Moose Creek entering from the east. The confluences of the Eureka and Friday creeks with Moose Creek are located ~ 0.5 km upstream and ~ 1 km downstream, respectively, from the Slate Creek confluence with Moose Creek. Both the Friday and Eureka creeks have been disturbed by historic placer Au mining (Bundtzen, 1978). Two Moose Creek samples (not shown) were collected during 2007; one upstream (07MC01) and one downstream (07MC02) of the Slate Creek confluence with Moose Creek. These samples were collected to compare hydrogeochemical data before and after the input of the mineralized/disturbed drainages.

The Stampede Creek field sampling was conducted in July of 2006 and the sampling locations are shown in Figure 2.4. As with Slate Creek, samples were collected upstream, downstream and within the mined areas, as well as from minor tributaries. Pore water (06STcore) was collected from a pulverized ore pile adjacent to the main drainage within the mine workings. Two samples (06ST13, 06ST18) were collected upstream and one sample (06ST15) downstream of the Clearwater Fork and Stampede Creek confluence to compare hydrogeochemical data before and after the Stampede Creek input (Figure 2.4).

Water samples were collected in HDPE bottles (HDPE amber bottles were used for As, Sb and Fe speciation samples) and field-filtered using 0.45 μm high capacity Geotech disposable filters. Additional samples were collected at a subset of locations (18 total) and filtered through 0.2 μm pore-size syringe filters to qualitatively determine a colloidal-fraction (as the difference in element concentrations between 0.2 and 0.45 μm-filtered samples). Water samples were field-preserved with ultrapure 6 M HNO_3 for major cation and trace metal analyses and with ultrapure 6 M HCl for Fe, As and Sb speciation analysis to pH ~ 2. Water samples for sulfide analysis were collected in 125 mL bottles and field-preserved with 1 mL 1 M zinc acetate and titrated with 6 N NaOH to pH $\geq$ 9. Fine-fraction (< 63 μm) streambed sediment samples were wet-sieved onsite through polyester screens and collected in HDPE bottles. All samples were stored at 4 °C until analysis.

The oxidation-reduction potential (ORP), pH, conductivity, and temperature were measured *in situ* (Table 2.1) using Oakton instruments (double junction ORPTestr10, ECTestr high+ and pH Testr30). The instruments were calibrated daily using standard solutions.

2.3.2 Analytical Methods

Water samples were analyzed using ion chromatography (Dionex ICS-2000) for major cation (IonPac CS12A column) and anion (IonPac AS19 column) composition. The operational parameters suggested in the IC column manuals were optimized using standard solutions before sample analysis. The mobile phase for cation analysis was methanesulfonic acid (MSA; supplied by Dionex). To optimize the cation peak resolution, the concentration of MSA was varied from 10 mM at the beginning of the analytical run (0 – 3 minutes), to 3 mM (2.5 – 25 minutes), followed by a linear increase to 15 mM (26.5 – 50 minutes). For the anion analysis, NaOH (Dionex) mobile phase was used. The optimum peak resolution was observed with the following sequence: 0.5 mM NaOH (0 – 3 minutes), linearly increased to 12 mM (3 – 12 minutes), and then linearly increased to 50 mM at 12 – 35 minutes. The conductivity cell temperature was set at 30 °C. Milli-Q water with the resistivity of 18.2 MΩ·cm, 0.2 μm-filtered and UV-irradiated (< 1 ppb total organic carbon) was used for preparing all solutions (Barnstead NANOpure® Diamond™).

Minor and trace elements of aqueous samples were measured using inductively coupled plasma mass spectrometry (ICP MS; Agilent 7500ce) (Creed et al., 1994). To remove $^{40}Ar^{35}Cl$ polyatomic interference during analysis of arsenic, the ICP MS was operated in a collision/reaction cell (CRC) mode using He gas. Streambed sediments were partially digested using a multi-acid digestion technique (Briggs and Meier, 2002) and analyzed by ICP MS (Perkin Elmer ELAN® 6000) for major/minor elemental composition.

Alkalinity was determined by titrating 100 mL of a filtered sample with 0.0200 N H_2SO_4 (Fisher) to a pH of 4.5 (Eaton and Franson, 2005). The resulting alkalinity (mg/L

$CaCO_3$) was calculated as 10 times the volume of 0.0200 N H_2SO_4. For alkalinities < 20 mg/L the titration was stopped in the range of pH from 4.3 to 4.6, and then continued using a micro-burette to reduce the pH by 0.3 units. The resulting alkalinity was calculated using the expression:

$$Alk_{total}, mg\,CaCO_3 / L = \frac{(2B - C) \times N \times 50{,}000}{mL\ sample}$$

where B is volume (mL) of H_2SO_4 used to the first recorded pH; C is total volume (mL) of H_2SO_4 to reach pH 0.3 unit lower; and N is normality of H_2SO_4 acid.

The concentration of dissolved sulfide was determined by potentiometric titration (Eaton and Franson, 2005) using a combination silver/sulfide electrode (Orion 94-16). The electrode performance was checked every 2 hours and calibration standards were measured every 4 hours. The ZnS precipitate formed during sample preservation was separated and dissolved in 50 mL of the alkaline antioxidant reagent and diluted to 100 mL volume with deoxygenated milli-Q water prior to the potential measurement; the alkaline antioxidant reagent was prepared by combining 80 g NaOH, 35 g ascorbic acid ($C_6H_8O_6$), 67 g Na_2H_2EDTA in deoxygenated milli-Q water and bringing the total volume to 1 L.

The oxidation state of As and Sb in water was determined using liquid chromatography (LC; Agilent 1100) coupled to an ICP MS (Agilent 7500ce). The separation was performed using an arsenic speciation column (Agilent G3154-65001, 4.6 mm×150 mm i.d.) and guard column (Agilent G3154-65002, 4.6 mm×10 mm i.d.) packed with chemical bonded hydrophilic anion exchange resin. The mobile phase for As speciation was prepared following Agilent recommendations (Agilent Technologies, 2000) of 2 mM NaH_2PO_4, 0.2 mM NaEDTA, and adjusted to pH 6 with 1 M NaOH; it also contained 50 ppb Ge as internal standard. Sensitivity optimization was performed at a forward radio-frequency (RF) power of 1400 W, LC injection volume of 50 µg/L, and detector count time of 0.5 seconds per point (^{75}As) with a total acquisition time of 800 seconds. The As^{3+} and As^{5+} peaks were centered at 112 and 435 seconds, respectively. The mobile phase for Sb speciation analysis consisted of 12 mM NaEDTA, 2 mM

phthalic acid, 3 % v/v methanol, 50 ppb In as internal standard, and the final volume adjusted to pH 4.5 with 1 M NaOH (modified from Zheng et al., 2000). Sensitivity optimization was performed at a RF power of 1500 W, LC injection volume of 100 µL, detector count time of 0.5 seconds per point (^{121}Sb, ^{123}Sb) with a total acquisition time of 450 seconds. The Sb^{3+} and Sb^{5+} peaks were centered at 210 and 130 seconds, respectively.

The aqueous Fe^{2+} and Fe_{total} were determined by UV visible spectrophotometry (UV VIS) using the ferrozine method (To et al., 1999). Calibration standards with 0.004 – 1.6 mg/L of Fe^{2+} were prepared daily by diluting aliquots of an Fe^{2+} stock solution (25 mM reagent grade $FeSO_4 \cdot 7H_2O$ in deoxygenated milli-Q water containing 1 % v/v ultrapure HCl) in deoxygenated milli-Q water. To prevent oxidation of Fe^{2+} in standard solutions and to reduce Fe^{3+} to Fe^{2+} in samples intended for the Fe_{total} measurement, 1 mL aliquot of reagent grade 10 % w/v hydroxylamine hydrochloride solution was added to each 40 mL of standard solution or sample in a 50 mL volumetric flask. Then a 1 mL aliquot of 4.9 mM ferrozine reagent was added to all samples, and the total volume of each sample was brought to 50 mL with milli-Q water. The concentration of Fe^{2+} was determined by measuring the absorbance at 562 nm; Fe^{3+} was calculated as the difference between Fe_{total} and Fe^{2+}. The Fe_{total} determined using this method was comparable (± 5 %) to Fe_{total} determined by ICP MS for all samples.

2.4 Results and discussion

Figure 2.5 shows the correlation between Sb and As in stream and sediment samples from the present study, as well as other samples collected within the TGP (Mueller et al., 2010). There is a high (and expected) correlation between Sb and As concentrations in water and bed-sediments, with some water samples exceeding EPA MCLs by up to two orders of magnitude. Of particular note are the generally elevated Sb concentrations in the aqueous (and to a lesser extent the sediment) samples from the Kantishna Hills sites. This observation motivates the present study, which is focused on characterizing the hydrogeochemical setting associated with the Kantishna area samples.

2.4.1 Major/Minor element aqueous chemistry

The *in situ* measurements of water from the Kantishna Hills sites are presented in Table 2.1. The lowest pH values were measured in waters directly derived from mine waste; pH 2.50 in pulverized ore pore water (06STcore) at the Stampede mine site and pH 2.83 in a tailings pile seep (05SC02) at Slate Creek. All stream water samples had pseudoneutral pH. Conductivities ranged from 512 to 2980 µS/cm in water samples from minor tributaries and 202 to 1014 µS/cm in main drainage samples. Similar pH and conductivities for the Slate Creek waters was reported by Eppinger et al. (2000).

The major and minor element composition of water samples are presented in Table 2.2. Waters of the main drainage and minor tributaries ranged in major-anion composition from bicarbonate to sulfate-dominant (Figure 2.6). The more sulfate-dominant waters correspond to samples collected within the mine workings, whereas the more bicarbonate-dominant waters were collected upstream of the mined areas or downstream beyond evidence of mining. The notable exceptions in anion composition are the springs (05SC14A, 05SC14B), pond (05SC16), and tailings seep (05SC02) samples. The chloride concentrations of the springs and pond samples are higher than stream samples, which suggest a significant degree of volume reduction due to (e.g.) evapotranspiration (Langmuir, 1997). In addition, the alkalinities (as mg/L $CaCO_3$) of the springs and pond samples were below detection (< 10 mg/L) even though the pH of the samples were in the range of 6.05 – 6.29. This significant lack of buffering capacity is also correlated with a large charge imbalance that indicates an anion component deficiency (Table 2.2). A rain event was occurring during sampling, so we speculate that this observation may be attributed to baseflow dilution coupled with an influx of dissolved organic carbon from surface runoff, which is in agreement with previous studies (Buffam et al., 2001; Petrone et al., 2006). The presence of organic acids was unaccounted for in alkalinity measurements. Conversely, the tailings seep sample (05SC02) also had effectively zero alkalinity; however, this sample was highly acidic (sulfate dominated), consistent with its location in the tailings pile. Furthermore, this sample indicates a significant cation deficiency which could possibly be associated with

loss of metals (e.g., Fe^{2+}) associated with rapid oxidation and precipitation during sample collection.

All water samples were calcium-magnesium dominant with respect to major-cations (Figure 2.6). The highest calcium concentrations were in the spring samples, which often correlate to higher water-rock interaction of subsurface waters. Similar chemical compositions of Slate Creek waters were reported by Eppinger et al. (2000).

The sum of dissolved base metals Zn, Cu, Cd, Pb, Co, and Ni are plotted in relation to pH in a Ficklin diagram (Figure 2.7; after Plumlee et al., 1999). The sum of base metals allows for differentiation between different geologic controls on water composition that would not otherwise be evident from concentration variations in major cations. The designated boundaries in the figure were proposed by Plumlee et al. (1992) to help classify different drainage compositions. The waters draining both the Slate Creek and Stampede mineral deposits can largely be classified as near-neutral pH, low base metal type waters. The acid water contributions from tailings seeps and other minor tributaries are quickly neutralized / diluted when mixing with the stream waters.

Within the main drainages calcite ($CaCO_3$) solubility appears to be the primary control on alkalinity. $CaCO_3$ saturation indices (SI), calculated using Visual MINTEQ, version 2.32 (Gustafsson, 2005), with inputs from the standard MINTEQ thermodynamic database, analytical totals and *in situ* pH values, indicate that all main drainage samples (and most minor tributaries) are at approximate saturation with respect to $CaCO_3$ (Figure 2.8). A tailings seep (05SC02) was found to be under-saturated, which is consistent with the lower pH value. Assuming equilibrium with atmospheric CO_2 pressure (35.5 Pa), the low alkalinity spring (05SC14A, 05SC14B) and pond (05SC16) samples are also below saturation. As stated in the alkalinity discussion above, this undersaturation with respect to $CaCO_3$ may be due to incomplete mixing of $CaCO_3$-rich baseflow and fresh rainwater runoff.

Calculated SI values indicate approximate saturation to oversaturation with respect to amorphous $Fe(OH)_3$ for all samples (Figure 2.8), but under-saturated with respect to Al and Mn minerals included in the standard MINTEQ database. This is

consistent with the observation of iron staining throughout the drainage, particularly near heavily mineralized zones, indicating precipitation of ferric-hydroxides. Several factors may explain the apparent oversaturation, including an incomplete thermodynamic database or errors associated with tabulated temperature corrections. In addition to these factors, the apparent oversaturation may in part be due to the presence of colloidal Fe. A comparison of 0.2 µm versus 0.45 µm-filtered sample data (Table 2.3) shows that up to 23% of total Fe (and Mn) may be associated with colloids ranging in size between the two filter pore sizes. Recalculating the $Fe(OH)_3$ SI using Fe total concentrations of the 0.2 µm-filtered samples results in a decrease in SI value (not shown); however, the calculations still indicate slight oversaturation. Colloidal Fe of < 0.2 µm-size fraction is also likely contributing to the "dissolved" Fe total concentrations, which is supported in literature (Bouby et al., 2004; Kuma et al., 1998; Pokrovsky et al., 2005; Pullin and Cabaniss, 2003). Nonetheless, the analytical Fe concentrations and calculated SI values indicate that ferric hydroxides are likely important substrates for sequestration of metal(loids) in this system via sorption and/or co-precipitation processes.

2.4.2 Aqueous speciation and redox potentials

Aqueous speciation was determined for the following redox-sensitive elements: S, N, Fe, As, and Sb. Sulfate concentrations ranged from < 0.5 to 2115 mg/L (Table 2.2). Sulfide was not detected in any water sample above detection limit (~ 0.03 mg/L), although a strong $H_2S(g)$ odor was noted during the collection of the Slate Creek spring (05SC14A) and pond (05SC16 and 07SC08) samples. Concentrations of N redox species (NO_3^-, NO_2^- and NH_4^+) were insignificant in all samples. Total Fe concentrations ranged from < 12 µg/L to 230 mg/L, with Fe^{2+}/ Fe^{3+} ratios between 0.1 and 31 (Table 2.4). Total As concentrations in surface and spring waters ranged from < 1 to 179 µg/L, with As^{3+}/As^{5+} ratios between 0.1 and 3. Total As concentration in pulverized ore pore water was 3554 µg/L, with a As^{3+}/As^{5+} ratio of 78 (Table 2.4). Lastly, Sb^{5+} concentrations in surface and spring waters ranged from < 1 to 699 µg/L and were 55 mg/L in the

pulverized ore pore water (Table 2.5). The reduced Sb^{3+} species was not found above the detection limit (~ 5 µg/L) in any sample.

The redox potential (E_H) of water samples was calculated from the analytical data based on two redox couples: Fe^{2+}/Fe^{3+} and As^{3+}/As^{5+}. In Figure 2.9, the E_H for the Fe^{2+}/Fe^{3+} couple as a function of pH is compared to the theoretical stability fields calculated from thermodynamic data in Langmuir (1997) for a simplified $Fe\text{-}O_2\text{-}H_2O$ system at dissolved concentrations of 10^{-5} M Fe (average for Kantishna field samples) at 25 °C and 10^5 Pa. It can be seen from the figure that (for the majority of the samples) the experimental E_H values fall in the regime expected for Fe^{2+} equilibrium with freshly precipitated $Fe(OH)_3(am)$. These observations are consistent with relatively slow dissolution of the Fe-bearing primary sulfide minerals (FeS_2, FeAsS) as compared to the equilibration of the Fe^{2+}/Fe^{3+} redox couple in oxygenated systems (Stefánsson et al., 2005; Stumm and Morgan, 1996). One exception is the acidic tailings seep (pH 2.83), which is comparatively more reduced than the main drainage and other tributaries, and is apparently under-saturated with respect to possible Fe^{3+} phases. Furthermore, it is suspected that oxidation and precipitation of metals (e.g., Fe^{2+}) may have occurred during sample collection based on a significant charge imbalance (cation deficiency; Table 2.2) of the sample, as discussed in the previous section. Precipitation would result in a high-biased E_H, so it is possible that the tailings seep waters may be a more reduced environment than calculated.

A similar analysis using the computed E_H values from the dissolved arsenic concentrations suggests that the aqueous As^{3+} and As^{5+} species maintain an apparent equilibrium (Figure 2.10). The calculations suggest an absence of any sulfide species, even when using 10 mM dissolved sulfur in the computation (Kantishna samples average 1 mM total sulfur). The calculations also suggest that two predominant forms ($H_2AsO_4^-$ /$HAsO_4^{2-}$) of As^{5+} would be present in solution depending on the pH. Furthermore, E_H calculated from the As^{3+}/As^{5+} redox couple compared to theoretical Sb stability fields (also plotted in Figure 2.10), suggests that the Sb^{3+} and Sb^{5+} species maintain an apparent equilibrium. Based on these As^{3+}/As^{5+}-determined E_H values, $Sb(OH)_6^-$ is the

predominant form of Sb^{5+} over the pH range of these waters. The thermodynamic data used for plotting theoretical stability fields for As species was obtained from Ferguson and Gavis (1972) and Vink (1996), and the data for Sb species from Wagman et al. (1982) and Brookins (1988).

A comparison of calculated E_H values based on the As^{3+}/As^{5+} and Fe^{2+}/Fe^{3+} redox couples is presented in Figure 2.11. While the correlation is very strong, there is an obvious offset between the potentials computed in the two cases. This may be associated to some extent with the apparent high E_H values resulting from inclusion of colloidal Fe in the dissolved total. However, it is also likely that there is disequilibrium between these redox pairs. These observations are in agreement with previous findings on the redox conditions in a cold groundwater (Lindberg and Runnels, 1984) and geothermal waters (Stefánsson et al., 2005; Stefánsson and Arnórsson, 2002). Possible explanations for this commonly observed disequilibrium have been postulated, to include improper sample preservation leading to a post-sampling shift in redox species concentrations and variations in tabulated standard E^0 data used to calculate E_H (Lindberg and Runnels, 1984). Nevertheless the high correlation leads us to speculate that the As redox chemistry is likely strongly influenced by the Fe chemistry, and heterogenous processes between dissolved As and solid phase Fe, as noted in a number of previous studies (Bednar et al., 2005; Herbel and Fendorf, 2006; Tufano et al., 2008; Weber et al., 2010).

2.4.3 Mobility and attenuation of Sb and As

The speciation and transport of Sb and As away from stibnite (Sb_2S_3) and arsenopyrite (FeAsS)-rich mineralization is important to the fate and attenuation of these species in the secondary environment. The total Sb and As concentrations in water and bed-sediment as a function of distance from headwater (i.e., regional background samples) for the 2005 and 2007 Slate Creek, and 2006 Stampede Creek sampling events is shown in Figures 2.12a, 2.12b, and 2.12c, respectively. Both main drainage and minor tributaries, and corresponding *in situ* pH, are plotted. A summary of Sb and As water and sediment concentrations is also provided in Table 2.5.

As shown in Figure 2.12a, there was considerable increase in dissolved Sb and As concentrations within and downstream of the Slate Creek (2005) mine workings compared to concentrations at the headwater (i.e., regional background (05SC01); [Sb] = 4.18 ppb, [As] = 5.3 ppb). The Sb and As concentrations in the main drainage increased significantly in the vicinity of the tailings seep and another minor tributary flowing from south of the mine disturbance. However, Sb (and to a lesser extent As) concentrations continue to increase downstream of the disturbed mining area, reaching a maximum of 665 ppb at 0.75 km from headwater. Antimony concentrations decrease one order of magnitude within another 3 km, but still remain one order of magnitude above (58.8 ppb) the EPA MCL (6 ppb) before merging with Moose Creek ~ 8 km from headwater. After merging with Moose Creek, Sb is diluted to below the water quality standard. Conversely, As appears to be less mobile in this environment than Sb. Dissolved As exceeds the EPA MCL (10 ppb) by ~ 3 times at its maximum concentration downstream of the mining disturbance and rapidly decreases to below the MCL within 0.8 km. Further downstream (4.5 km), a significant concentration of As (239 ppb) from a minor tributary (~ ¼ the size of the main drainage) near an exposed FeAsS-rich tailings pile was deposited into the main drainage. However, an increase in dissolved As concentration was not observed 200 m downstream of the confluence, indicating that As was rapidly attenuated via partitioning and/or dilution.

The dissolved Sb and As concentrations from the 2007 Slate Creek sampling event (Figure 2.12b) were slightly elevated compared to the 2005 sampling event (Figure 2.12a). The lower 2005 results are correlated with total discharge; stream water levels were ~ 0.5 meters higher in 2005 than in 2007. The higher 2005 water levels are presumed to be groundwater contribution as atmospheric precipitation for several weeks prior to sampling was minimal (the 2005 National Atmospheric Deposition Program (NAPD) recorded levels of snow accumulation and spring rain events were greater in 2005 than in 2007). Although the exact 2005 main drainage locations were not re-sampled in 2007, the same pond (05SC15, 07SC08) and tailings seep (05SC02, 07SC03) near headwater were re-sampled and can be directly compared. The 2007 pond had 22%

and 4% higher Sb and As concentrations, respectively. This is consistent with the overall higher Sb/As concentrations of the main drainage resulting from lower water levels (less dilution). Conversely, the 2005 tailings seep contained 120% more Sb and 158% more As than in 2007. In addition, the pH of water in 2005 (2.83) was markedly lower than 2007 (5.62). This may be explained by the flushing (a light rain began minutes prior to sampling) of secondary sulfate salts that were deposited on the tailings through evaporation. These metal salts can store acid and metal(loid)s in solid form that can dissolve readily during a rainstorm runoff, resulting in a high influx of acid and metal(loid)s into the drainage system (Nordstrom and Alpers, 1999; Plumlee et al., 1999).

The 2007 Sb and As concentrations in Moose Creek upstream of the Friday, Slate, and Eureka creek confluences (not shown in Figure 2.12b) were both < 1 ppb (07MC01), indicating a lack of substantial Sb and As input upstream and/or that dilution, adsorption, and (co)precipitation processes have significantly reduced metalloid concentrations (Table 2.5). The samples from the Friday and Eureka creeks were collected ~ 0.8 km upstream from the junction with Moose Creek and contained 1.66 ppb Sb and 3.49 ppb As, and 8.94 ppb Sb and 3.54 ppb As, respectively. The Moose Creek sample (07MC02) collected ~ 0.5 km downstream of the Friday Creek confluence (downstream of all three confluences) contained 4.27 ppb Sb and 2.20 ppb As. The impact of input from the upstream mining-effected drainages on the Moose Creek water quality is minimized largely through dilution as Moose Creek is over several times the volume of the three tributaries.

Antimony was detected in the Stampede Creek (Figure 2.12c) at concentrations ~ 2 times less than the Slate Creek drainage. Elevated Sb concentrations (11 to 16 ppb) above presumed regional background concentration (2.65 ppb) were detected in samples collected upstream of any known disturbance, whereas As concentrations remained < 1 ppb. Pore water collected from the refined, pulverized ore pile along the bank of the main drainage contained significant Sb (55 mg/L) and As (3.5 mg/L) concentrations. Similar to the Slate Creek drainage, the maximum dissolved Sb concentration (264 ppb) was detected ~ 0.9 km downstream from the mine site, and remained over one order of

magnitude above (82.7 ppb) the MCL before merging with the Clearwater Fork ~ 3.6 km from the mine site (4.3 km from headwater). Downstream (150 m) of the confluence with Clearwater Fork, Sb is diluted to 28.5 ppb. Conversely, dissolved As only marginally exceeded the EPA standard in one main drainage sample (06ST07; 10.2 ppb) and quickly attenuated. Clearwater Fork Sb (< 2 ppb) and As (< 1 ppb) concentrations from samples (06ST13, 06ST18) collected upstream of the Stampede Creek confluence were minimal. The unnamed drainage contained 11.7 ppb Sb (As < 1 ppb). It is unknown if the drainage has been affected by historic mining activity or if the Sb detected is a result of natural weathering processes.

Antimony and As mobility in an aerobic aqueous environment is moderated by (co)precipitation and/or adsorption with amorphous metal (hydr)oxides (Filella et al., 2002; Leuz et al., 2006a; Roddick-Lanziolotta et al., 2002; Smedley and Kinniburgh, 2002; Tighe et al., 2005; Wilson et al., 2010), which is supported by the high concentrations in < 63 μm-size fraction bed-sediment samples downstream of the mining-effected areas. However, in comparing the water to the sediment Sb and As downstream profiles (Figures 2.12a and 2.12c), it can be seen that bed-sediments are effectively decoupled from the water column. In other words, minimal mixing between the sediment and water/suspended particles limits the rate of bedload transport, which has been observed in previous studies (Smith, 1999, and references therein). Antimony and As sediment concentrations in relation to Fe sediment concentrations as a function of distance from headwater is shown for Slate Creek and Stampede Creek main drainage samples in Figure 2.13. The ratios of Sb and As to Fe in sediments yield similar downstream sediment dispersion profiles to that of total Sb and As concentrations, indicating a strong correlation between Sb/As and Fe in bed-sediment. This correlation suggests that sorption and (co)precipitation with Fe (hydr)oxides is an important pathway for the attenuation of Sb and As in natural waters.

The predominant form of As in the Slate and Stampede creeks is As^{5+}. The percent of the As^{5+} species in the main drainage as a function of distance from the headwater is shown in Figure 2.14. In all cases, As^{5+} % decreases in the area of exposed

tailings but quickly increases to approximate background levels within 1-3 km from the source. The As^{3+} species was dominant in the pore water (06STcore), a tributary originating from the mined area (05SC03), a spring (05SC14A), and both pond (05SC16, 07SC08) samples. Due to the small volume input of these tributaries and the relatively fast (possibly bio-mediated) oxidation of As^{3+} to As^{5+} in oxidized waters (Bruneel et al., 2003; Oremland et al., 2001; Saltikov and Newman, 2003), As^{5+} remains the dominant species in the main drainages. A summary of As speciation in water samples is presented in Table 2.4.

The predominant form of Sb in all samples is Sb^{5+}. Antimony originating from pore water of the pulverized ore, and perhaps the slightly reduced environment of the spring and pond, was expected to have detectable concentrations of reduced species, but Sb^{3+} was not detected in any sample. However, the Sb^{3+} detection limit (~ 5 ppb) was elevated to that of Sb^{5+} (1 ppb) due to poor peak resolution. The sample preservative (HCl) used for the Sb^{3+}/Sb^{5+} redox couple was found to spectrally interfere with the elution of the Sb^{3+} species, thus increasing its detection limit. The detection of the thermodynamically unstable As^{3+} species but not the Sb^{3+} species in these waters suggests slower oxidation kinetics for As^{3+} or stabilization via complexation. This observation has been has been supported in literature (Leuz et al., 2006b; Mitsunobu et al., 2006). It also may suggest that HCl in an inadequate preservative for the Sb^{3+}/Sb^{5+} redox couple.

The behavioral difference of downstream transport of Sb and As can be explained through Sb/As aqueous speciation. In aerobic conditions at mildly acidic to pseudoneutral pH, As^{5+} has a high affinity for mineral surfaces, thereby As is effectively immobilized by sorption and (co)precipitation with metal (hydr)oxides (Bissen and Frimmel, 2003; Smedley and Kinniburgh, 2002). Conversely, Sb^{5+} has a lower affinity for mineral surfaces and can be transported further distances (Belzile et al., 2001; Casiot et al., 2007; Filella et al., 2002; Wilson el al., 2010). These results are in agreement with previous studies of Sb and As mobility in mining-impacted water (Ashley et al., 2003; Casiot et al., 2005, 2007).

2.5 Summary

Elevated concentrations of Sb and As in both water and bed-sediments are associated with legacy mining activities at the Slate Creek and Stampede Creek sites within the Kantishna Hills. Water quality of both drainage systems is compromised several kilometers downstream from the mineralized source. Dissolved Sb concentrations in Slate Creek exceeds the EPA MCL by over two orders of magnitude near the mine workings and remains one order of magnitude above until the mergence with Moose Creek (~ 8 km from headwater). Dissolved As concentrations also exceed the MCL by ~ 3 times near the mine workings; however, As rapidly decreases to below the water quality standard within 1.5 km. Similar results are seen for the Stampede Creek drainage, although at slightly lower concentrations. The behavioral difference between Sb and As is attributed to aqueous speciation and different affinities to mineral surfaces, namely Fe (hydr)oxides. The predominant form of Sb and As in main drainage waters is the +V oxidation state, with As^{3+} predominating in minor tributaries (pulverized ore pore water, pond, and spring samples). The As^{5+} species is affectedly immobilized by its high affinity for mineral surfaces, whereas the lower affinity of Sb^{5+} for mineral surfaces allows for further downstream transport. The redox potentials calculated from the Fe^{2+}/Fe^{3+} and As^{3+}/As^{5+} redox couples indicate the species maintain apparent equilibrium in these waters. A strong correlation between the Fe and As redox potentials is observed; however, an obvious offset between the potentials suggests a disequilibrium between the redox pairs. High correlation was found in downstream dispersion between Sb/As and Fe concentrations in bed-sediment, indicating that sorption and (co)precipitation with iron (hydr)oxides is an important pathway for the attenuation of Sb and As in natural waters.

Acknowledgements

The authors express gratitude to National Park Service personnel (the late Phil Brease and Lucy Tyrrell) for access and logistical support; Kunaljeet Tanwar, Anastasia Ilgen, and Sarah Petitto for field work assistance; Richard Goldfarb (USGS, Denver, CO) for collaborative efforts; and, Anastasia Ilgen for analytical consultations. This research

was financially supported by the USGS MRERP grant 06HQGR0177, NSF grants CBET-0404400 and CHE-0431425, and the Discover Denali Research Fellowship (funded by the National Park Service and the Denali Education Center).

References

Ackermann, S., Giere, R., Newville, M., Majzlan, J., 2009. Antimony sinks in the weathering crust of bullets from Swiss shooting ranges. Sci. Total Environ. 407(5), 1669–1682.

Agilent Technologies Inc., 2000. As Speciation Analysis Handbook.

Ashley, P.M., Craw, D., Graham, B.P., Chappell, D.A., 2003. Environmental mobility of antimony around mesothermal stibnite deposits, New South Wales, Australia and southern New Zealand. J. Geochem. Explor. 77(1), 1-14.

Belzile, N., Chen, Y.-W., Wang, Z., 2001. Oxidation of antimony(III) by amorphous iron and manganese oxyhydroxides. Chem. Geol. 174(4), 379-387.

Bednar, A.J., Garbarino, J.R., Ranville, J.F., Wildeman, T.R., 2005. Effects of iron on arsenic speciation and redox chemistry in acid mine water. J. Geochem. Explor. 85(2), 55-2.

Bissen, M., Frimmel, F.H., 2003. Arsenic – A review. Part I: Occurrence, toxicity, speciation, mobility. Acta Hydroch. Hydrob. 31(1), 9-18.

Bouby, M., Geckeis, H., Manh, T.N., Yun, J.-I., Dardenne, K., Schäfer, T., Walther, C., Kim, J.-I., 2004. Laser-induced breakdown detection combined with asymmetrical flow field-flow fractionation: application to iron oxi/hydroxide colloid characterization. J. Chromatogr. 1040(1), 97-104.

Briggs, P.H., Meier, A.L., 2002. The determination of forty-two elements in geological materials by inductively coupled plasma - mass spectrometry, Chapter I in: Taggart Jr., J.E. (Ed.), Analytical methods for chemical analysis of geologic and other materials, US Geological Survey. Open-File Report 02-223.

Brookins, D.G., 1988. Eh-pH Diagrams for Geochemistry. Springer-Verlag, Berlin, New York, pp. 30-31.

Bruneel, O., Personne J.-C., Casiot, C., Leblanc, M., Elbaz-Poulichet, F., Mahler, B.J., Le Fleche, A., Grimont, P.A.D., 2003. Mediation of arsenic oxidation by Thiomonas sp. in acid mine drainage (Carnoules, France). J. Appl. Microbiol. 95(3), 492-499.

Buffam, I., Galloway, J.N., Blum, L.K., McGlathery, K.J., 2001. A stormflow/baseflow comparison of dissolved organic matter concentrations and bioavailability in an Appalachian stream. Biogeochemistry 53(3), 269-306.

Bundtzen, T.K., 1978. A history of mining in the Kantishna Hills. Alaska Journal 8(2), 150-161.

Bundtzen, T.K., 1981. Geology and mineral deposits of the Kantishna Hills, Mount McKinley quadrangle, Alaska: Fairbanks, Alaska, University of Alaska Fairbanks, M.S. thesis, pp. 238.

Bundtzen, T.K., 1983. Mineral-resource modeling, Kantishna-Dunkle mine-study areas, Alaska Division of Geological & Geophysical Surveys Report of Investigation 83-12, p. 51.

Bundtzen, T.K., 1994. Kantishna district, in: Plafker, G., Berg, H.C. (Eds.), Metallogeny and major mineral deposits of Alaska. The geology of North America, v. G-1. Geological Society of America, Colorado, pp. 872-873.

Bundtzen, T.K., Turner, D.L., 1979. Geochronology of metamorphic and igneous rocks in the Kantishna Hills, Mount McKinley quadrangle, Alaska, in: Alaska Division of Geological & Geophysical Surveys, Short Notes on Alaskan Geogeology – 1978: Alaska Division of Geological & Geophysical Surveys Geological Report 61F, pp. 25-30.

Capps, S.R., 1918. Mineral resources of the Kantishna region, in: U.S. Geological Survey Staff, Mineral resources of Alaska, report on progress of investigations in 1916: U.S. Geol. Surv. Bull., 662, pp. 279-332.

Casiot, C., Lebrun, S., Morin, G., Bruneel, O., Personne, J.C., Elbaz-Poulichet, F., 2005. Sorption and redox processes controlling arsenic fate and transport in a stream impacted by acid mine drainage. Sci. Total Environ. 347(1-3), 122-130.

Casiot, C., Ujevic, M., Munoz, M., Seidel, J.L., Elbaz-Poulichet, F., 2007. Antimony and arsenic mobility in a creek draining an antimony mine abandoned 85 years ago (upper Orb basin, France). Appl. Geochem. 22(4), 788-798.

Creed, J.T., Brockhoff, C.A., Martin, T.D, 1994. EPA method 200.8, Revision 5.4, Determination of trace elements in waters and wastes by inductively coupled plasma – mass spectrometry. U.S. Environmental Protection Agency.

Davis, J.A., 1922. The Kantishna Region. Alaska Territorial Department of Mines Miscellaneous Report, MR-66-0, p. 85.

Eaton, A.D., Franson, M.A.H., 2005. Standard methods for the examination of water & wastewater. 21st Centennial Edition. Amer Public Health Assn., Washington D.C.

Ebbley Jr., N., Wright, W.S., 1948. Antimony deposits in Alaska. U.S. Bureau of Mines Report of Investigations 4173, p. 41.

Eppinger, R.G., Griggs, P.H., Crock, J.G., Meier, A.L., Sutley, S.J., Theodorakos, P.M., 2000. Environmental-geochemical study of the Slate Creek antimony deposit, Kantishna Hills, Denali National Park and Preserve, Alaska. Studies by the U.S. Geological Survey in Alaska , 2000, U.S Geological Survey Professional Paper 1662.

Ferguson, J.F., Gavis, J., 1972. A review of the arsenic cycle in natural waters. Water Res. 6(11), 1259-1274.

Filella, M., Belzile, N., Chen, Y.-W., 2002. Antimony in the environment: a review focused on natural waters: II. Relevant solution chemistry. Earth Sci. Rev. 59(1-4), 265-285.

Guo, T., DeLaune, R.D., Patrick Jr., W.H., 1997. The influence of sediment redox chemistry on chemically active forms of arsenic, cadmium, chromium, and zinc in estuarine sediment. Environ. Int. 23(3), 305-316.

Gustafsson, J.P., 2005. Visual Mineq version 2.32. KTH, Royal Institute of Technology, Sweden.

Harvey, C.F., Swartz, C.H., Badruzzaman, A.B.M., Keon-Blute, N., Yu, W., Ali, M.A., Jay, J., Beckie, R., Niedan, V., Brabander, D., Oates, P.M., Ashfaque, K.N., Islam, S., Hemond, H.,F. Ahmed, M.F., 2002. Arsenic mobility and groundwater extraction in Bangladesh. Science 298(5598), 1602-1606.

Herbel, M., Fendorf, S., 2006. Biogeochemical processes controlling the speciation and transport of arsenic within iron coated sands. Chem. Geol. 228(1-3), 16-32.

Kuma, K., Katsumoto, A., Kawakami, H., Takatori, F., Matsunaga, K., 1998. Spatial variability of Fe(III) hydroxide solubility in the water column of the northern North Pacific Ocean. Deep Sea Res. Part I: Oceanographic Research Papers 45(1), 91–113.

Langmuir, D., 1997. Aqueous Environmental Geochemistry. Prentice Hall, New Jersey.

Langner, H.W., Inskeep,W.P., 2000. Microbial reduction of arsenate in the presence of ferrihydrite. Environ. Sci. Technol. 34(15), 3131–3136.

Leuz, A.-K., Monch, H., Johnson, C.A., 2006a. Sorption of Sb(III) and Sb(V) to goethite: influence on Sb(III) oxidation and mobilization. Environ. Sci. Technol. 40(23), 7277-7282.

Leuz, A.-K., Hug, S.J., Wehrli, B., Johnson, C.A., 2006b. Iron-mediated oxidation of antimony(III) by oxygen and hydrogen peroxide compared to arsenic(III) oxidation. Environ. Sci. Technol. 40(8), 2565-2571.

Lindberg, R.D., Runnells, D.D., 1984. Ground water redox reactions: an analysis of equilibrium state applied to Eh measurements and geochemical modeling. Science 225(4665), 925-927.

Lingren, W., 1933. Mineral Deposits, 4th ed. McGraw-Hill, New York.

Mitsunobu, S., Harada, T., Takahashi, Y., 2006. Comparison of antimony behavior with that of arsenic under various soil redox conditions. Environ. Sci. Technol. 40(23), 7270–7276.

Moffit, F.H., 1933. The Kantishna district, in: U.S. Geological Survey Staff, Mineral Resources of Alaska, report on investigations in 1930: US Geological Survey Bulletin, 836-D, pp. 301-388.

Mueller, S.H., Goldfarb, R.J., Verplanck, P.L., Trainor, T.P., Sanzolone, R.F., Adams, M., 2010. Surface-water, ground-water, and sediment geochemistry of Epizonal and shear-hosted mineral deposits in the Tintina Gold Province – arsenic and antimony distribution and mobility, in: Gough, L.P., Day, W.C. (Eds.), Chapter G of Recent U.S. Geological Survey Studies in the Tintina Gold Province, Alaska, United States, and Yukon, Canada–Results of a 5-Year Project. Scientific Investigations Report 2007-5289-G.

Nam, S.-H., Yang, C.-Y., An, Y.-J., 2009. Effects of antimony on aquatic organisms (larva and embryo *Oryzias latipes, Moina macrocopa, Simocephalus mixtus,* and *Pseudokirchneriella subcapitata*). Chemosphere 75(7), 889-893.

Nordstrom, D., Alpers, C.N., 1999. Geochemistry of acid mine waters, in: Plumlee G.S., Logsdon, M.J. (Eds.), The Environmental Geochemistry of Mineral Deposits, Part A: Processes, Methods, and Health Issues. Society of Economic Geologists, Reviews in Econ. Geol. 6A, 133-160.

Oremland, R.S., Newman, D.K., Kail, B.W., Stolz, J.F., 2001. Bacterial respiration of arsenate and its significance in the environment, in: Frankenberger Jr., W.T. (Ed.), Environmental Chemistry of Arsenic, Marcel Dekker, New York, pp. 273–296.

Petrone, K.C., Jones, J.B., Hinzman, L.D., Boone, R.D., 2006. Seasonal export of carbon, nitrogen, and major solutes from Alaskan catchments with discontinuous permafrost. J. Geophys. Res. 111, G02020, doi:10.1029/2005JG000055.

Plumlee, G.S., Smith, K.S., Ficklin, W.H., Briggs, P.H., 1992. Geological and geochemical controls on the composition of mine drainages and natural drainages in mineralized areas, v. 1 of Water-rock interaction, Proceedings of the 7th International Symposium on Water-Rock Interaction, Park City, Utah, July 13-18, 1992: Rotterdam, A.A. Balkema, 1, 419-422.

Plumlee, G.S., Smith, K.S., Montour, W.R, Ficklin, W.H., Mosier, E.L., 1999. Geologic controls on the composition of natural waters and mine waters draining diverse mineral-deposit types, in: Filipek L.H., Plumlee, G.S. (Eds.), The Environmental Geochemistry of Mineral Deposits, Part B: Case Studies and Research Topics. Society of Economic Geologists, Reviews in Econ. Geol. 6B, 373-407.

Pokrovsky, O.S., Dupré, B., Schott, J., 2005. Fe-Al-organic colloids control of trace elements in peat soil solutions: results of ultrafiltration and dialysis. Aquat. Geochem. 11(3), 241-278.

Pullin, M., Cabaniss, S.E., 2003. The effects of pH, ionic strength, and iron-fulvic acid interactions on the kinetics of non-photochemical iron transformations. I. Iron(II) oxidation and iron(III) colloid formation. Geochim. Cosmochim. Acta 67(21), 4067-4077.

Roddick-Lanzilotta, A.J., McQuillan, A.J., Craw, D., 2002. Infrared spectroscopic characterisation of arsenate (V) ion adsorption from mine waters, Macraes mine, New Zealand. Appl. Geochem., 17(4), 445-454.

Ryu, J.-H., Gao, S., Dahlgren, R.A., Zierenberg, R.A., 2002. Arsenic distribution, speciation and solubility in shallow groundwater of Owens Dry Lake, California. Geochim. Cosmochim. Acta 66(17), 2981-2994.

Saltikov, C.W., Newman, D.K., 2003. Genetic identification of a respiratory arsenate reductase. Proc. Natl. Acad. Sci. U.S.A. 100 (19), 10983–10988.

Scheinost, A.C., Rossberg, A., Vantelon, D., Xifra, I., Kretzschmar, R., Leuz, A.-K., Funke, H., Johnson, C.A., 2006. Quantitative antimony speciation in shooting-range soils by EXAFS spectroscopy. Geochim. Cosmochim. Acta 70(13), 3299–3312.

Smedley, P.L., Kinniburgh, D.G., 2002. A review of the source, behaviour and distribution of arsenic in natural waters. Appl. Geochem. 17(5), 517-568.

Smith, K.S., Ficklin, W.H., Plumlee, G.S., Meier, A.L., 1992. Metal and arsenic partitioning between water and suspended sediment at mine-drainage sites in diverse geologic settings, in: Kharaka, Y.K., Maest, A.S., (Eds.), Low temperature environments, v. 1 of Water-rock interaction, Proceedings of the 7th International Symposium on Water-Rock Interaction, Park City, Utah, July 13-18, 1992: Rotterdam, A.A. Balkema, 1, 443-447.

Smith, K.S., Ficklin, W.H., Plumlee, G.S., Meier, A.L., 1993. Computer simulations of the influence of suspended iron-rich particulates on trace metal-removal from mine-drainage waters., in: Proceedings of the Mined Land Reclamation Symposium, Billings, Montana., March 21-27, 1993 2, 107-115.

Smith, K.S., 1999. Metal sorption on mineral surfaces: an overview with examples relating to mineral deposits, in Plumlee, G.S., Logsdon, M.J. (Eds.), The Environmental Geochemistry of Mineral Deposits, Part A: Processes, Techniques, and Health Issues. Society of Economic Geologists, Reviews in Econ. Geol. 6A, 161-182.

Stefánsson, A., Arnórsson, S., Sveinbjörnsdóttir, A.E., 2005. Redox reactions and potentials in natural waters at disequilibrium. Chem. Geol. 221(3-4), 289-311.

Stefánsson, A., Arnórsson, S., 2002. Gas pressures and redox reactions in geothermal fluids in Iceland. Chem. Geol. 190(1-4), 251-271.

Stumm, W., Morgan, J.J., 1996. Aquatic Chemistry, 3rd edition. John Wiley and Sons, Inc. New York.

Takahashi, Y., Minamikawa R., Hattori K.H., Kurishima K., Kihou N. & Yuita K,.2004. Arsenic behavior in paddy fields during the cycle of flooded and non-flooded periods. Environ. Sci. Technol. 38(4), 1038-1044.

Tighe, M., Lockwood, P., Wilson, S., 2005. Adsorption of antimony(V) by floodplain soils, amorphous iron(III) hydroxide and humic acid. J. Environ. Monit. 7, 1177-1185.

To, T., Nordstrom, D., Cunningham, K., Ball, J., McCleskey, R., 1999. New method for the direct determination of dissolved Fe(III) concentration in acid mine water. Environ. Sci. Technol. 33(5) 807-813.

Tufano, K.J., Reyes, C., Saltikov, C.W., Fendorf, S., 2008. Reductive processes controlling arsenic retention: revealing the relative importance of iron and arsenic reduction. Environ. Sci. Technol. 42(22), 8283-8289.

Vaughan, D.J., 2006. Arsenic. Elements, 2(2), 71-75.

Vink, B.W., 1996. Stability relations of antimony and arsenic compounds in the light of revised and extended Eh-pH diagrams. Chem. Geol. 130(1-2), 21-30.

Wagman, D.D., Evans, W.H., Parker, V.B., Schumm, R.H., Halow, I., Bailey, S.M., Churney, K.L., Nuttall, R.L., 1982. The NBS Tables of Chemical Thermodynamic Properties: Selected Values for Inorganic and C1 and C2 Organic Substances in SI units. J. Phys. Chem. Ref. Data, 11 (Suppl. 2), 2-79, 2-80.

Weber, F.-A., Hofacker, A.F., Voegelin, A., Kretzschmar, R., 2010. Temperature dependence and coupling of iron and arsenic reduction and release during flooding of a contaminated soil. Environ. Sci. Technol. 44(1), 116-122.

Wilson, S.C., Lockwood, P.V., Ashley, P.M., Tighe, M., 2010. The chemistry and behaviour of antimony in the soil environment with comparisons to arsenic: a critical review. Environ. Pollut. 158(5), 1169-1181.

Zheng, J., Ohata, M., Furuta, N., 2000. Antimony speciation in environmental samples by using high-performance liquid chromatography coupled to inductively coupled plasma mass spectrometry. Anal. Sci. 16(1), 75-80.

Zobrist, J., Dowdle, P.R., Davis, J.A., Oremland, R.S., 2000. Mobilization of arsenite by dissimilatory reduction of adsorbed arsenate. Environ. Sci. Technol. 34(22), 4747–4753.

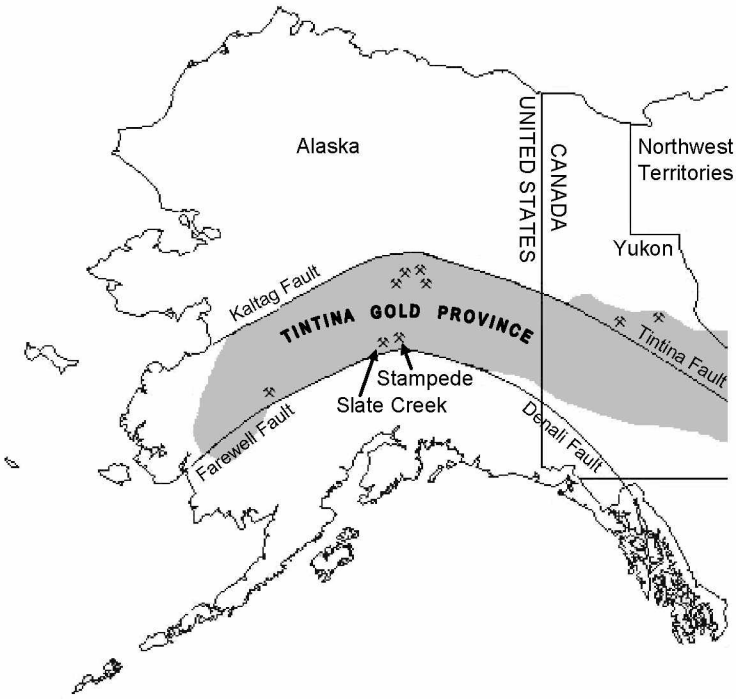

Figure 2.1 Map outlining the Tintina Gold Province (shaded area), major faults, and the Stampede Creek and Slate Creek study areas (modified from Eppinger et al., 2000).

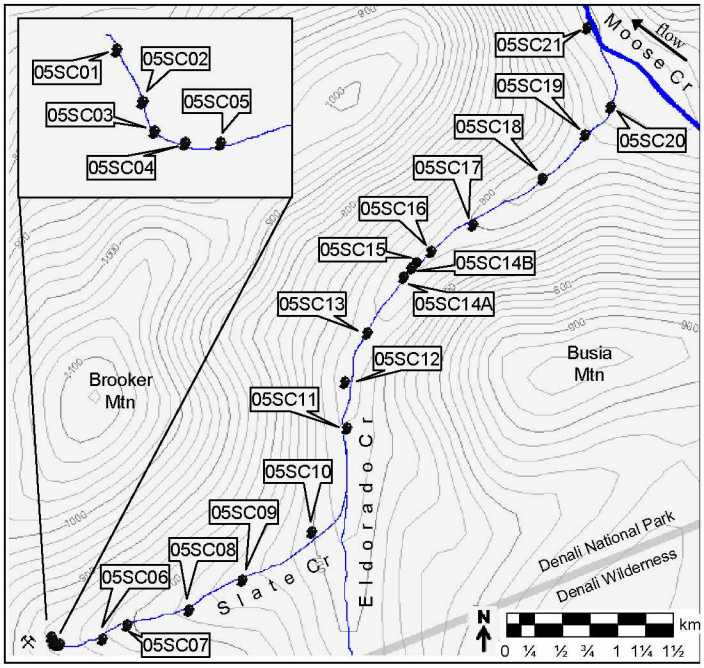

Figure 2.2 Slate Creek (2005) water and bed-sediment sampling locations.

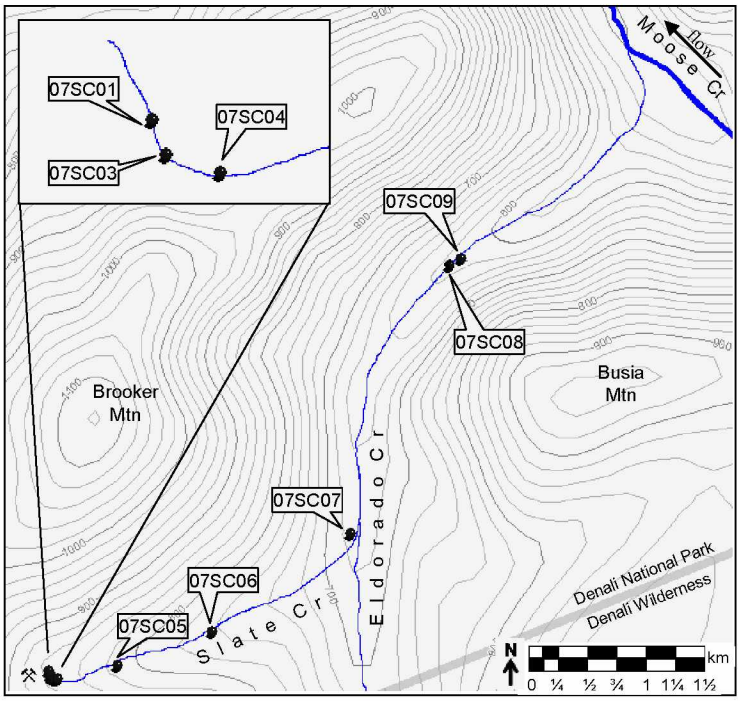

Figure 2.3 Slate Creek (2007) water and bed-sediment sampling locations.

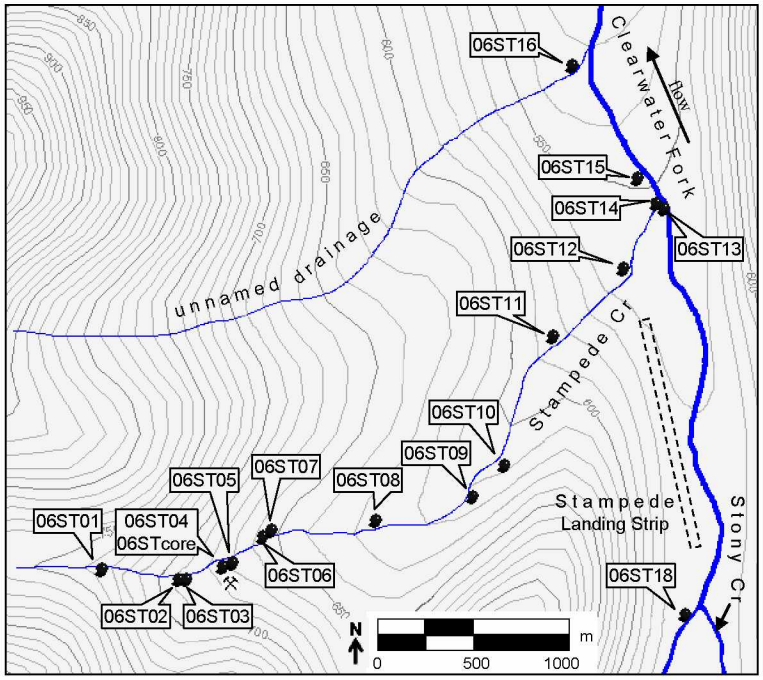

Figure 2.4 Stampede Creek (2006) water and bed-sediment sampling locations.

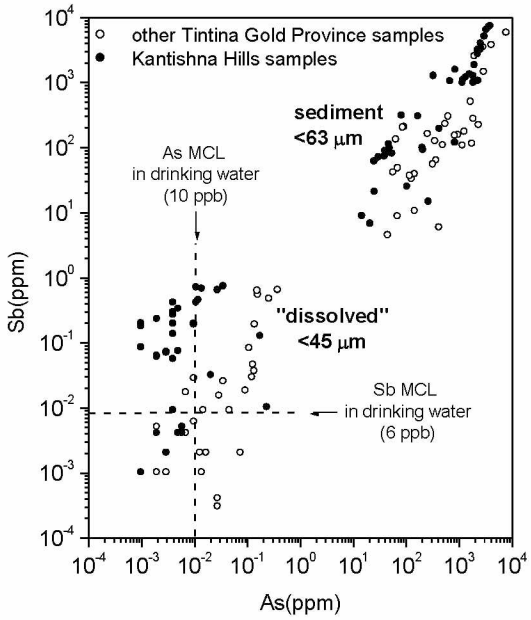

Figure 2.5 Correlation between antimony and arsenic concentrations in water and bed-sediments collected from streams draining legacy mining operations in the Tintina Gold Province (Mueller et al., 2010), including the Kantishna Hills district. Antimony and arsenic concentrations in several water samples exceed EPA MCLs (6 ppb Sb, 10 ppb As) up to two orders of magnitude.

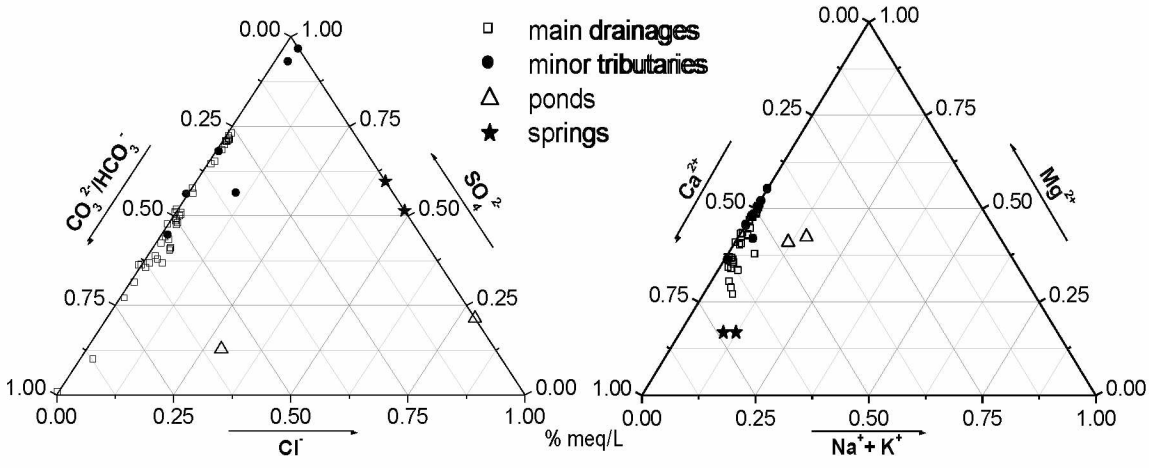

Figure 2.6 Ternary diagrams of water samples from the Kantishna Hills.

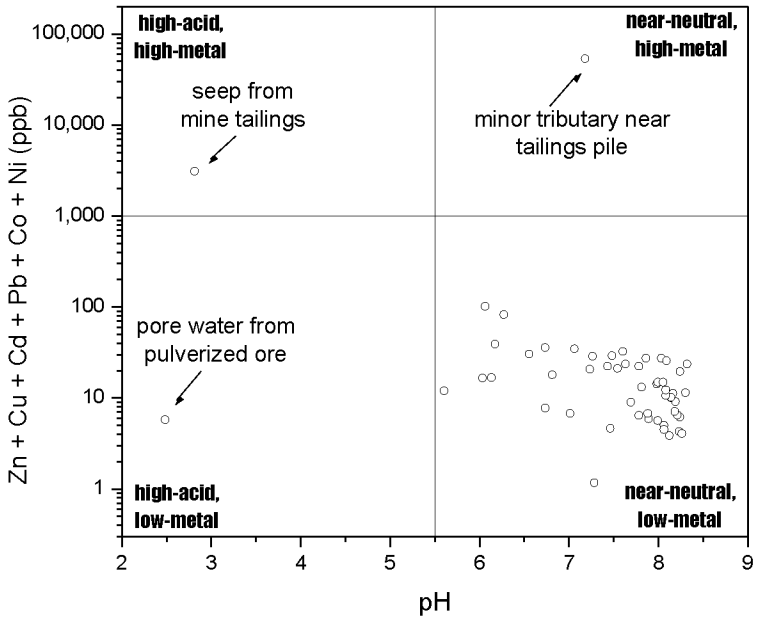

Figure 2.7 Ficklin diagram (after Plumlee et al., 1999) showing the sum of dissolved base metals Zn, Cu, Cd, Pb, Co, and Ni as a function of pH in waters draining legacy antimony mines in the Kantishna Hills. The designated boundaries were proposed by Plumlee et al. (1992) to help classify different drainage compositions.

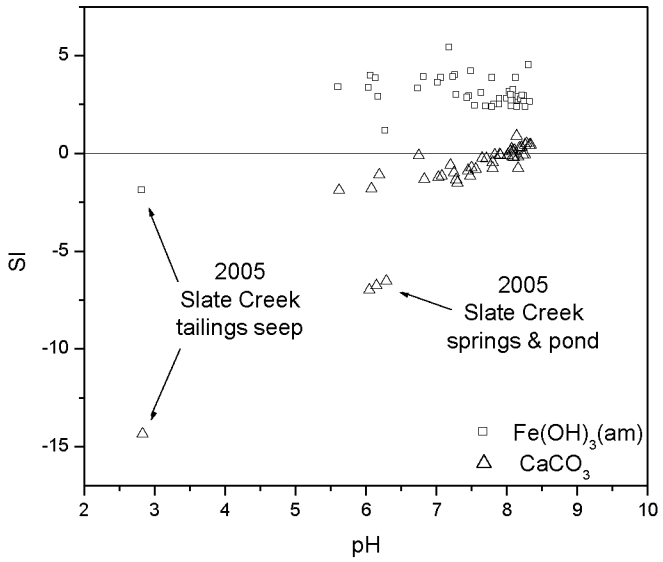

Figure 2.8 Calculated saturation indices for calcite ($CaCO_3$) and amorphous ferrihydrite ($Fe(OH)_3$) as a function of pH for the Kantishna Hills mine-drainage and minor tributary waters.

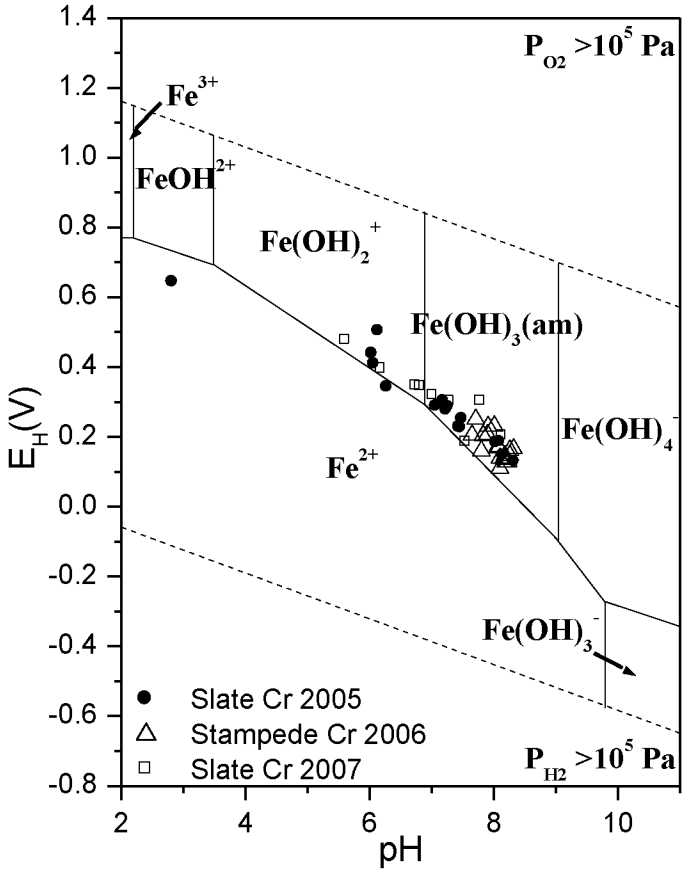

Figure 2.9 E_H-pH diagram showing calculated E_H values based on the Fe^{2+}/Fe^{3+} redox couple. The boundaries show stable phases in a simplified Fe-O_2-H_2O system at dissolved concentrations of 10^{-5} M Fe at 25 °C and 10^5 Pa. The diagram indicates that the majority of waters are in approximate equilibrium with amorphous $Fe(OH)_3$. Thermodynamic data was obtained from Langmuir (1997).

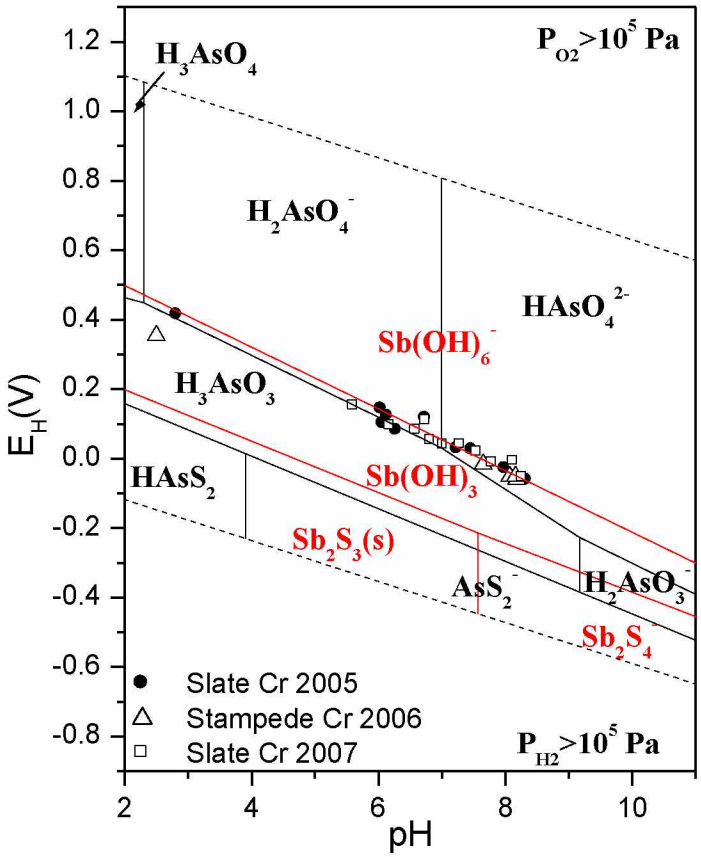

Figure 2.10 E_H-pH diagram showing calculated E_H values based on the As^{3+}/As^{5+} redox couple. The boundaries (black lines) show stable phases in a simplified As-S-H_2O system at dissolved concentrations of 10^{-6} M As and 10^{-2} M S at 25 °C and 10^5 Pa. Stable Sb phases (red lines) for a Sb-S-H_2O system (10^{-8} M Sb and 10^{-3} M S at 25 °C and 10^5 Pa) are over-plotted for theoretical comparison. Arsenic thermodynamic data was obtained from Wagman et al. (1982) and Brookins (1988), and antimony data from Ferguson and Gavis (1972) and Vink (1996).

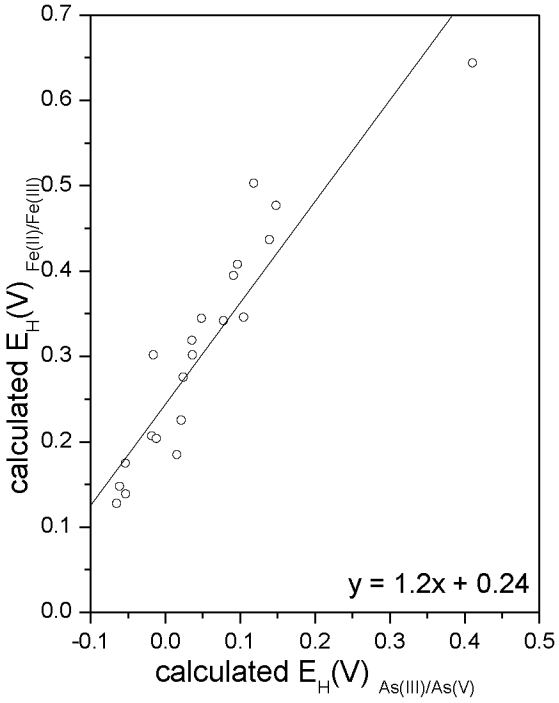

Figure 2.11 A comparison of calculated E_H values based off the As^{3+}/As^{5+} and Fe^{2+}/Fe^{3+} redox couples. Although the figure shows a strong correlation between the potentials, the offset indicates a potential disequilibrium between the redox pairs.

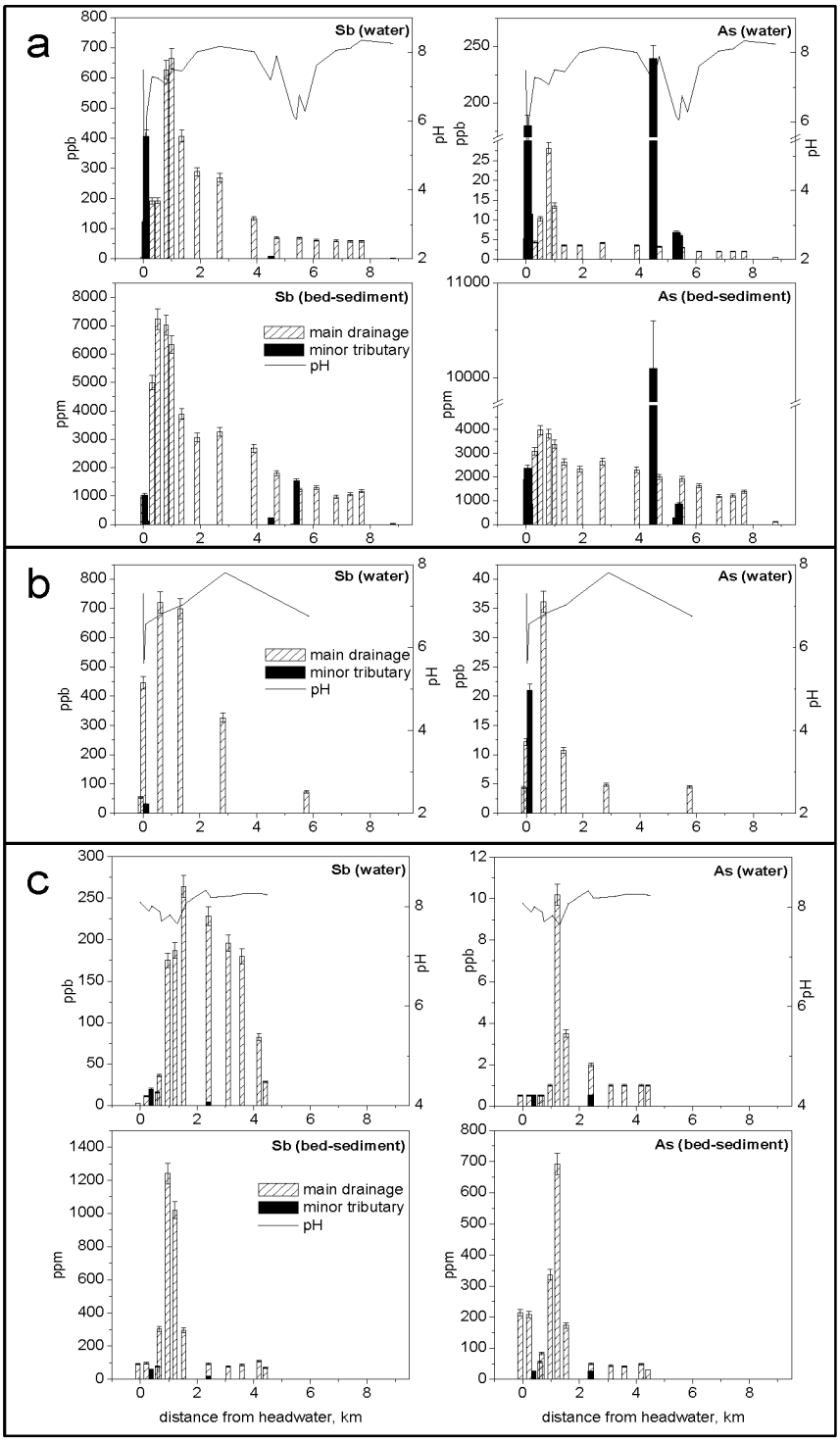

Figure 2.12 Total antimony and arsenic concentrations in water and bed-sediment as a function of distance from headwater in (a) Slate Creek 2005, (b) Slate Creek 2007 (water only), and (c) Stampede Creek 2006 samples. Both main drainage (striped bar) and minor tributaries (solid bar), and corresponding pH (line), are plotted.

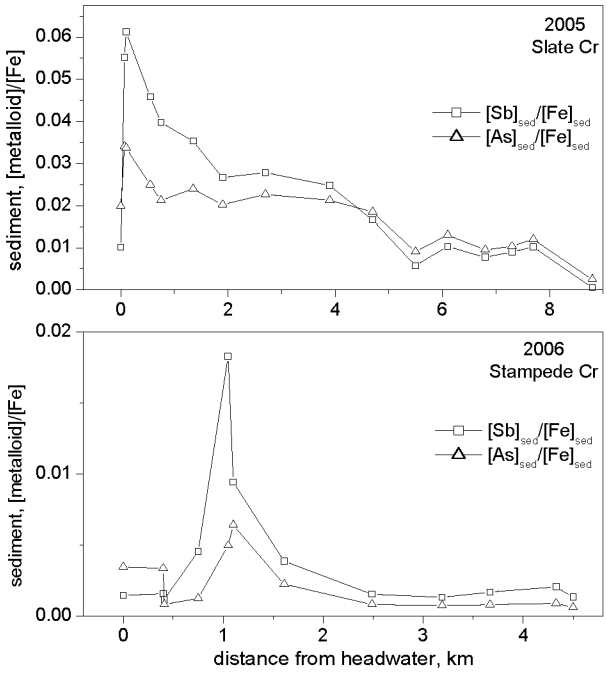

Figure 2.13 The ratios of Sb and As to Fe in sediment with distance from headwater yield similar downstream profiles to total Sb and As sediment concentrations (Figure 2.12), indicating a strong correlation between Sb/As and Fe in bed-sediment.

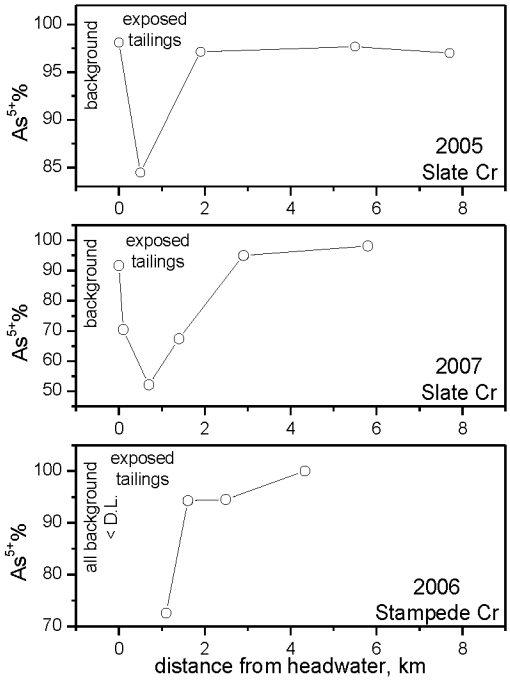

Figure 2.14 Percent of As^{5+} species in main drainage waters as a function of distance from headwater. In all cases, As^{5+} % decreases in the area of exposed mine workings but quickly increases to approximate background levels within 1-3 km from the source.

Table 2.1 Kantishna Hills sample descriptions and *in situ* measurements

Sample ID	Sample type/location	Dist. from headwater km	Cond µS/cm	pH (±0.5)	Temp °C	ORP mV
05SC01	Slate Cr (~background)	0.00	202	7.48	8.8	-
05SC02	tailings seep	0.02	1816	2.83	12.0	-
05SC03	minor tributary	0.04	512	6.08	10.7	-
05SC04	Slate Cr	0.07	210	7.28	9.6	-
05SC05	Slate Cr	0.10	386	7.25	9.0	-
05SC06	Slate Cr	0.55	393	7.08	10.4	-
05SC07	Slate Cr	0.75	388	7.50	10.1	-
05SC08	Slate Cr	1.35	345	7.45	10.3	-
05SC09	Slate Cr	1.90	339	8.00	9.4	-
05SC10	Slate Cr	2.70	354	8.16	9.9	-
05SC11	Slate Cr	3.90	309	8.01	8.1	-
05SC12	tributary near tailings	4.49	2710	7.20	8.1	-
05SC13	Eldorado Cr	4.70	334	7.88	6.2	-
05SC14A	small spring	5.30	2040	6.15	3.3	-
05SC14B	small spring	5.40	2060	6.05	2.8	-
05SC15	Eldorado Cr	5.50	442	6.75	7.1	-
05SC16	pond adjacent to Eldorado	5.70	2980	6.29	12.0	-
05SC17	Eldorado Cr	6.10	471	7.62	7.8	-
05SC18	Eldorado Cr	6.80	494	8.05	8.2	-
05SC19	Eldorado Cr	7.30	498	8.11	9.0	-
05SC20	Eldorado Cr	7.70	499	8.34	9.1	-
05SC21	Moose Cr	8.80	286	8.25	8.6	-
06ST01	Stampede Cr (~background)	0.00	838	8.08	3.5	293
06ST02	Stampede Cr	0.40	881	7.91	3.9	-
06ST03	minor tributary	0.41	727	8.01	3.8	330
06ST04	Stampede Cr	0.69	856	7.90	3.9	334
06STcore	pulverized ore pore water	0.73	-	2.50	-	-
06ST05	Stampede Cr	0.75	901	7.71	3.8	339
06ST06	Stampede Cr	1.05	961	7.83	4.8	328
06ST07	Stampede Cr	1.10	999	7.65	4.5	187
06ST08	Stampede Cr	1.61	1014	8.07	7.0	322
06ST09	minor tributary	2.31	521	8.32	11.5	321
06ST10	Stampede Cr	2.49	945	8.18	8.5	327
06ST11	Stampede Cr	3.19	909	8.21	9.8	335
06ST12	Stampede Cr	3.67	894	8.26	10.3	337
06ST13	Clearwater Cr	-	356	8.26	9.1	318
06ST14	Stampede Cr	4.33	522	8.16	6.6	325
06ST15	Clearwater Cr	4.50	420	8.23	8.4	327
06ST16	unnamed drainage	-	235	7.80	5.1	298
06ST18	Clearwater Cr	-	329	8.20	10.7	312
07SC01	Slate Cr	0.00	237	7.30	4.7	90-100
07SC03	tailings seep	0.04	658	5.62	11.0	158
07SC04	Slate Cr	0.10	360	6.57	6.6	120
07SC05	Slate Cr	0.70	432	6.83	7.6	96
07SC06	Slate Cr	1.40	487	7.03	8.3	101
07SC07	Slate Cr	2.90	432	7.80	7.9	189
07SC08	pond adjacent to Eldorado	5.70	1255	6.19	12.8	228
07SC09	Eldorado Cr	5.75	732	6.75	6.4	124
07EK01	Eureka Cr	-	223	8.14	6.6	155
07MC01	Moose Cr	-	301	8.08	9.0	120
07MC02	Moose Cr	-	345	7.56	9.5	67
07FR01	Friday Cr	-	224	8.28	6.6	168

"-" = not determined

Table 2.2 Major and minor element composition of water samples from Kantishna Hills

Sample ID	Cl^- mg/L (±0.03%)	SO_4^- mg/L (±0.08%)	Alk. as $CaCO_3$ mg/L (±10%)	Na^+ mg/L (±0.72%)	K^+ mg/L (±1.01%)	Mg^{2+} mg/L (±0.42%)	Ca^{2+} mg/L (±0.40%)	Charge Balance (%)
05SC01	1.2	28	73.1	0.83	0.26	11.2	22.4	0
05SC02	25	2004	0	0.5	0.62	52.6	69.3	-55
05SC03	22	171	98.0	0.52	0.42	31.9	59.9	-4
05SC04	1.1	34	71.2	0.97	0.31	11.8	23.4	0
05SC05	2.4	89	114	0.85	0.33	30.2	43.4	5
05SC06	3.4	93	104	0.69	0.37	27.7	44.7	5
05SC07	3.4	99	105	0.67	0.34	27.2	45.4	3
05SC08	2.2	85	90.7	0.72	0.38	24.6	41.1	6
05SC09	2.3	89	85.4	0.8	0.34	24.8	40.4	6
05SC10	2.2	90	93.2	0.96	0.38	26.1	42.0	6
05SC11	2.3	57	104	1.4	0.54	18.2	40.6	4
05SC12	55	2115	90.7	4.9	2.7	245	422	-7
05SC13	2.3	73	101	1.4	0.53	19.1	42.8	2
05SC14A	65	224	0	23.5	2.4	69.1	469	65
05SC14B	100	233	0	25.1	2.4	70.5	463	59
05SC15	5.3	88	138	2.6	0.57	21.0	62.2	2
05SC16	485	203	0	139	5.5	187	355	37
05SC17	8.4	93	148	4	0.77	24.8	73.1	6
05SC18	8.4	104	148	3.6	0.75	26.1	71.0	4
05SC19	8.4	106	150	3.6	0.67	23.0	66.3	-1
05SC20	8.6	110	151	3.9	0.73	26.2	77.1	5
05SC21	3	62	77.9	2.9	0.65	12.2	40.4	3
06ST01	6	331	141	0.86	0.95	51.4	108	-1
06ST02	6	342	154	0.99	1.14	56.5	109	-1
06ST03	3.7	290	144	0.85	1.10	54.0	74.5	-5
06ST04	6	336	157	0.94	1.17	57.9	101	-2
06ST05	7.6	354	151	1.02	1.22	63.9	102	-1
06ST06	6	404	174	1.08	1.26	71.3	103	-4
06ST07	5	429	176	1.19	1.36	76.5	106	-4
06ST08	6	448	192	1.33	1.36	77.9	106	-6
06ST09	3.77	117	155	1.08	1.18	27.5	70.4	2
06ST10	6.2	390	157	1.44	1.34	70.4	99.9	-3
06ST11	6	368	156	1.4	1.27	66.5	97.1	-3
06ST12	6.4	362	180	1.46	1.28	65.2	96.1	-5
06ST13	2.6	88	94.5	5.15	0.85	19.0	42.9	2
06ST14	3.5	175	99.4	0.89	0.77	34.7	57.2	0
06ST15	2.6	118	98.0	3.66	0.77	23.4	46.0	-1
06ST16	<0.20	40	77.8	0.92	0.32	11.8	30.7	3
06ST18	2.4	80	87.1	1.25	0.88	14.9	40.0	-3
07SC01	<0.20	32.5	63.1	0.802	0.088	10.4	20.9	0
07SC03	<0.20	144	125	0.636	0.435	30.0	59.6	0
07SC04	<0.20	<0.50	134	0.759	0.122	15.9	27.4	1
07SC05	<0.20	91.2	93.8	0.697	0.204	21.8	35.3	-2
07SC06	<0.20	97.4	103	0.654	0.238	25.0	40.9	1
07SC07	<0.20	73.1	88.0	0.731	0.276	22.2	35.6	5
07SC08	114	65.9	327	28.8	0.842	54.4	103	-1
07SC09	7.71	29.0	288	8.02	0.567	29.2	89.9	5
07EK01	1.27	172	137	1.02	0.564	32.6	70.0	-1
07MC01	1.61	42.7	79.0	3.68	0.460	7.85	32.4	-2
07MC02	2.62	56.3	94.5	3.71	0.624	10.9	41.3	0
07FR01	1.04	151	160	0.967	1.53	28.2	79.0	0

"-" = not determined

Table 2.3 Ratios of iron and manganese concentrations of 0.2 µm and 0.45 µm-filtered samples to estimate percent colloidal-fraction in water samples.

Sample ID	[Fe] 0.2 µm/ [Fe] 0.45 µm	% colloidal formation	[Mn] 0.2 µm/ [Mn] 0.45 µm	% colloidal formation
06ST01	-	-	0.91	9
06ST03	-	-	1.0	0
06ST05	-	-	0.81	19
06ST07	0.91	9	0.99	1
06ST10	-	-	0.85	15
06ST11	-	-	0.77	23
06ST14	0.99	1	0.97	3
06ST16	0.95	5	0.99	1
06ST17	0.95	5	1.0	0
06ST18	-	-	0.95	5
07SC01	0.97	3	1.0	0
07SC03	0.77	23	1.0	0
07SC04	0.80	20	0.98	2
07SC05	0.79	21	1.0	0
07SC06	0.92	8	1.0	0
07SC07	0.84	16	0.89	11
07SC08	0.77	23	0.93	7
07SC09	0.77	23	0.84	16

"-" = not determined

Table 2.4 Oxidation state of As (determined by LC-ICP-MS) and Fe (determined by UV-Vis) in water samples

Sample ID	Description	As(III) µg/L	As(V) µg/L	[As(III)]/ [As(V)]	Fe(II) mg/L	Fe(III) mg/L	[Fe(II)]/ [Fe(III)]
05SC01	Slate Cr (~background)	<1	5.20	-	0.097	0.018	5.3
05SC02	tailings seep	13.8	165	0.1	50.4	183.9	0.3
05SC03	minor tributary	7.75	2.96	2.6	8.99	4.40	2.0
05SC04	Slate Cr	-	-	-	0.335	0.320	1.0
05SC05	Slate Cr	2.50	8.70	0.3	0.663	0.308	2.1
05SC06	Slate Cr	-	-	-	0.914	0.344	2.7
05SC07	Slate Cr	-	-	-	0.517	0.293	1.8
05SC08	Slate Cr	-	-	-	0.082	0.014	5.7
05SC09	Slate Cr	<1	3.42	-	<0.012	<0.012	-
05SC10	Slate Cr	-	-	-	0.013	0.002	6.0
05SC11	Slate Cr	-	-	-	<0.012	<0.012	-
05SC12	tributary near tailings	-	-	-	27.0	13.1	2.1
05SC13	Eldorado Cr	-	-	-	<0.012	<0.012	-
05SC14A	small spring	3.53	3.05	1.2	3.290	2.99	1.1
05SC14B	small spring	3.05	3.22	0.9	3.40	2.63	1.3
05SC15	Eldorado Cr	<1	2.93	-	-	-	-
05SC16	pond adjacent to Eldorado	3.86	1.74	2.2	0.051	0.004	12.6
05SC18	Eldorado Cr	-	-	-	0.025	0.010	2.7
05SC19	Eldorado Cr	-	-	-	0.015	0.009	1.7
05SC20	Eldorado Cr	<1	1.94	-	<0.012	<0.012	-
06ST01	Stampede Cr (~background)	<1	<1	-	0.019	0.003	7.4
06ST02	Stampede Cr	<1	<1	-	<0.012	0.004	-
06ST03	minor tributary	<1	<1	-	<0.012	0.007	-
06ST04	Stampede Cr	-	-	-	0.015	0.005	3.3
06STcore	pulverized ore pore water	3509	45	78	-	-	-
06ST05	Stampede Cr	<1	<1	-	<0.012	<0.012	-
06ST06	Stampede Cr	-	-	-	0.025	0.005	5.0
06ST07	Stampede Cr	3.49	7.40	0.5	0.339	0.029	11.7
06ST08	Stampede Cr	<1	3.30	-	0.036	0.007	4.9
06ST09	small creek	-	-	-	0.090	0.003	31.9
06ST10	Stampede Cr	<1	1.89	-	0.028	0.004	7.5
06ST11	Stampede Cr	-	-	-	0.020	0.002	8.8
06ST12	Stampede Cr	-	-	-	<0.012	<0.012	-
06ST13	Clearwater Cr	-	-	-	0.012	0.003	3.6
06ST14	Stampede Cr	<1	1.0	-	0.119	0.010	12.5
06ST15	Clearwater Cr	-	-	-	0.038	0.004	9.4
06ST16	unnamed drainage	-	-	-	0.087	0.004	24.4
06ST18	Clearwater Cr	-	-	-	0.018	0.002	8.5
07SC01	Slate Cr	<1	4.01	-	0.034	0.046	0.7
07SC03	tailings seep	8.92	10.2	0.9	3.03	3.74	0.8
07SC04	Slate Cr	2.33	8.61	0.3	-	-	-
07SC05	Slate Cr	15.4	18.8	0.8	0.860	0.876	1.0
07SC06	Slate Cr	2.85	7.20	0.4	0.275	0.261	1.1
07SC07	Slate Cr	<1	4.64	-	0.005	0.086	0.1
07SC08	pond adjacent to Eldorado	4.54	1.53	3.0	0.696	0.276	2.5
07SC09	Eldorado Cr	<1	4.43	-	0.555	0.337	1.6
07EK01	Eureka Cr	<1	3.54	-	<0.012	<0.012	-
07MC01	Moose Cr	<1	<1	-	<0.012	<0.012	-
07MC02	Moose Cr	<1	2.15	-	0.090	0.048	1.9
07FR01	Friday Cr	<1	3.39	-	<0.012	<0.012	-

"-" = not determined

Table 2.5 Total Sb and As concentrations in water and bed-sediment samples

Sample ID	Sample type/location	Dist. from headwater km	Sb_{water} µg/L	$Sb_{sediment}$ mg/kg	As_{water} µg/L	$As_{sediment}$ mg/kg
05SC01	Slate Cr (~background)	0.00	4.18	968	5.3	1,900
05SC02	tailings seep	0.02	124	1,040	180	2,370
05SC03	minor tributary	0.04	407	116	11.4	855
05SC04	Slate Cr	0.07	192	4,990	4.4	3,080
05SC05	Slate Cr	0.10	193	7,230	10.3	3,980
05SC06	Slate Cr	0.55	626	7,020	28.2	3,820
05SC07	Slate Cr	0.75	665	6,330	13.6	3,380
05SC08	Slate Cr	1.35	407	3,890	3.6	2,640
05SC09	Slate Cr	1.90	289	3,070	3.5	2,330
05SC10	Slate Cr	2.70	269	3,260	4.2	2,650
05SC11	Slate Cr	3.90	134	2,680	3.5	2,300
05SC12	tributary near tailings	4.49	9.64	223	239	10,100
05SC13	Eldorado Cr	4.70	70.6	1,800	3.2	2,000
05SC14A	small spring	5.30	<0.3	14.4	6.9	272
05SC14B	small spring	5.40	<0.3	1,530	6.1	875
05SC15	Eldorado Cr	5.50	68.9	1,220	3	1,920
05SC16	pond adjacent to Eldorado	5.70	3.72	189	5.9	435
05SC17	Eldorado Cr	6.10	62.2	1,300	2	1,640
05SC18	Eldorado Cr	6.80	59.6	972	2	1,190
05SC19	Eldorado Cr	7.30	58.7	1,060	2	1,220
05SC20	Eldorado Cr	7.70	58.8	1,170	2	1,380
05SC21	Moose Cr	8.80	3.38	24.6	<1	107
06ST01	Stampede Cr (~background)	0.00	2.65	90.7	<1	214
06ST02	Stampede Cr	0.40	11.2	97.1	<1	208
06ST03	minor tributary	0.41	19.8	59.8	<1	25.5
06ST04	Stampede Cr	0.69	15.9	78.6	<1	55.7
06STcore	pulverized ore pore water	0.73	55,000	-	3509	-
06ST05	Stampede Cr	0.75	36.3	305	<1	83.9
06ST06	Stampede Cr	1.05	175	1,240	1	336
06ST07	Stampede Cr	1.10	187	1,020	10.2	692
06ST08	Stampede Cr	1.61	264	296	3.5	173
06ST09	minor tributary	2.31	4.55	20.5	<1	25.8
06ST10	Stampede Cr	2.49	228	94.2	2	49.9
06ST11	Stampede Cr	3.19	196	78.6	1	43.8
06ST12	Stampede Cr	3.67	180	87.0	1	41.4
06ST13	Clearwater Cr	-	1.88	8.7	<1	15.0
06ST14	Stampede Cr	4.33	82.7	110	1	48.2
06ST15	Clearwater Cr	4.50	28.5	69.5	<1	31.2
06ST16	unnamed drainage	-	11.7	71.1	<1	39.7
06ST18	Clearwater Cr	-	1.7	6.6	<1	21.5
07SC01	Slate Cr	0.00	54.6	-	4.38	-
07SC03	tailings seep	0.04	31.3	-	21.0	-
07SC04	Slate Cr	0.10	446	-	12.2	-
07SC05	Slate Cr	0.70	720	-	36.1	-
07SC06	Slate Cr	1.40	699	-	10.7	-
07SC07	Slate Cr	2.90	327	-	4.88	-
07SC08	pond adjacent to Eldorado	5.70	4.56	-	6.17	-
07SC09	Eldorado Cr	5.75	73.2	-	4.52	-
07EK01	Eureka Cr	-	8.94	-	3.54	-
07MC01	Moose Cr	-	0.632	-	0.647	-
07MC02	Moose Cr	-	4.27	-	2.20	-
07FR01	Friday Cr	-	1.66	-	3.49	-

"-" = not determined

Chapter 3: Conclusions and Future Work

This project provides a detailed hydrogeochemical analysis of water and sediment samples associated with streams draining legacy antimony (Sb) mines in the Kantishna Hills District, Denali National Park and Preserve, Alaska. Of particular interest in this study was the use of Sb, As and Fe speciation analysis of waters to provide correlation of oxidation state with transport characteristics along a downstream profile. The results show that there is a good correlation between redox chemistry and transport which leads to an improved understanding of the mobility and chemical fate of Sb and As in these systems. This further provides information essential to predicting water quality impacts on streams draining Sb and As-rich mineralized areas within the Kantishna District, and more broadly, to areas with similar types of mineralization and hydrogeochemical characteristics.

One of the major findings in this work is that the aqueous Sb and As concentrations are largely limited by dilution and by adsorption and (co)precipitation processes. The predominant form of Sb in water is the oxidized Sb^{5+} species, whereas As is detected in mixed As^{3+}/As^{5+} oxidation states. The differences in oxidation state play an important role in mineral surface sorption tendencies and subsequent downstream mobility. Water quality of both the Slate Creek and Stampede Creek is compromised several kilometers downstream from the source, with maximum Sb and As concentrations exceeding respective EPA MCLs by two orders of magnitude. Although Sb concentrations remain above the MCL throughout the length of the Slate Creek/Eldorado Creek and Stampede Creek drainages, Sb (and As) concentrations decrease (largely through dilution) to below the MCL after merging with larger drainage systems. However, the localized Sb and As contamination within these drainages may be of ecological concern several kilometers downstream from the mining-effected areas.

Detectable concentrations of sulfide were expected to be found in at least the pond and spring samples due to the strong $H_2S(g)$ odor omitting from the waters during collection. Sulfide was also expected in the tailings seep due to its proximity to the source. It may be possible that detectable S^{2-} concentrations were present but oxidized to

SO_4^{2-} prior to analysis. Furthermore, the lack of S^{2-} in the samples may be due to analytical error. The silver/sulfide electrode voltage readings of standard solutions during analysis were half that of standards analyzed during a test run the day prior. Standard solutions were remade and the electrode was maintained, but the readings remained the same and the analytical run was completed. The sulfide analytical method and noted problems are described in further detail in Appendix A.6. Given my analytical S^{2-} results may be in question, future work should include additional sampling of waters and sediment impacted by the oxidative weathering of sulfide-rich mineralization to further investigate the redox processes of sulfur in similar subarctic aquatic environments. Of particular interest may be comparing oxidation states of S and As in a downstream profile to examine possible correlations between these elements in aerobic aqueous environments.

Figure 3.1 shows a simplified conceptual pathway for the oxidative weathering of primary sulfide minerals and the subsequent downstream mobilization and/or sequestration of associated Sb and As. Additional research is required to improve the understanding of these pathway processes. Minimizing the amount of colloidal material in aqueous samples is important to avoiding the over-estimation of "dissolved" Fe (and Mn, Al), as well as metal(loid)s that sorb to the colloidal material. Future work could focus on a series of ultrafiltration experiments to further examine the degree in which Sb and As is associated with colloids in the water column. Furthermore, determining the chemical identity of these colloids and the speciation of Sb and As associated with them would provide valuable information toward understanding the behavior of Sb and As in natural aquatic environments.

Future work should also include exploring different sample preservatives suitable for aqueous Sb speciation analysis via LC-ICP-MS. The reason for this is two-fold. First, as mentioned in Chapter 2 (and further described in Appendix A.1), HCl spectrally interferes with the elution of the Sb^{3+} species. Significant effort was put towards minimizing the affects of HCl (through modifying the mobile phase constituents, concentrations and pH, as well as LC flow rate and injection volume), but a detection

limit lower than ~ 5 ppb was not obtained. Achieving a lower Sb^{3+} detection limit is essential to the characterization of Sb in natural aquatic environments. Secondly, the absence of Sb^{3+} in water samples in this study may suggest that HCl is not an adequate preservative for the Sb^{3+}/ Sb^{5+} redox couple.

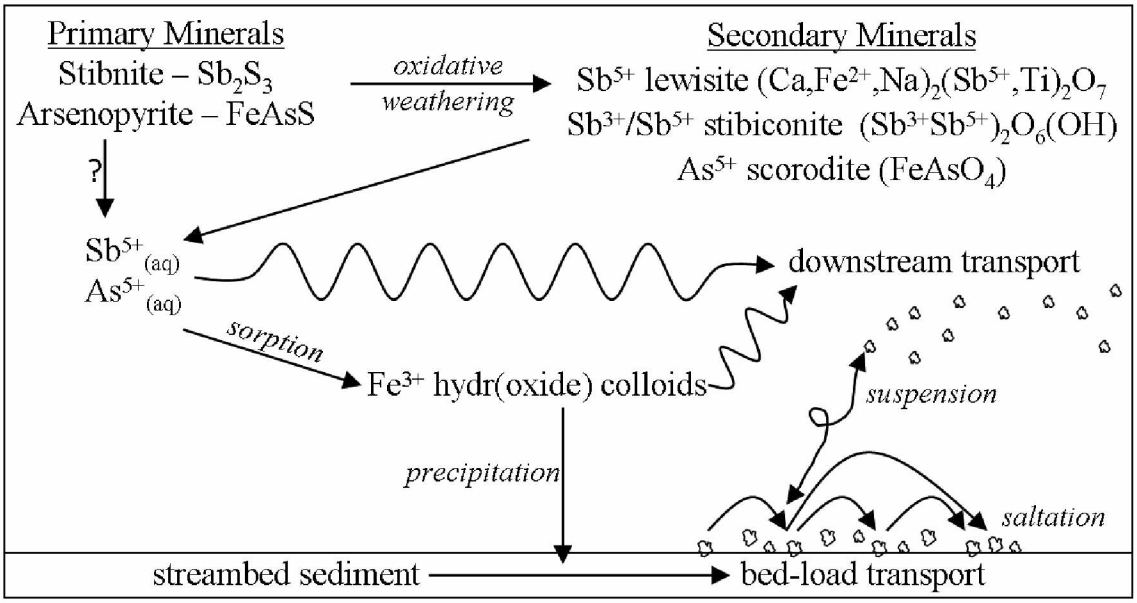

Figure 3.1 Simplified conceptual pathways for the oxidative weathering of primary sulfide minerals and subsequent downstream mobilization and/or sequestration of associated antimony and arsenic.

Appendix

A.1 Antimony Speciation Analysis of HCl-Preserved Samples by Liquid Chromatography-Inductively Coupled Plasma-Mass Spectrometry and Standard Preparation

There were several challenges associated with the method development for Sb speciation of HCl field-preserved samples by liquid chromatography (LC) coupled to an inductively coupled plasma-mass spectrometer (ICP-MS). Two of the most notable challenges were addressing the spectral interferences caused by HCl and preparing adequate Sb^{3+} and Sb^{5+} LC standards.

Spectral anomaly caused by HCl and LC analysis optimization

Using HCl as a sample preservative causes a spectral anomaly that interferes with the quantitation of the Sb^{3+} peak. The Sb^{3+} detection limit in LC standards without the addition of HCl is approximately 1 ppb, whereas with the addition of 44 mM HCl (the concentration used in my field samples) increases the detection limit to approximately 5 ppb. Figure A.1 shows a spectral comparison of the injection of a 44 mM HCl solution to that of pure water. The spectral dip, peak and subsequent tailing caused by the addition of HCl occurs approximately at the same retention time as the Sb^{3+} species (~ 210 s).

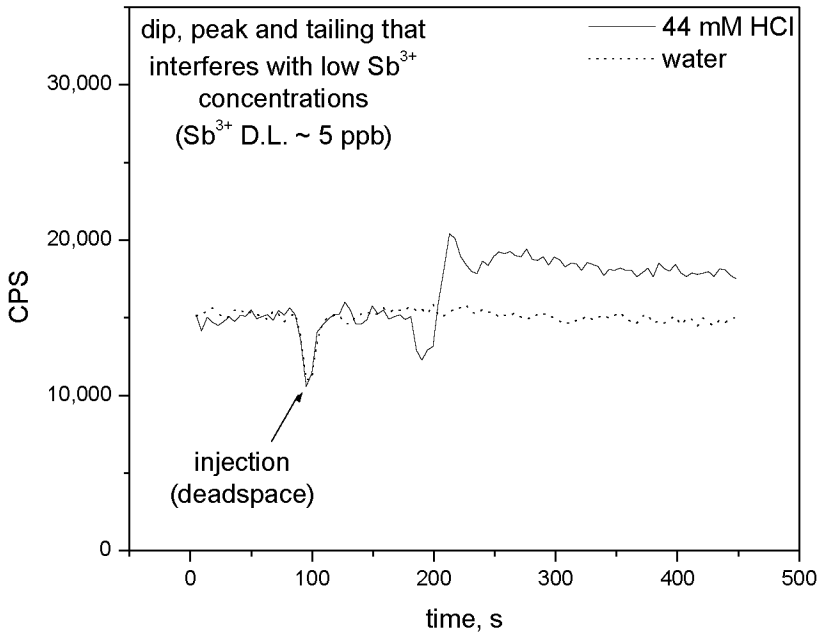

Figure A.l Comparison of chromatograms resulting from the analysis of a 44 mM HCl solution to that of pure water.

Several attempts were made to overcome the affects of the HCl sample preservative through modification of the mobile phase (concentrations and pH), LC flow rate, and varying sample injection volume. Although significant improvements were made on Sb^{3+} and Sb^{5+} peak resolution and overall detection limits throughout the optimization process, the lowest Sb^{3+} detection limit achieved was ~ 5 ppb. The operating conditions for the LC, including the optimized mobile phase (modified from Zheng et al., 2000), are presented in Table A.1. General operating settings for the ICP-MS are presented in Table A.2.

Table A.1 Operating conditions for the LC instrument

instrument	Agilent 1100
column	Arsenic Speciation column (Agilent G3154-65001)
mobile phase	12 mM Na_2EDTA 2 mM phthalic acid 3 vol% methanol 1 M NaOH (for pH adjustment) pH 4.5 50 ppb In (internal standard)
flow rate	1.0 mL/min
injection volume	100 µL
column temperature	ambient

Table A.2 Operating settings for the ICP-MS instrument

instrument	Agilent 7500ce
all tuning parameters	tune as required for stable and maximum counts
data acquisition mode	time resolved analysis
integration time	0.5 s
isotopes monitored	^{121}Sb, ^{123}Sb, ^{115}In
total analysis time	600 s

LC standard preparation

Preparing LC standards of pure Sb^{3+} or Sb^{5+} oxidation state is desirable but not essential to adequately quantify sample data. The concentration of each peak (species) in the standard can be determined from the ratio of the peak areas and the total Sb results from the ICP-MS.

Antimony(III) standards were prepared using $SbCl_3(s)$ or $Sb_2O_3(s)$. Preparing a stock solution of specific concentration was difficult due to the low solubility of both compounds (there was always solid still present in solution even when preparing solutions at concentrations orders of magnitude below the theoretical solubility constants). Heating the solution to aid is dissolution significantly increased the amount of Sb^{5+}, so applying heat was avoided. The purest Sb^{3+} standards were achieved by placing the desired amount of solid in deoxygenated water in an amber bottle and storing it in the refrigerator for up to one month. Filtered aliquots of the stock solution were diluted with deoxygenated water and the concentrations were determined by ICP-MS.

A chromatogram of a Sb standard prepared from $SbCl_3$ in 44 mM HCl solution is shown in Figure A.2.

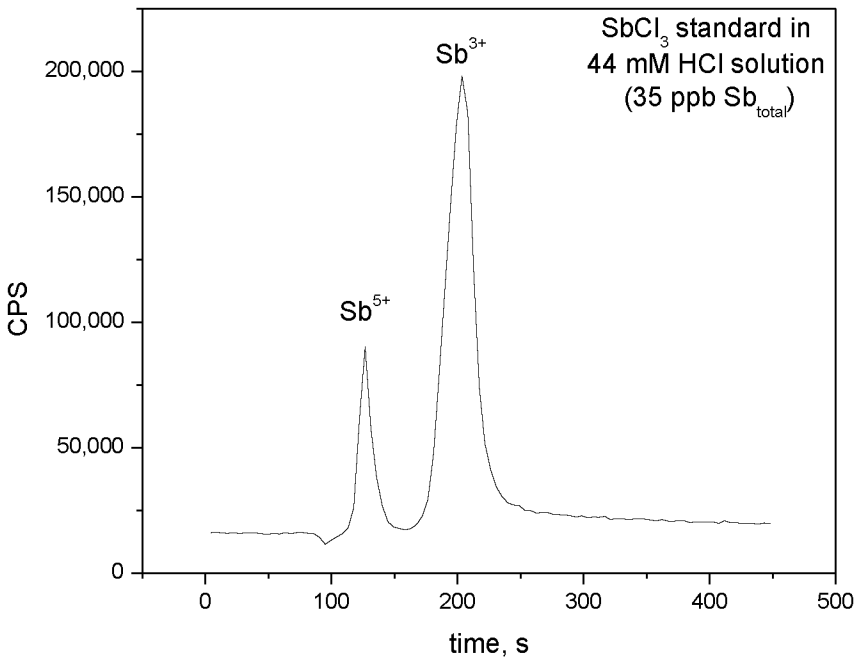

Figure A.2 Chromatogram resulting from the analysis of a $SbCl_3$ standard in 44 mM HCl solution.

Antimony(V) standards were prepared using $KSb(OH)_6$(s), $SbCl_5$(l) or Sb_2O_5(s). Of the three compounds, $KSb(OH)_6$ was preferred as it fully dissolved (with aide of a hot plate) and was effectively pure Sb^{5+} (or more correctly, Sb^{3+} was below the HCl-imposed detection limit of ~ 5 ppb). $KSb(OH)_6$ (potassium pyroantimonate) can also be purchased in solution to negate the dissolution step. Figure A.3 shows a chromatogram of a Sb standard prepared from $KSb(OH)_6$ in 44 mM HCl solution.

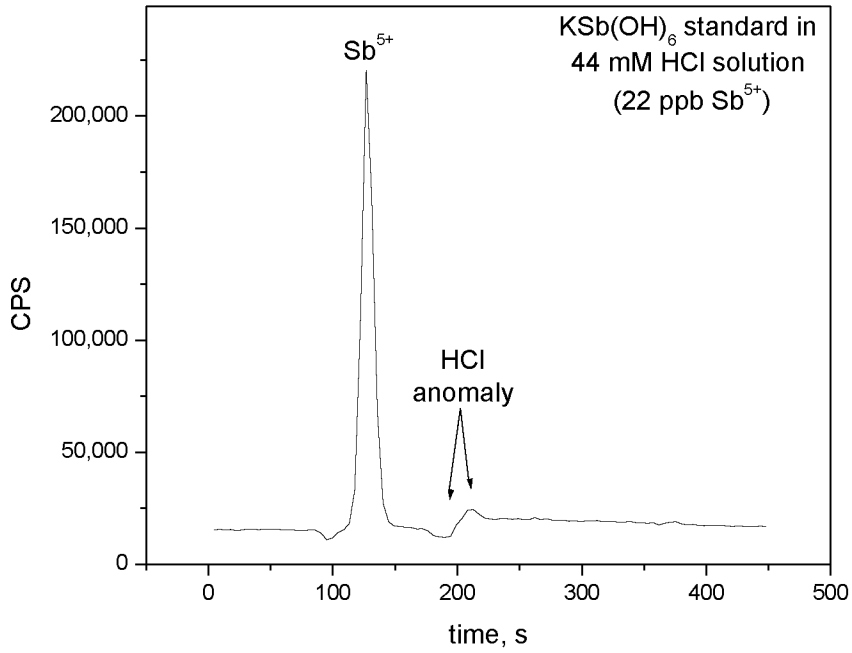

Figure A.3 Chromatogram resulting from the analysis of a $KSb(OH)_6$ standard in 44 mM HCl solution.

Preparation of Sb^{5+} standards from $SbCl_5(l)$ must be done in a fume hood. ***Mixing the $SbCl_5$ liquid with water leads to a violent exothermic reaction.*** Add $SbCl_5$ drop-wise; do not pour. Standards prepared from Sb_2O_5 can be done, but it is challenging and time consuming to get the solid to dissolve.

A.2 LC-ICP-MS Operation Tips, Cautions and Troubleshooting

In order to operate the LC pump and injection sequences WITHOUT the ICP-MS turned on (for flushing/rinsing purposes), the LC remote cord must be disconnected from the back of the ICP-MS. Otherwise, the LC will not operate.

LC pump and column care

- Before hooking up the column, flush mobile phase (or pure water) through the lines and collect it in a waste receptacle for a couple minutes. This will avoid depositing any solids that may have formed in the tubing (from evaporation) onto your column, or running someone else's mobile phase through your column.
- Double check the LC pump speed before hooking up your column. The LC pump speed can be increased to make flushing the lines go faster, however, be sure to **decrease the pump speed to a safe operating speed/pressure for your column**, or it will become damaged.
- It is best to condition a column by pumping mobile phase through the column for a couple hours before beginning analysis, particularly if a different mobile phase (different pH or concentrations, etc.) is being used than the last time. Collect the effluent in a waste receptacle.
- Avoid pump air-lock. If the LC has not been operated in a while, the fluid in the tubing may have evaporated. If the pump does not start taking up mobile phase within the 10 seconds or so of turning the pump on, it is likely air-locked. Continued pump operation without mobile phase present (for lubrication) will damage the pump. The tubing must be primed with fluid before continuing. This can be done with a syringe.
    - If fluid can be seen through the clear tubing but the pump is still not taking up fluid, an air bubble is likely lodged in the glass mobile phase inlet filter. Carefully tapping the filter (do not break) will encourage the air bubble to travel up through the line, allowing fluid to travel.

- The rate of evaporation in the lines can be decreased if the glass mobile phase inlet filter is stored in a bottle of water in between uses.

ICP-MS care, settings, and tuning for LC

- **Turn the ICP-MS peristaltic pump up to at least 0.35 rps** (for a LC pump setting of 1 mL/min) so that the spray chamber does not fill with mobile phase. The plasma torch will shut down if fluid collects in the spray chamber (and it can damage the torch shield).
- Add an internal standard (20-50 ppb) to the mobile phase to aid in tuning the ICP for LC needs. Determine that you are getting adequate counts of your internal standard. Tune the ICP as necessary.

Improving LC analytical performance and speed

- Keep the tubing as short as possible between the column and ICP nebulizer to minimize peak spreading.
- Add 2-3 vol. % methanol to mobile phase to improve sensitivity (proven effective for Sb and As speciation analysis).
- Set the autosampler to "prefetch" sample vials. This prompts the autosampler to fetch a vial while a previous sample is moving still moving through the column. This leads to a faster injection cycle.
- Select the "overlapped injection mode" for a faster injection cycle.

Avoiding cross-contamination and troubleshooting

- Analyze a couple blank samples at the beginning of every run to verify the column or instrument is not contaminated.
- Program the LC autosampler to perform a "needle wash" in between every standard and sample. This will prompt the autosampler to grab a vial from a designated location in the sample tray and inject a cleaning solution (while also rinsing the outside of the needle). This rinse solution (e.g., 2-5% HNO_3) will be

flushed through the needle seat and into the injection valve, but will be directed to the drain off the injection valve rather than being pushed onto the column. Make certain that the **rinse vial is uncapped** so the needle isn't continually contaminated from contact with a septum. Change out the rinse vial with fresh solution periodically (~ every 30 samples).

- If cross-contamination between samples is suspected (carry-over from the sample before), increase the analysis time or rinse time, or analyze blank samples in between samples of known high concentration.
- If contamination still persists after increasing rinse times and/or is present in pure water injections, determine if the contamination is coming from the column or the instrument. Remove the column and perform another water injection. If the contamination disappears, then the contamination is obviously associated with the column itself. Depending on the level of contamination, the column may need flushed with mobile phase or pure water for several hours (also see "passivating procedure" below). This should be done with the ICP off to conserve argon gas. Double check calculations used to make standards and sample dilutions. (If using the arsenic speciation column, it is safe to run a 3% methanol solution through the column to aid in decontamination.)
- If contamination is still present with the column removed, then the contamination likely lies somewhere within the injection or drain system. Perform the following sequence of decontamination efforts:
    - Perform another couple of water injections to verify that fluid is coming out of the drain that is connected to the injection valve. There will not be a lot of volume discharging, but you should see a few drops emerge from the drain tubing. If not, the tubing is plugged up with solids and the effluent is backing up into the injection valve. (Solids may form in the drain if adequate rinsing is not performed after analysis of concentrated standards and samples! When in doubt – rinse!) Replace the tubing and make several rinse injections to see if the problem is fixed. If not, then the

injection valve may need taken apart and the parts cleaned or replace. *But first attempt the following troubleshooting steps first.*

- Clean the needle seat and the needle with 5-10% HNO_3 with cotton swabs, followed by a water rinse. The needle seat and the needle can also be removed and flushed more thoroughly with the acid through a syringe. See if that fixed it.
- Perform a "passivating procedure" (as direct by Agilent), which is a more aggressive rinsing sequence. You must follow all the steps of the sequence and verify that you end with a neutral pH or run risk of damaging LC parts. **Do NOT connect the column or ICP-MS.** Direct all effluent to a waste receptacle. Pump the following fluids through the LC system at 5 mL/min and make periodic injections of the corresponding fluids, followed by several water injections.
    1. H_2O flush (20 minutes)
    2. Isopropyl alcohol flush (15 min)
    3. H_2O flush (15 min)
    4. 37.8% (6 M) HNO_3 flush (30 min)
    5. H_2O flush until effluent reaches ~ pH 7 (this step has taken me ~1.5 hrs)
- If contamination is still present, you may need to look into replacing parts. Also visit the following Agilent website. It contains several helpful links on LC topics.

http://www.chem.agilent.com/en-US/Support/FAQs/LC/Hardware/LC-MS/Pages/CategorizedFAQs.aspx

A.3 Cation Program for Ion Chromatography

Pressure.LowerLimit =		200 [psi]
	Pressure.UpperLimit =	3000 [psi]
	%A.Equate =	"%A"
	CR_TC =	On
	LoadPosition	
	Data_Collection_Rate =	5.0 [Hz]
	CellTemperature.Nominal =	30.0 [°C]
	ColumnTemperature.Nominal =	30.0 [°C]
	Suppressor_Type =	CSRS_4mm
	; Pump_ECD.H2SO4 =	0.0
	; Pump_ECD.MSA =	20.0
	; Pump_ECD.Other eluent =	0.0
	; Pump_ECD.Recommended Current =	66
	Suppressor_Current =	66 [mA]
-3.500	Pump_ECD_Relay_1.Closed	Duration=138.00
	Concentration =	20.00 [mM]
	Flow =	1.00 [mL/min]
0.000	Concentration =	10.00 [mM]
	Flow =	1.00 [mL/min]
	ECD_1.AcqOn	
	Pump_InjectValve.InjectPosition	Duration=30.00
	Concentration =	10.00 [mM]
	Flow =	1.00 [mL/min]
2.500	Concentration =	3.00 [mM]
25.000	Concentration =	3.00 [mM]
26.500	Concentration =	15.00 [mM]
	Flow =	1.50 [mL/min]
50.000	ECD_1.AcqOff	
	Concentration =	15.00 [mM]
	Flow =	1.50 [mL/min]
	End	

A.4 Anion Program for Ion Chromatography

CR_TC =	On	
	Pressure.UpperLimit =	3000 [psi]
	%A.Equate =	"%A"
	Data_Collection_Rate =	5.0 [Hz]
	CellTemperature =	30.0 [°C]
	ColumnTemperature =	30.0 [°C]
	Suppressor_Type =	ASRS_4mm
	; Pump_ECD.Carbonate =	0.0
	; Pump_ECD.Bicarbonate =	0.0
	; Pump_ECD.Hydroxide =	20.0
	; Pump_ECD.Tetraborate =	0.0
	; Pump_ECD.Other eluent =	0.0
	; Pump_ECD.Recommended Current =	50
	Suppressor_Current =	80 [mA]
	Flow =	1.00 [mL/min]
-2.500	Pump_ECD_Relay_1.Closed	Duration=0.10
	Pressure.LowerLimit =	200
	Pressure.UpperLimit =	3000
	%A.Equate =	"%A"
	LoadPosition	
	Concentration =	0.50 [mM]
	Curve =	5
0.000	Autozero	
	Pump_InjectValve.InjectPosition	Duration=200.00
	ECD_1.AcqOn	
2.000	Pump_ECD_Relay_1.Open	
	Pump_ECD_Relay_1.State	Open
3.000	Concentration =	0.50 [mM]
	Curve =	5
12.000	Concentration =	12.00 [mM]
	Curve =	5
35.000	Concentration =	50.00 [mM]
	Curve =	5
36.000	Concentration =	0.50 [mM]
	Curve =	5
36.000	ECD_1.AcqOff	
	End	

A.5 Alkalinity Titration

Modified from A. D. Eaton, L. S. Clesceri, E. W. Rice, A. E. Greenberg and M. A.H. Franson. Standard Methods for Examination of Water and Wastewater, 21st edition, Amer Public Health Assn, 2005, p. 2-27 – 2-29

Apparatus

1. pH meter with a combination electrode
2. Burette 25 mL
3. Microburette 5 or 10 mL
4. Stirring plate, stir bars
5. Beaker 150-200 mL

Reagents

0.0200 N H_2SO_4 – dilute commercially available stock solution

DI H_2O

Na_2CO_3 0.05 N - Dry Na_2CO_3 at 250 ^oC for 4 hours, cool in desiccator. Weigh 1.325 g of Na_2CO_3 and dilute to 500 mL with DI H_2O and stir. Do not keep for more than 1 week. Buffer solutions for pH meter calibration.

Procedure

Prepare check standards of Na_2CO_3 by diluting stock solution.

mL stock diluted to 1 L	mg alk/L as $CaCO_3$
4.0	10
19.98	50

Calibrate the pH meter.

All solutions and samples should be at room temperature.

Titrate 100 mL of sample or check standard with 0.0200N H_2SO_4 using regular burette and 5 mL microburette (for fine adjustments). The stirring action should be vigorous enough near the end of titration to break the surface to allow rapid equilibrium

of CO_2 between the solution and atmosphere. Stop the titration at exact pH of 4.5 and record volume.

Calculation:

$$Alk_{total}, mg\,CaCO_3 / L = ml(titrant) \times 10$$

if the normality of H_2SO_4 solution is different than 0.02 N:

$$Alk_{total}, mg\,CaCO_3 / L = \frac{A \times N \times 50{,}000}{ml(sample)}$$

A – mL standard acid used

N – normality of standard acid

For alkalinities less than 20 mg/l: titrate with 0.0200 N H_2SO_4 and stop the titration in the range of pH 4.3 to 4.7, record the volume acid used and exact pH. Carefully add more titrant using microburette to reduce the pH exactly 0.30 pH unit and again record the volume.

Calculation:

$$Alk_{total}, mgCaCO_3 / L = \frac{(2B - C) \times N \times 50{,}000}{ml(sample)}$$

B – mL titrant used to the first recorded pH

C – total mL titrant to reach pH 0.3 unit lower

N – normality of H_2SO_4 acid

A.6 Ion-Selective Electrode Method for Sulfide Analysis

Retrieved from Standard methods for the examination of water and wastewater, 21 ed., 2005; edited by Eaton A.D., Clesceri L.S., Rise E.W. and Greenberg A.E.
Orion Silver/Sulfide electrode instruction manual.

(Note: I potentially had electrode problems during analysis. The voltage readings of my standards during my practice run were similar to voltages obtained by someone else (Anastasia Ilgen) for standards of equivalent concentrations. The next morning (during my 'real' experimental run), the voltage readings of my standards were nearly half as the night before. (For example, a standard of ~ 9 ppm had a reading of -755 mV initially and then was -447 mV the following day.) I remade the standards, but the voltage readings were the same as the initial standards made the evening before. I followed electrode maintenance steps per the electrode instruction manual with no change in performance. Despite this, I carried on with the experiment. Sulfide was not detected in any sample above the method detection limit. The electrode gave consistent voltage readings for check standards throughout the experiment.)
Detection level: 0.032 mg/L ($1x10^{-6}$M) – 100 mg/L

Apparatus

1. Silver/sulfide electrode
2. Double junction reference electrode
3. Electrode polishing strips
4. pH-mater with millivolt scale, capable of 0.1-mV resolution
5. Electrochemical cell: Make suitable cell from a 150 mL beaker and a sheet of rigid plastic (PVC or acrylic) with holes drilled to allow insertion of the electrodes and a tube for flushing the headspace with nitrogen
6. Gas dispersion tube: Use to deaerate water for preparing reagents and standards
7. Magnetic stirrer and stirring bar

Reagents

Alkaline antioxidant reagent (AAR)

In a 1 L volumetric flask add:

~600 mL deaerated reagent water

80 g NaOH

35 g ascorbic acid

67 g Na_2H_2EDTA

Swirl to dissolve and dilute to 1 L.

The color of resulting solution should be from colorless to yellow. Store in a tightly capped brown glass bottle. Discard when solution becomes brown.

Lead perchlorate, 0.1 M

In 100 mL reagent water, dissolve

4.60 g $Pb(ClO_4)_2 \cdot 3H_2O$

(see further instructions below)

Sulfide stock solution, 130 mg/L

Use sodium sulfide nonahydrate ($Na_2S \cdot 9H_2O$) crystals

Use degassed water (Ar or N_2)

(see further instructions below)

Standardize $Pb(ClO_4)_2$ by titrating with Na_2H_2EDTA

$$2Pb(ClO_4)_2 \cdot 3H_2O + Na_2H_2EDTA \rightarrow Pb_2EDTA + Na_2H_2(ClO_4)_4 + 6H_2O$$

[Note: Put a known amount of moles of Na_2H_2EDTA in a flask; titrate with lead perchlorate solution to the end point; # of moles of $2Pb(ClO_4)_2 \cdot 3H_2O$ = 2 x # of moles of + Na_2H_2EDTA; concentration of lead perchlorate = # of moles/volume of the solution used.]

Make 0.1 M Na_2H_2EDTA solution. Dissolve 37.225 g Na_2H_2EDTA in a 1,000 mL volumetric flask with DI water, heat up a little bit. If have difficulties dissolving

add a small amount of NaOH. Filter the solution. This solution needs to be normalized by titration with $CaCO_3$.

Make a standard $CaCO_3$ solution. Use dried $CaCO_3$ (dry in an oven at 250 °C for at least 2 hours, cool in a desiccator). Weight 0.250 g in a beaker, add ~25 mL of DI water, and add dilute HCl drop wise, until dissolved. Add another 2 drops. Transfer to 250 mL volumetric flask.

Make a pH 10 buffer solution. Dissolve 16.9 g ammonium chloride (NH_4Cl) in 143 mL conc ammonium hydroxide (NH_4OH).

Make the indicators. Dissolve 0.05 g Eriochrome Black T in 10 g triethanolamine. Dissolve 0.05 g xylenol orange in 10 mL DI water.

Pipet 50-mL aliquots of the standard $CaCO_3$ solution into three or four 250-mL Erlenmeyer flasks. Add 7-8 mL of pH 10 buffer to the first sample, 15 mL of DI water, and 3 drops of Eriochrome Black T and titrate immediately with Na_2H_2EDTA solution until the light red solution turns a light sky blue. Repeat for the replicates.

Titrations must be performed quickly because ammonia will evaporate and thus the pH of the solution will change.

Calculate the molarity of the Na_2H_2EDTA from the volume of Na_2H_2EDTA used in the titration of each aliquot.

$CaCO3 + Na_2H_2EDTA \rightarrow CaEDTA + Na_2CO_3$

$$C_{Na2\,H\,2EDTA} = \frac{V_{CaCO3} \times [CaCO_3]}{V_{EDTA}}$$

The results for the replicates should be very close, if not – repeat titration.

Titrating procedure for $Pb(ClO_4)_2$ standardization with known concentration Na_2H_2EDTA solution.

$2Pb(ClO_4)_2 \cdot 3H_2O \times XylOr + Na_2H_2EDTA \rightarrow Pb_2EDTA + Na_2H_2(ClO_4)_4 + 6H_2O +$ Xyl.Or. Use spectrophotometer to detect the end point of titration.

Prepare 10-15 50 mL beakers. Put 2 mL of ~0.1 M $Pb(ClO_4)_2$ in each, add 1 mL of Xylenol orange, and 30 mL of DI water. Titrate with Na_2H_2EDTA solution until color starts to change from red-purple to yellow, to each subsequent sample add 0.1 mL more Na_2H_2EDTA.

When it seems that color of each subsequent sample does not change anymore, add 2 mL extra to the last sample (over titrate).

Prepare 2 end members - one with 2 mL of Pb solution, 30 mL of H_2O and 1 mL of Xyl.Or., another end member - 2 mL Na_2H_2EDTA solution, 1 mL Xylenol orange and 30 mL H_2O. Measure the absorbance spectra using spectrophotometer, record the absorbance at 578 nm.

As soon as absorbance is approximately equal to the blank Na_2H_2EDTA, it is the end point.

Calculate the $Pb(ClO_4)_2$ solution concentration:

$$C_{Pb(ClO4)2} = \frac{V_{EDTA} \times [EDTA]}{0.002L}$$

Preparing sulfide stock solution, 130 mg/L

Use sodium sulfide nonahydrate ($Na_2S \cdot 9H_2O$) crystals

Use degassed water (Ar or N_2)

Preferably remove single crystals of $Na_2S \cdot 9H_2O$ from reagent bottle with nonmetallic tweezers; quickly rinse in degassed reagent water. Blot crystal dry with tissue, than rapidly transfer to a tared, stoppered weighing bottle containing 5 – 10 mL degassed reagent water. Repeat procedure until desired amount of sodium sulfide is in weighing bottle. Avoid excess agitation and mixing of the solution with atmospheric oxygen. Add the rest of the water. (3.75 g $Na_2S \cdot 9H_2O$ diluted to a final volume of 500 mL will give a stock solution of which 1 mL = 1.00 mg S^{2-}). Standardize the solution using iodometric method or ***titration with 0.1M $Pb(ClO_4)_2$.***

Iodometric method *(for standardizing S^{2-} stock solution)*:

Standard iodine solution, 0.0250 N: Dissolve 20 to 25 g KI in a little water and add 3.2 g iodine. After iodine has dissolved, dilute to 1,000 mL and standardize against 0.0250 N $Na_2S_2O_3$, using starch solution as indicator.

Standard sodium thiosulfate solution, 0.0250 N: Dissolve 6.205 g of $Na_2S_2O_3 \cdot 5H_2O$ in distilled water. Add 1.5 mL 6N NaOH or 0.4 g solid NaOH and dilute to 1,000 mL. Standardize with bi-iodate ($KH(IO_3)_2$) solution.

Starch solution: Dissolve 2 g laboratory-grade soluble starch and 0.2 g salicylic acid, as a preservative, in 100 mL hot distilled water.

Hydrochloric acid, HCl, 6N

Measure from a burette into a 500 mL flask an amount of iodine solution estimated to be in excess over the amount of sulfide present. Add distilled water, if necessary, to bring volume to about 20 mL. Add 2 mL 6N HCl. Pipet 200 mL sample into flask, discharging sample under solution surface. If iodine color disappears, add more iodine until color remains. Back-titrate with $Na_2S_2O_3$

solution, adding a few drops of starch solution as end point is approached, and continuing until blue color disappears.

Calculation:

One milliliter 0.0250N iodine solution reacts with 0.4 mg S^{2-}:

$$mgS^{2-} / L = \frac{[(A \times B) - (C \times D)] \times 16000}{mL(sample)}$$

A = mL iodine solution

B = normality of iodine solution

C = mL $Na_2S_2O_3$

D = normality of $Na_2S_2O_3$ solution

0.1M $Pb(ClO_4)_2$ titration (*for standardizing the S^{2-} stock solution*)

Pipet 50 mL sulfide stock solution into the electrochemical cell. Insert Ag/S electrode and reference electrode and read initial potential. Titrate with 0.1 M $Pb(ClO_4)_2$. Let electrode potential stabilize and record potential after each addition. Locate equivalence point: 1. as the end point is approached, add smaller and equal increments (0.1 or 0.2 mL) at longer intervals, so that the exact end point can be determined; 2. plot a differential titration curve if the exact end point cannot be determined by inspecting the data. Plot change in instrument reading for equal increments of $Pb(ClO_4)_2$ against volume of $Pb(ClO_4)_2$ added, using average of burette readings before and after each addition:

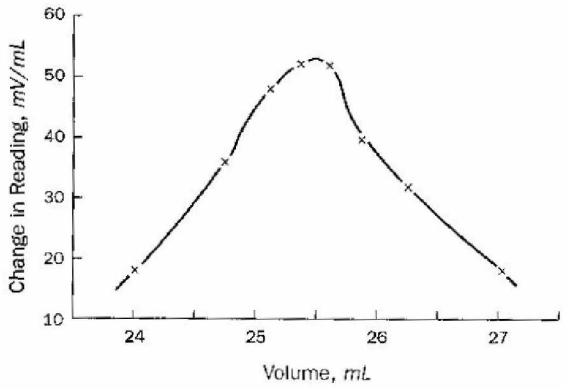

Figure A.4 Change in potential reading during titration with $Pb(ClO_4)_2$

Calculate the function F_1 for points before the equivalence point

$$F_1 = (V_0 + V) \times 10^{E/m}$$

V_o = volume of stock solution, mL

V = titrant volume, mL

E = potential, Mv

M = slope of calibration curve, mV/log unit.

Plot F_1 as a function of titrant volume. Extrapolate to find the intersection with the x-axis; that is, the equivalence point. Calculate sulfide concentration in the stock solution from:

$$C = \frac{V_{eq}[Pb]}{V_0}$$

C = sulfide concentration, mg/L

Veq = equivalence volume

[Pb] = concentration of Pb in titrant, mg/L

Vo = volume of stock solution, mL

Store stock solution in a tightly capped bottle for 1 week or less.

Store in a fume hood!

Prepare sulfide standards daily by serial dilution of stock. Add AAR and 1 M $Zn(C_2H_3O_2)_2$ solutions to 100 mL volumetric flasks. Add sulfide solutions and dilute to volume with DRW (or DASW). Refer to table A.3 for volumes:

Table A.3 Sulfide standard solutions

Dilution	*Alkaline Antioxidant Reagent mL*	*Sulfide solution*	*Sulfide solution mL*	*1M Zink Acetate mL*
1:10	45	Stock	10	0.15
1:100	50	Stock	1	0.15
1:1 000	45	1:100	10	0.14
1:10 000	50	1:100	1	0.15

Prepare at least one standard with a concentration less than the lowest sample concentration.

Sulfide analysis procedure

Check electrode performance and calibrate daily. Check electrode potential in a sulfide standard every 2 hours. The procedure depends on the sulfide concentration and the time between sample collection and sulfide determination. If the total sulfide concentration is greater than 0.03 mg/L and the time delay is only a few minutes, sulfide can be determined directly. Otherwise, precipitate ZnS, let it settle. Then decant as much supernatant as possible without loss of precipitate. Refill bottle with distilled water, shake to resuspend the precipitate and quickly withdraw a sample. If interfering substances (thiosulfate, sulfite and organic compounds) are present in high concentration, settle, decant, and refill a second time.

- Check electrode performance: Pipet 50 mL AAR, 50 mL DWR, and 1 mL sulfide stock solution into the measurement cell. Place Ag/S and reference electrodes in the solution and read potential. Add 10 mL stock solution and read potential. The change in potential should be -28±2 mV. If it is not, follow the troubleshooting procedure in the electrode manual.

- Calibration: Place electrodes in the most dilute standard but use calibration standards that bracket the sulfide concentrations in the samples. Record potential when the rate of change is less than 0.3 mV/min. (This may take up to 30 min for very low sulfide concentrations, i.e., less than 0.03 mg/L.) Rinse electrodes, blot dry with a tissue, and read potential of the next highest standard. For a meter that can be calibrated directly in concentration, follow manufacturer's directions. For other meters, plot potential as a function of the logarithm (base 10) of the sulfide concentration. For potentials in the linear range, calculate the slope and intercept of the linear portion of the calibration plot.

Sulfide determination by comparison with calibration curve, with ZnS precipitation: Place filter with ZnS precipitate in a 150 mL beaker containing a stir bar. Wash sample bottle with 50 mL AAR and 20 mL DRW and pour the washings into the beaker. Stir to dissolve precipitate. Remove filter with forceps while rinsing it into the beaker with a minimum amount of DRW. Quantitatively transfer to a 100 mL volumetric flask and dilute to mark with DRW. Pour into the electrochemical cell and place the electrodes in the solution. Measure potential: record potential when the rate of change is less than 0.3 mV/min. Read sulfide concentration from the calibration curve. Alternatively, for potentials in the linear range, calculate the sulfide concentration from:

$$S_{tot} = 10^{\frac{E-b}{m}}$$

E = electrode potential

B and m are the intercept and slope of the calibration curve. For a meter that can be calibrated directly in concentration, follow the manufacturer's directions.

Sulfide determination by standard addition with or without ZnS precipitate: Measure the Ag/S-ISE electrode potential as in c. Add sulfide stock solution and measure potential again. Calculate sulfide concentration as follows:

$$C_o = \frac{fC_s}{(1+f)10^{\frac{Es-Eo}{m}} - 1}$$

Co and Cs = sulfide concentrations in sample and known addition

Eo and Es = potentials measured for sample and known addition

m = slope of calibration curve (approximately 28 mV/logS^{2-})

f = ratio of known addition volume to sample volume

Sulfide determination by titration, with ZnS precipitation: Filter the sample. Place filter with ZnS precipitate in a 150 mL beaker containing a stir bar. Wash sample bottle with 50 mL AAR and 20 mL DRW and pour the washings into the beaker. Stir to dissolve precipitate. Remove filter with forceps while rinsing it into the beaker with a minimum amount of DRW. Quantitatively transfer to a 100 mL volumetric flask and dilute to mark with DRW. Pour into the electrochemical cell and place the electrodes in the solution. Titrate with lead perchlorate solution. The concentration of the lead perchlorate solution should be ~10-20 times as concentrated as sulfide concentration in the sample. Use standardized 0.1 M lead perchlorate solution to make up the needed concentration. Use the same procedure as for standardizing the sulfide stock solution. The minimum sulfide concentration for determination by titration is 0.3 mg/L (10^{-5} M)

Table A.4 Reagents for sulfide ion-selective analysis

Chemical	**Amount, concentration**
NaOH	80 g
ascorbic acid	35 g
Na_2H_2EDTA	67 g
$Na_2S{\cdot}9H_2O$ crystals	3.75 g
$Pb(ClO_4)_2{\cdot}3H_2O$	4.60 g
$Zn(C_2H_3O_2)_2{\cdot}2H_2O$	~110 g 1 M solution
Ar or N_2 gas	
KI	20 to 25 g
I_2	3.2 g
$Na_2S_2O_3{\cdot}5H_2O$	6.205 g (0.0250 N)
Starch, laboratory-grade	2 g
$KH(IO_3)_2$	
Salicylic acid	0.2 g
$CaCO_3$	~ 1 g
NH_4Cl	~ 20 g
NH_4OH, conc.	~ 150 mL
Eriochrome Black T	0.05 g
Triethanolamine	10 g
Xylenol orange	0.05 g
HCl	6N

A.7 Sample Locations and Complete Analytical Data Tables

The Global Positioning System (GPS) coordinates, sample descriptions, and *in situ* measurements associated with each sample location are provided in Table A.5. The remaining tables (Tables A.6 through A.14) in this appendix are complete tables of analytical data (unless already presented in Chapter 2) and are provided for reference.

Table A.5 Kantishna Hills sample descriptions, locations and *in situ* measurements

Sample ID	Sample type/location	Dist. from headwater (km)	Latitude (NAD27AK)	Longitude (NAD27AK)	Cond µS/cm	pH	T °C	ORP mV
05SC01	Slate Cr (~bkgd)	0.00	63.48229	-151.07211	202	7.48	8.8	-
05SC02	tailings seep	0.02	63.48194	-151.07170	1816	2.83	12.0	-
05SC03	minor tributary	0.04	63.48174	-151.07152	512	6.08	10.7	-
05SC04	Slate Cr	0.07	63.48166	-151.07106	210	7.28	9.6	-
05SC05	Slate Cr	0.10	63.48166	-151.07051	386	7.25	9.0	-
05SC06	Slate Cr	0.55	63.48173	-151.06209	393	7.08	10.4	-
05SC07	Slate Cr	0.75	63.48263	-151.05811	388	7.50	10.1	-
05SC08	Slate Cr	1.35	63.48439	-151.04726	345	7.45	10.3	-
05SC09	Slate Cr	1.90	63.48680	-151.03754	339	8.00	9.4	-
05SC10	Slate Cr	2.70	63.49068	-151.02502	354	8.16	9.9	-
05SC11	Slate Cr	3.90	63.49900	-151.01881	309	8.01	8.1	-
05SC12	tributary near tailings	4.49	63.50268	-151.01915	2710	7.20	8.1	-
05SC13	Eldorado Cr	4.70	63.50666	-151.01517	334	7.88	6.2	-
05SC14A	small spring	5.30	63.51112	-151.00856	2040	6.15	3.3	-
05SC14B	small spring	5.40	63.51112	-151.00856	2060	6.05	2.8	-
05SC15	Eldorado Cr	5.50	63.51191	-151.00706	442	6.75	7.1	-
05SC16	pond adjacent to Eldorado	5.70	63.51315	-151.00360	2980	6.29	12.0	-
05SC17	Eldorado Cr	6.10	63.51505	-150.99380	471	7.62	7.8	-
05SC18	Eldorado Cr	6.80	63.51903	-150.98360	494	8.05	8.2	-
05SC19	Eldorado Cr	7.30	63.52254	-150.97591	498	8.11	9.0	-
05SC20	Eldorado Cr	7.70	63.52474	-150.97130	499	8.34	9.1	-
05SC21	Moose Cr	8.80	63.52992	-150.96660	286	8.25	8.6	-
06ST01	Stampede Cr (~bkgd)	0.00	63.74156	-150.38647	838	8.08	3.5	293
06ST02	Stampede Cr	0.40	63.74110	-150.37843	881	7.91	3.9	-
06ST03	minor tributary	0.41	63.74110	-150.37762	727	8.01	3.8	330
06ST04	Stampede Cr	0.69	63.74166	-150.37367	856	7.90	3.9	334
06STcore	pulverized ore pore water	0.73	63.74166	-150.37367	-	2.50	-	-
06ST05	Stampede Cr	0.75	63.74183	-150.37262	901	7.71	3.8	339
06ST06	Stampede Cr	1.05	63.74306	-150.36943	961	7.83	4.8	328
06ST07	Stampede Cr	1.10	63.74340	-150.36855	999	7.65	4.5	187
06ST08	Stampede Cr	1.61	63.74387	-150.35741	1014	8.07	7.0	322
06ST09	minor tributary	2.31	63.74503	-150.34612	521	8.32	11.5	321
06ST10	Stampede Cr	2.49	63.74646	-150.34384	945	8.18	8.5	327
06ST11	Stampede Cr	3.19	63.75250	-150.33865	909	8.21	9.8	335
06ST12	Stampede Cr	3.67	63.75571	-150.33115	894	8.26	10.3	337
06ST13	Clearwater Cr	-	63.75996	-150.32440	356	8.26	9.1	318
06ST14	Stampede Cr	4.33	63.76022	-150.32520	522	8.16	6.6	325
06ST15	Clearwater Cr	4.50	63.76175	-150.32570	420	8.23	8.4	327
06ST16	unnamed drainage	-	63.77009	-150.33885	235	7.80	5.1	298
06ST17	Stampede Cr	3.19	63.75250	-150.33865	494	8.1	7.1	334
06ST18	Clearwater Cr	-	63.73885	-150.32790	329	8.20	10.7	312
07SC01	Slate Cr	0.00	63.48208	-151.07211	237	7.30	4.7	90
07SC03	tailings seep	0.04	63.48194	-151.07170	658	5.62	11.0	158
07SC04	Slate Cr	0.10	estimated[1]	estimated[1]	360	6.57	6.6	120
07SC05	Slate Cr	0.70	estimated[1]	estimated[1]	432	6.83	7.6	96
07SC06	Slate Cr	1.40	estimated[1]	estimated[1]	487	7.03	8.3	101
07SC07	Slate Cr	2.90	estimated[1]	estimated[1]	432	7.80	7.9	189
07SC08	pond adjacent to Eldorado	5.70	63.51315	-151.00360	1255	6.19	12.8	228
07SC09	Eldorado Cr	5.75	estimated[1]	estimated[1]	732	6.75	6.4	124
07EK01	Eureka Cr	-	estimated[1]	estimated[1]	223	8.14	6.6	155
07MC01	Moose Cr	-	estimated[1]	estimated[1]	301	8.08	9.0	120
07MC02	Moose Cr	-	estimated[1]	estimated[1]	345	7.56	9.5	67
07FR01	Friday Cr	-	estimated[1]	estimated[1]	224	8.28	6.6	168

"-" = not determined

[1] Location on map estimated from site description (due to error associated with the collection of GPS coordinate)

Table A.6 Elemental composition of filtered (0.45 µm) water samples by ICP-MS

Sample ID	Lab	Ag µg/L	Al µg/L	As µg/L	Ba µg/L	Be µg/L	Bi µg/L	Ca mg/L	Cd µg/L	Ce µg/L	Co µg/L	Cr µg/L
05SC01	USGS[1]	<3	3.8	5.3	5.06	<0.05	< 0.2	22.4	<0.02	0.02	0.17	<1
05SC02	USGS[1]	<3	6490	180	9.85	2.2	< 0.2	67.8	5.61	127	266	10.5
05SC03	USGS[1]	<3	9.5	11.4	17.3	<0.05	< 0.2	57.7	0.08	0.05	11.4	1.6
05SC04	USGS[1]	<3	15.5	4.4	4.8	<0.05	< 0.2	22.5	0.03	0.25	1.61	<1
05SC05	USGS[1]	<3	7.6	10.3	6.14	<0.05	< 0.2	39.4	0.02	0.09	1.89	<1
05SC06	USGS[1]	<3	10	28.2	7.79	<0.05	< 0.2	38.9	0.03	0.08	3.33	<1
05SC07	USGS[1]	<3	5.6	13.6	8.08	<0.05	< 0.2	41.7	0.02	0.04	2.89	<1
05SC08	USGS[1]	<3	4	3.6	7.04	<0.05	< 0.2	35.9	0.04	0.02	1.08	<1
05SC09	USGS[1]	<3	5.2	3.5	7.83	<0.05	< 0.2	34.6	0.03	0.02	0.54	<1
05SC10	USGS[1]	<3	4.3	4.2	8.44	<0.05	< 0.2	36.4	0.02	0.01	0.17	<1
05SC11	USGS[1]	<3	3.9	3.5	12	<0.05	< 0.2	37.3	<0.02	< 0.01	0.04	<1
05SC12	USGS[1]	<3	11.3	239	27.9	0.2	< 0.2	459	132	1.36	93.6	<1
05SC13	USGS[1]	<3	3	3.2	13.1	<0.05	< 0.2	40.7	0.07	< 0.01	0.13	<1
05SC14A	USGS[1]	<3	7.1	6.9	44.7	0.2	< 0.2	465	<0.02	1.4	0.76	<1
05SC14B	USGS[1]	<3	6	6.1	47.7	0.3	< 0.2	463	<0.02	1.44	0.59	2.8
05SC15	USGS[1]	<3	9.1	3	14.6	<0.05	< 0.2	59	0.09	0.3	0.62	1.7
05SC16	USGS[1]	<3	3.2	5.9	81.6	<0.05	< 0.2	350	0.75	0.01	2.91	4.7
05SC17	USGS[1]	<3	9.8	2	19.6	<0.05	< 0.2	63.9	0.09	0.17	0.77	<1
05SC18	USGS[1]	<3	12.1	2	19.5	<0.05	< 0.2	65.6	0.08	0.1	0.48	<1
05SC19	USGS[1]	<3	13.7	2	21	<0.05	< 0.2	69.8	0.08	0.08	0.48	<1
05SC20	USGS[1]	<3	15.5	2	20.8	<0.05	< 0.2	68.6	0.07	0.07	0.42	<1
05SC21	USGS[1]	<3	3.1	<1	19.2	<0.05	< 0.2	37.9	<0.02	0.01	0.06	<1
06ST01	USGS[1]	<3	4.1	<1	8.57	<0.05	< 0.2	113	<0.02	0.02	0.24	<1
06ST02	USGS[1]	<3	4.4	<1	8.56	<0.05	< 0.2	113	<0.02	0.02	0.22	<1
06ST03	USGS[1]	<3	10.5	<1	25.8	<0.05	< 0.2	76	0.06	0.06	0.04	<1
06ST04	USGS[1]	<3	5.5	<1	11.8	<0.05	< 0.2	107	<0.02	0.03	0.12	<1
06ST05	USGS[1]	<3	4.8	<1	12	<0.05	< 0.2	108	<0.02	0.03	0.87	<1
06ST06	USGS[1]	<3	4.6	1	11.4	<0.05	< 0.2	108	0.03	0.03	0.56	<1
06ST07	USGS[1]	<3	4.4	10.2	11.3	<0.05	< 0.2	112	0.03	0.03	1.59	<1
06ST08	USGS[1]	<3	3.9	3.5	11.2	<0.05	< 0.2	113	<0.02	0.01	0.39	<1
06ST09	USGS[1]	<3	5.7	<1	18	<0.05	< 0.2	72.2	<0.02	0.07	0.9	<1
06ST10	USGS[1]	<3	4.3	2	13.4	<0.05	< 0.2	110	<0.02	0.02	0.38	<1
06ST11	USGS[1]	<3	3.8	1	15	<0.05	< 0.2	106	<0.02	0.02	0.12	<1
06ST12	USGS[1]	<3	4.4	1	15.6	<0.05	< 0.2	105	<0.02	0.02	0.12	<1
06ST13	USGS[1]	<3	38.9	<1	23.8	<0.05	< 0.2	43.5	0.03	0.52	0.81	<1
06ST14	USGS[1]	<3	29	1	13.8	<0.05	< 0.2	59	<0.02	0.22	0.97	<1
06ST15	USGS[1]	<3	35.8	<1	20.4	<0.05	< 0.2	49	<0.02	0.43	0.36	<1
06ST16	USGS[1]	<3	34.8	<1	11.8	<0.05	< 0.2	31.2	<0.02	0.2	0.73	<1
06ST17	USGS[1]	<3	27.6	1	10.6	<0.05	< 0.2	57.5	<0.02	0.22	0.32	<1
06ST18	USGS[1]	<3	49.7	<1	16.1	<0.05	< 0.2	42.7	0.02	0.67	0.74	<1
07SC01	UAF	0.011	2.9	4.4	3.4	0.016	-	-	0.017	0.017	0.148	0.104
07SC03	UAF	< 0.01	11.1	21.0	17.3	0.060	-	-	0.163	0.063	21.3	0.051
07SC04	UAF	< 0.01	4.7	12.2	4.4	0.005	-	-	0.026	0.035	1.507	0.209
07SC05	UAF	< 0.01	6.5	36.1	6.2	0.016	-	-	0.030	0.063	3.294	0.034
07SC06	UAF	< 0.01	3.7	10.7	7.4	0.010	-	-	0.031	0.026	2.942	0.036
07SC07	UAF	< 0.01	8.9	4.9	5.8	0.001	-	-	0.019	0.029	0.244	0.012
07SC08	UAF	< 0.01	43.5	6.2	19.6	0.063	-	-	0.226	0.635	0.824	0.285
07SC09	UAF	< 0.01	4.4	4.5	16.4	0.042	-	-	0.081	0.111	0.516	0.111
07EK01	UAF	< 0.01	2.7	3.5	13.8	< 0.01	-	-	0.044	< 0.01	0.198	0.020
07MC01	UAF	< 0.01	4.1	0.6	15.5	< 0.01	-	-	0.014	0.018	0.505	0.108
07MC02	UAF	< 0.01	2.6	2.2	19.2	< 0.01	-	-	0.018	0.014	0.474	0.075
07FR01	UAF	< 0.01	3.7	3.5	23.7	< 0.01	-	-	0.230	0.015	0.268	0.078

" - " = not determined

[1] Lamothe, P.J., Meier, A.L., Wilson, S.A., 2002. The determination of forty-four elements in aqueous samples by inductively coupled plasma-mass spectrometry. Chapter H, US Geological Survey Open File Report 02-223-H.

Table A.6 *Continued*

Sample ID	Cs µg/L	Cu µg/L	Dy µg/L	Er µg/L	Eu µg/L	Fe µg/L	Ga µg/L	Gd µg/L	Ge µg/L	Ho µg/L
05SC01	< 0.02	1.4	0.006	< 0.005	< 0.005	112	< 0.05	0.007	< 0.05	< 0.005
05SC02	0.15	289	13.6	7.38	2.79	234000	1.7	15.2	0.36	2.33
05SC03	< 0.02	1.3	0.01	0.007	< 0.005	13300	< 0.05	0.01	< 0.05	< 0.005
05SC04	< 0.02	2.1	0.03	0.02	0.007	598	< 0.05	0.03	< 0.05	0.006
05SC05	< 0.02	1.4	0.01	0.01	< 0.005	931	< 0.05	0.01	< 0.05	< 0.005
05SC06	< 0.02	1.1	0.02	0.01	< 0.005	1420	< 0.05	0.01	< 0.05	< 0.005
05SC07	< 0.02	0.95	0.006	0.006	< 0.005	784	< 0.05	0.008	< 0.05	< 0.005
05SC08	< 0.02	0.95	< 0.005	< 0.005	< 0.005	73	< 0.05	0.005	< 0.05	< 0.005
05SC09	< 0.02	1.1	< 0.005	< 0.005	< 0.005	<50	< 0.05	< 0.005	< 0.05	< 0.005
05SC10	< 0.02	1	< 0.005	< 0.005	< 0.005	<50	< 0.05	< 0.005	< 0.05	< 0.005
05SC11	< 0.02	0.71	< 0.005	< 0.005	< 0.005	<50	< 0.05	< 0.005	< 0.05	< 0.005
05SC12	0.12	5.5	0.31	0.24	0.04	44000	0.3	0.26	0.1	0.075
05SC13	< 0.02	0.6	< 0.005	< 0.005	< 0.005	<50	< 0.05	< 0.005	< 0.05	< 0.005
05SC14A	0.14	1.2	0.73	0.55	0.13	6680	< 0.05	0.6	0.05	0.16
05SC14B	0.15	1.3	0.78	0.58	0.14	6400	< 0.05	0.65	< 0.05	0.16
05SC15	< 0.02	6	0.04	0.02	0.01	142	< 0.05	0.04	< 0.05	0.008
05SC16	0.4	1.8	0.005	0.008	0.007	<50	< 0.05	<0.005	< 0.05	< 0.005
05SC17	< 0.02	5.2	0.02	0.02	0.008	60	< 0.05	0.03	< 0.05	0.006
05SC18	< 0.02	4.6	0.02	0.01	0.005	<50	< 0.05	0.01	< 0.05	< 0.005
05SC19	< 0.02	4	0.01	0.01	0.007	<50	< 0.05	0.01	< 0.05	< 0.005
05SC20	< 0.02	3.7	0.01	0.01	0.005	<50	< 0.05	0.01	< 0.05	< 0.005
05SC21	< 0.02	0.56	0.005	< 0.005	< 0.005	<50	< 0.05	0.007	< 0.05	< 0.005
06ST01	< 0.02	1.6	0.009	0.006	< 0.005	<50	< 0.05	0.006	< 0.05	< 0.005
06ST02	< 0.02	1.8	0.005	< 0.005	< 0.005	<50	< 0.05	< 0.005	< 0.05	< 0.005
06ST03	< 0.02	2.2	0.02	0.01	0.007	<50	< 0.05	0.02	< 0.05	< 0.005
06ST04	< 0.02	1.9	0.007	0.006	< 0.005	<50	< 0.05	0.009	< 0.05	< 0.005
06ST05	< 0.02	2	0.009	0.005	< 0.005	<50	< 0.05	0.007	< 0.05	< 0.005
06ST06	< 0.02	2	0.008	0.006	< 0.005	<50	< 0.05	0.01	< 0.05	< 0.005
06ST07	< 0.02	2.1	0.008	0.005	< 0.005	392	< 0.05	0.01	< 0.05	< 0.005
06ST08	< 0.02	2.3	0.006	< 0.005	< 0.005	<50	< 0.05	< 0.005	< 0.05	< 0.005
06ST09	< 0.02	4	0.02	0.01	0.005	68	< 0.05	0.02	< 0.05	< 0.005
06ST10	< 0.02	2.4	0.007	0.005	< 0.005	<50	< 0.05	0.005	< 0.05	< 0.005
06ST11	< 0.02	2.6	0.005	0.006	< 0.005	<50	< 0.05	0.005	< 0.05	< 0.005
06ST12	< 0.02	9.8	0.006	0.005	< 0.005	<50	< 0.05	0.006	< 0.05	< 0.005
06ST13	< 0.02	1.4	0.05	0.02	0.01	<50	< 0.05	0.055	< 0.05	0.009
06ST14	< 0.02	2.9	0.03	0.02	0.008	120	< 0.05	0.03	< 0.05	0.006
06ST15	< 0.02	1.9	0.04	0.02	0.01	<50	< 0.05	0.051	< 0.05	0.008
06ST16	< 0.02	2.5	0.03	0.02	0.007	95	< 0.05	0.04	< 0.05	0.009
06ST17	< 0.02	3.1	0.04	0.02	0.007	148	< 0.05	0.03	< 0.05	0.007
06ST18	< 0.02	1.5	0.05	0.02	0.01	<50	< 0.05	0.064	< 0.05	0.009
07SC01	-	1.915	0.005	0.003	< 0.01	76.650	-	< 0.01	-	< 0.01
07SC03	-	0.863	0.009	0.008	< 0.01	6818	-	< 0.01	-	< 0.01
07SC04	-	1.566	0.007	0.005	< 0.01	1362	-	< 0.01	-	< 0.01
07SC05	-	1.236	0.012	0.010	< 0.01	1608	-	< 0.01	-	< 0.01
07SC06	-	1.068	0.005	0.004	< 0.01	529	-	< 0.01	-	< 0.01
07SC07	-	1.399	0.007	0.006	< 0.01	100	-	< 0.01	-	< 0.01
07SC08	-	4.213	0.093	0.061	< 0.01	1079	-	0.094	-	< 0.01
07SC09	-	1.427	0.056	0.047	< 0.01	812	-	0.038	-	< 0.01
07EK01	-	1.148	< 0.01	< 0.01	< 0.01	10.99	-	< 0.01	-	< 0.01
07MC01	-	1.118	< 0.01	< 0.01	< 0.01	13.95	-	< 0.01	-	< 0.01
07MC02	-	0.738	< 0.01	< 0.01	< 0.01	108.4	-	< 0.01	-	< 0.01
07FR01	-	2.174	< 0.01	< 0.01	0.010	8.516	-	< 0.01	-	< 0.01

Table A.6 *Continued*

Sample ID	K mg/L	La µg/L	Li µg/L	Lu µg/L	Mg mg/L	Mn µg/L	Mo µg/L	Na mg/L	Nb µg/L	Nd µg/L	Ni µg/L
05SC01	0.3	0.02	< 0.1	< 0.1	10.5	26.1	< 2	0.86	< 0.2	0.02	1.7
05SC02	0.63	54.1	4.6	0.9	50.6	11400	< 2	0.6	0.29	52.7	533
05SC03	0.4	0.06	1.5	< 0.1	29.3	747	< 2	0.54	< 0.2	0.02	32.9
05SC04	0.31	0.12	0.4	< 0.1	10.6	80.4	< 2	0.89	< 0.2	0.1	5
05SC05	0.31	0.06	1.5	< 0.1	25.1	150	< 2	0.78	< 0.2	0.04	6.7
05SC06	0.32	0.08	1	< 0.1	23.5	309	< 2	0.72	< 0.2	0.04	11.8
05SC07	0.35	0.06	1.4	< 0.1	24	285	< 2	0.71	< 0.2	0.02	11
05SC08	0.36	0.04	1.1	< 0.1	19.9	116	< 2	0.7	< 0.2	0.02	6.8
05SC09	0.35	0.03	0.8	< 0.1	20.4	58	< 2	0.78	< 0.2	0.02	4.7
05SC10	0.38	0.02	1.1	< 0.1	21.4	20.4	< 2	0.86	< 0.2	< 0.01	3.4
05SC11	0.49	0.01	1.3	< 0.1	15.8	4.6	< 2	1.37	< 0.2	< 0.01	1.8
05SC12	2.84	3.32	15.4	< 0.1	256	17000	< 2	5.06	< 0.2	0.51	150
05SC13	0.48	0.01	1.4	< 0.1	16.9	14.4	< 2	1.41	< 0.2	< 0.01	2.2
05SC14A	2.27	0.73	12.3	< 0.1	64.6	663	< 2	22.8	< 0.2	1.05	11.5
05SC14B	2.47	0.75	13.2	< 0.1	67.1	685	< 2	24.7	< 0.2	1.11	11.8
05SC15	0.58	0.33	2.2	< 0.1	19	52.8	< 2	2.23	< 0.2	0.2	4.3
05SC16	4.86	< 0.01	32.8	< 0.1	212	947	< 2	nr	< 0.2	0.01	8.9
05SC17	0.65	0.19	2.5	< 0.1	20.5	48.6	< 2	3.27	< 0.2	0.12	4.1
05SC18	0.68	0.12	2.8	< 0.1	22.6	43.8	< 2	3.28	< 0.2	0.08	4.2
05SC19	0.76	0.1	2.3	< 0.1	24.1	42.5	< 2	3.48	< 0.2	0.06	4.3
05SC20	0.76	0.08	3.1	< 0.1	23.2	37	< 2	3.38	< 0.2	0.05	4.3
05SC21	0.59	0.02	2.8	< 0.1	10.6	3.7	< 2	2.68	< 0.2	0.01	1.2
06ST01	0.94	0.02	7.5	< 0.1	47.2	2.7	< 2	0.8	0.54	0.02	1.6
06ST02	1.09	0.02	8.3	< 0.1	52	0.7	< 2	0.89	< 0.2	0.02	1.8
06ST03	1.01	0.09	6.7	< 0.1	50	3.2	< 2	0.78	< 0.2	0.1	8.5
06ST04	1.13	0.04	8.4	< 0.1	54.1	0.9	< 2	0.9	< 0.2	0.04	3.1
06ST05	1.2	0.04	9.2	< 0.1	57.9	3.6	< 2	0.95	< 0.2	0.03	3.9
06ST06	1.22	0.04	9.1	< 0.1	66	40.5	< 2	1.01	< 0.2	0.04	6.9
06ST07	1.33	0.04	9.3	< 0.1	69.6	155	< 2	1.09	< 0.2	0.04	13.2
06ST08	1.38	0.03	9.4	< 0.1	72.7	40.6	< 2	1.26	< 0.2	0.02	8.8
06ST09	1.08	0.05	4.2	< 0.1	25	125	< 2	1.01	< 0.2	0.06	5.2
06ST10	1.38	0.03	10	< 0.1	67.6	24.1	< 2	1.39	< 0.2	0.02	6
06ST11	1.32	0.03	9.7	< 0.1	63.9	13.3	< 2	1.37	0.52	0.02	4.4
06ST12	1.32	0.03	8.7	< 0.1	63	7.4	< 2	1.43	< 0.2	0.02	4.4
06ST13	0.78	0.35	5.3	< 0.1	17.6	14.5	< 2	5.21	< 0.2	0.28	2.6
06ST14	0.72	0.14	5.7	< 0.1	32.8	41.7	< 2	0.84	< 0.2	0.15	4.6
06ST15	0.76	0.3	5.5	< 0.1	22.7	22	< 2	3.79	< 0.2	0.27	3
06ST16	0.33	0.17	2.8	< 0.1	11.2	10.4	< 2	0.96	< 0.2	0.19	2.2
06ST17	0.67	0.15	5.7	< 0.1	30.9	44.9	< 2	0.77	< 0.2	0.16	5.1
06ST18	0.91	0.49	4.2	< 0.1	15.1	19.6	< 2	1.43	< 0.2	0.34	3.1
07SC01	0.205	0.029	-	< 0.01	14.6	14.7	-	1.374	0.027	-	-
07SC03	0.699	0.066	-	< 0.01	38.6	1690.0	-	1.131	0.021	-	-
07SC04	0.242	0.055	-	< 0.01	20.7	136.3	-	1.237	0.021	-	-
07SC05	0.386	0.090	-	< 0.01	29.4	336.2	-	1.229	0.033	-	-
07SC06	0.419	0.069	-	< 0.01	33.5	334.2	-	1.159	0.014	-	-
07SC07	0.458	0.044	-	< 0.01	29.4	15.7	-	1.255	0.024	-	-
07SC08	2.024	0.348	-	0.012	86.5	242.8	-	50.080	0.394	-	-
07SC09	1.170	0.086	-	0.008	43.7	107.4	-	13.270	0.091	-	-
07EK01	1.131	0.013	-	< 0.01	47	2.128	-	2.221	0.013	-	-
07MC01	0.683	0.013	-	< 0.01	11.2	3.935	-	5.527	0.018	-	-
07MC02	0.868	0.012	-	< 0.01	15.3	29.7	-	5.735	0.014	-	-
07FR01	2.236	0.021	-	< 0.01	41.9	0.4	-	1.950	0.021	-	-

Table A.6 *Continued*

Sample ID	P mg/L	Pb µg/L	Pr µg/L	Rb µg/L	Sb µg/L	Sc µg/L	Se µg/L	SiO2 mg/L	Sm µg/L	SO4 mg/L	Sr µg/L	Ta µg/L
05SC01	< 0.01	<0.05	< 0.01	0.37	4.18	0.8	< 1	5.6	< 0.01	25	88.1	< 0.02
05SC02	0.05	11	13.1	3.43	124	13.1	1.6	13.9	11.1	829	290	0.2
05SC03	< 0.01	<0.05	< 0.01	0.69	407	0.9	< 1	6.1	< 0.01	151	160	< 0.02
05SC04	< 0.01	0.08	0.03	0.39	192	0.8	< 1	5.6	0.03	30	90	< 0.02
05SC05	< 0.01	<0.05	0.01	0.36	193	0.8	< 1	5.2	< 0.01	84	130	< 0.02
05SC06	< 0.01	<0.05	< 0.01	0.44	626	0.8	< 1	5.2	< 0.01	89	136	< 0.02
05SC07	< 0.01	<0.05	< 0.01	0.5	665	0.8	< 1	5.4	< 0.01	92	153	< 0.02
05SC08	< 0.01	<0.05	< 0.01	0.44	407	0.8	< 1	5.3	< 0.01	80	141	< 0.02
05SC09	< 0.01	<0.05	< 0.01	0.35	289	0.8	< 1	5.6	< 0.01	83	142	< 0.02
05SC10	< 0.01	<0.05	< 0.01	0.36	269	0.9	< 1	5.6	< 0.01	84	157	< 0.02
05SC11	< 0.01	<0.05	< 0.01	0.3	134	1	< 1	7.8	< 0.01	53	166	< 0.02
05SC12	< 0.01	0.05	0.15	2.82	9.64	2.3	4	18.1	0.08	1960	1980	0.03
05SC13	< 0.01	<0.05	< 0.01	0.36	70.6	1.2	< 1	8.2	< 0.01	69	189	< 0.02
05SC14A	< 0.01	<0.05	0.2	2.31	<0.3	2.8	2.5	12.8	0.32	204	3020	< 0.02
05SC14B	< 0.01	<0.05	0.21	2.44	<0.3	3	2.5	14.3	0.35	195	3130	< 0.02
05SC15	< 0.01	<0.05	0.05	0.5	68.9	1.3	< 1	8.5	0.04	80	321	< 0.02
05SC16	< 0.01	0.06	< 0.01	5.79	3.72	2.4	10.5	26.4	< 0.01	171	10600	< 0.02
05SC17	< 0.01	<0.05	0.03	0.58	62.2	1.2	< 1	8	0.02	84	414	< 0.02
05SC18	< 0.01	<0.05	0.02	0.6	59.6	1.2	< 1	8	0.01	98	427	< 0.02
05SC19	< 0.01	0.1	0.02	0.68	58.7	1.2	< 1	8.5	< 0.01	102	456	< 0.02
05SC20	< 0.01	<0.05	0.01	0.68	58.8	1.2	< 1	8	< 0.01	101	442	< 0.02
05SC21	< 0.01	<0.05	< 0.01	0.46	3.38	1.2	< 1	8.5	< 0.01	57	218	< 0.02
06ST01	< 0.01	<0.05	< 0.01	0.88	2.65	0.6	< 1	4.6	< 0.01	330	424	0.1
06ST02	< 0.01	<0.05	< 0.01	1	11.2	0.6	< 1	4.4	< 0.01	353	439	0.06
06ST03	< 0.01	<0.05	0.02	1.38	19.8	0.7	< 1	5.7	0.02	285	275	0.05
06ST04	< 0.01	<0.05	< 0.01	1.12	15.9	< 0.6	< 1	4.6	< 0.01	344	406	0.04
06ST05	< 0.01	<0.05	< 0.01	1.16	36.3	0.6	< 1	4.7	< 0.01	361	405	0.03
06ST06	< 0.01	<0.05	< 0.01	1.2	175	0.6	< 1	4.5	< 0.01	397	422	0.03
06ST07	< 0.01	<0.05	< 0.01	1.24	187	0.6	< 1	4.6	< 0.01	431	429	0.02
06ST08	< 0.01	<0.05	< 0.01	1.19	264	0.6	< 1	4.6	< 0.01	439	463	0.02
06ST09	< 0.01	<0.05	0.01	0.6	4.55	< 0.6	< 1	3.5	0.01	117	408	0.02
06ST10	< 0.01	<0.05	< 0.01	1.07	228	0.6	< 1	4.5	< 0.01	403	480	< 0.02
06ST11	< 0.01	<0.05	< 0.01	0.96	196	0.6	< 1	4.5	< 0.01	374	471	0.09
06ST12	< 0.01	0.4	< 0.01	0.91	180	0.6	< 1	4.5	< 0.01	371	467	0.05
06ST13	< 0.01	<0.05	0.08	0.62	1.88	0.7	1	5.5	0.05	89	232	0.04
06ST14	< 0.01	0.07	0.04	0.47	82.7	< 0.6	< 1	3.8	0.03	177	265	0.03
06ST15	< 0.01	<0.05	0.06	0.57	28.5	0.6	< 1	4.8	0.05	118	238	< 0.02
06ST16	< 0.01	<0.05	0.04	0.14	11.7	< 0.6	< 1	3.9	0.04	40	141	0.02
06ST17	< 0.01	0.06	0.04	0.49	82.5	< 0.6	< 1	3.7	0.04	161	250	< 0.02
06ST18	< 0.01	<0.05	0.1	0.87	1.7	< 0.6	< 1	4.7	0.06	83	232	< 0.02
07SC01	< 0.01	0.308	0.014	-	54.57	0.74	< 0.01	-	< 0.01	-	91.2	-
07SC03	< 0.01	0.296	< 0.01	-	31.26	0.85	< 0.01	-	< 0.01	-	229	-
07SC04	< 0.01	0.292	< 0.01	-	446.00	0.74	< 0.01	-	< 0.01	-	107	-
07SC05	< 0.01	0.318	< 0.01	-	720	0.755	< 0.01	-	< 0.01	-	139	-
07SC06	< 0.01	0.314	< 0.01	-	699	0.803	< 0.01	-	< 0.01	-	188	-
07SC07	< 0.01	0.310	< 0.01	-	327	0.784	< 0.01	-	< 0.01	-	180	-
07SC08	< 0.01	0.420	0.094	-	4.56	1.38	76.42	-	0.076	-	3665	-
07SC09	< 0.01	0.306	0.019	-	73.22	1.20	15.12	-	0.023	-	1063	-
07EK01	< 0.01	0.317	< 0.01	-	8.94	0.76	1.05	-	< 0.01	-	528	-
07MC01	< 0.01	0.321	< 0.01	-	0.63	1.09	0.72	-	< 0.01	-	258	-
07MC02	< 0.01	0.291	< 0.01	-	4.27	1.14	1.34	-	< 0.01	-	338	-
07FR01	< 0.01	0.391	< 0.01	-	1.66	0.81	0.65	-	< 0.01	-	498	-

Table A.6 *Continued*

Sample ID	Tb µg/L	Th µg/L	Ti µg/L	Tl µg/L	U µg/L	V µg/L	W µg/L	Y µg/L	Yb µg/L	Zn µg/L	Zr µg/L
05SC01	< 0.005	< 0.2	< 0.5	<0.1	0.42	<0.5	< 0.5	0.03	0.005	1.2	< 0.2
05SC02	2.14	40.4	12.3	0.4	34.3	2.8	< 0.5	68.8	6.05	1890	< 0.2
05SC03	< 0.005	< 0.2	2.4	<0.1	< 0.1	<0.5	< 0.5	0.12	0.006	52.3	< 0.2
05SC04	0.005	< 0.2	< 0.5	<0.1	0.54	<0.5	< 0.5	0.17	0.02	18.9	< 0.2
05SC05	< 0.005	< 0.2	1.4	<0.1	1.6	<0.5	< 0.5	0.09	0.01	10	< 0.2
05SC06	< 0.005	< 0.2	1.4	<0.1	1.01	<0.5	< 0.5	0.12	0.01	17.3	< 0.2
05SC07	< 0.005	< 0.2	1.5	<0.1	0.84	<0.5	< 0.5	0.06	0.007	13.2	< 0.2
05SC08	< 0.005	< 0.2	1.2	<0.1	0.56	<0.5	< 0.5	0.04	< 0.005	12.7	< 0.2
05SC09	< 0.005	< 0.2	1.2	<0.1	0.8	<0.5	< 0.5	0.03	< 0.005	7.4	< 0.2
05SC10	< 0.005	< 0.2	1.3	<0.1	1.26	<0.5	< 0.5	0.02	< 0.005	5.1	< 0.2
05SC11	< 0.005	< 0.2	0.8	<0.1	1.23	<0.5	< 0.5	0.02	< 0.005	2.9	< 0.2
05SC12	0.04	< 0.2	29.3	<0.1	37.5	<0.5	< 0.5	7.18	0.17	51400	22
05SC13	< 0.005	< 0.2	1	<0.1	1.86	<0.5	< 0.5	0.03	< 0.005	23.4	< 0.2
05SC14A	0.095	< 0.2	3.4	<0.1	2.7	0.6	< 0.5	6.16	0.53	2.7	55.1
05SC14B	0.097	< 0.2	3.2	<0.1	2.5	1.2	< 0.5	6.31	0.55	2.3	62.7
05SC15	0.006	< 0.2	1.2	<0.1	1.85	<0.5	< 0.5	0.35	0.03	23.6	3.3
05SC16	< 0.005	< 0.2	1.8	<0.1	1.53	1.2	< 0.5	0.23	0.01	65.2	58.5
05SC17	< 0.005	< 0.2	1.4	<0.1	1.96	<0.5	< 0.5	0.23	0.02	21.2	2.5
05SC18	< 0.005	< 0.2	1.5	<0.1	2.17	<0.5	< 0.5	0.18	0.01	17.1	2
05SC19	< 0.005	< 0.2	1.5	<0.1	2.2	<0.5	< 0.5	0.16	0.009	15.7	1.6
05SC20	< 0.005	< 0.2	1.6	<0.1	2.16	<0.5	< 0.5	0.14	0.007	14.2	1.5
05SC21	< 0.005	< 0.2	0.9	<0.1	1.19	<0.5	< 0.5	0.04	< 0.005	2.3	< 0.2
06ST01	< 0.005	< 0.2	4.9	<0.1	4.89	<0.5	1.06	0.05	0.008	1.4	< 0.2
06ST02	< 0.005	< 0.2	5.5	<0.1	7.95	<0.5	< 0.5	0.05	0.005	1.9	< 0.2
06ST03	< 0.005	< 0.2	4.1	<0.1	3.52	<0.5	< 0.5	0.14	0.01	3.6	< 0.2
06ST04	< 0.005	< 0.2	5.3	<0.1	7.59	<0.5	< 0.5	0.08	0.005	1.4	< 0.2
06ST05	< 0.005	< 0.2	5.9	<0.1	7.76	<0.5	< 0.5	0.08	0.008	1.9	< 0.2
06ST06	< 0.005	< 0.2	6.2	<0.1	7.78	<0.5	< 0.5	0.08	0.008	3.2	< 0.2
06ST07	< 0.005	< 0.2	6.8	<0.1	7.54	<0.5	< 0.5	0.09	0.006	5.8	< 0.2
06ST08	< 0.005	< 0.2	6.8	<0.1	7.52	<0.5	< 0.5	0.06	< 0.005	2.9	< 0.2
06ST09	< 0.005	< 0.2	1.9	<0.1	2.75	<0.5	< 0.5	0.13	0.01	0.9	0.2
06ST10	< 0.005	< 0.2	6	<0.1	6.9	<0.5	< 0.5	0.06	0.006	2.1	< 0.2
06ST11	< 0.005	< 0.2	5.5	<0.1	6.36	<0.5	1.04	0.07	0.006	1.7	< 0.2
06ST12	< 0.005	< 0.2	5.8	<0.1	6.08	<0.5	< 0.5	0.07	0.006	4.2	< 0.2
06ST13	0.009	< 0.2	1.3	<0.1	1.2	<0.5	< 0.5	0.26	0.02	1.1	< 0.2
06ST14	0.006	< 0.2	2.7	<0.1	2.74	<0.5	< 0.5	0.18	0.02	1.3	0.2
06ST15	0.007	< 0.2	1.6	<0.1	1.68	<0.5	< 0.5	0.24	0.02	1	< 0.2
06ST16	0.005	< 0.2	0.7	<0.1	1.03	<0.5	< 0.5	0.21	0.02	0.8	< 0.2
06ST17	0.005	< 0.2	2.4	<0.1	2.5	<0.5	< 0.5	0.2	0.02	1.7	0.2
06ST18	0.008	< 0.2	1	<0.1	1.47	<0.5	< 0.5	0.28	0.02	1.5	< 0.2
07SC01	< 0.01	0.026	0.434	< 0.01	0.327	0.077	-	0.052	< 0.01	3.181	-
07SC03	< 0.01	0.007	0.490	0.029	0.065	0.019	-	0.234	< 0.01	101	-
07SC04	< 0.01	0.010	0.420	< 0.01	0.421	0.095	-	0.071	< 0.01	8.176	-
07SC05	< 0.01	0.015	0.435	< 0.01	0.469	0.028	-	0.140	< 0.01	24.5	-
07SC06	< 0.01	< 0.01	0.469	< 0.01	0.399	0.021	-	0.065	< 0.01	13.0	-
07SC07	< 0.01	< 0.01	0.508	< 0.01	0.776	0.060	-	0.072	< 0.01	4.572	-
07SC08	0.015	0.221	0.885	< 0.01	0.699	0.091	-	0.824	< 0.01	15.9	-
07SC09	< 0.01	0.010	0.656	< 0.01	2.124	0.098	-	0.774	< 0.01	35.4	-
07EK01	< 0.01	< 0.01	0.462	< 0.01	5.648	0.034	-	0.045	< 0.01	5.795	-
07MC01	< 0.01	< 0.01	0.698	< 0.01	0.788	0.243	-	0.043	< 0.01	1.759	-
07MC02	< 0.01	< 0.01	0.664	< 0.01	1.157	0.184	-	0.045	< 0.01	2.817	-
07FR01	< 0.01	< 0.01	0.490	< 0.01	3.401	0.067	-	0.053	< 0.01	17.4	-

Table A.7 Elemental composition of filtered (0.45 µm) water samples by ICP-AES

Sample ID	Lab	Ag µg/L	Al µg/L	As µg/L	B µg/L	Ba µg/L	Be µg/L	Ca mg/L	Cd µg/L	Co µg/L	Cr µg/L	Cu µg/L	Fe µg/L	K mg/L
05SC01	USGS[1]	<1	<10	<100	<5	5	<10	22.4	<5	<10	<10	<10	138	0.26
05SC02	USGS[1]	<1	6360	124	<5	10	<10	69.3	6.6	158	<10	290	203000	0.62
05SC03	USGS[1]	<1	<10	<100	<5	17	<10	59.9	<5	<10	<10	<10	12100	0.42
05SC04	USGS[1]	<1	10	<100	<5	4.9	<10	23.4	<5	<10	<10	<10	563	0.31
05SC05	USGS[1]	<1	<10	<100	<5	6.8	<10	43.4	<5	<10	<10	<10	845	0.33
05SC06	USGS[1]	<1	<10	<100	<5	8.3	<10	44.7	<5	<10	<10	<10	1290	0.37
05SC07	USGS[1]	<1	<10	<100	<5	8.3	<10	45.4	<5	<10	<10	<10	715	0.34
05SC08	USGS[1]	<1	<10	<100	<5	7.8	<10	41.1	<5	<10	<10	<10	133	0.38
05SC09	USGS[1]	<1	<10	<100	<5	8.6	<10	40.4	<5	<10	<10	<10	60	0.34
05SC10	USGS[1]	<1	<10	<100	<5	9.5	<10	42	7.8	<10	<10	<10	28	0.38
05SC11	USGS[1]	<1	<10	<100	<5	13	<10	40.6	<5	<10	<10	<10	<20	0.54
05SC12	USGS[1]	1.8	12	242	<5	29	<10	422	133	81	<10	<10	35700	2.7
05SC13	USGS[1]	<1	<10	<100	<5	14	<10	42.8	<5	<10	<10	<10	26	0.53
05SC14A	USGS[1]	2.7	<10	<100	<5	46	<10	469	<5	<10	11	<10	6250	2.4
05SC14B	USGS[1]	2.5	<10	<100	<5	47	<10	463	<5	<10	<10	<10	5840	2.4
05SC15	USGS[1]	<1	<10	<100	<5	15	<10	62.2	<5	<10	<10	<10	181	0.57
05SC16	USGS[1]	3	<10	<100	<5	80	<10	355	<5	<10	<10	<10	65	5.5
05SC17	USGS[1]	<1	<10	<100	<5	22	<10	73.1	<5	<10	<10	<10	107	0.77
05SC18	USGS[1]	<1	<10	<100	<5	21	<10	71	<5	<10	<10	<10	42	0.75
05SC19	USGS[1]	<1	<10	<100	<5	19	<10	66.3	<5	<10	<10	<10	20	0.67
05SC20	USGS[1]	<1	11	<100	<5	21	<10	77.1	<5	<10	<10	<10	<20	0.73
05SC21	USGS[1]	<1	<10	<100	<5	21	<10	40.4	<5	<10	<10	<10	<20	0.65
05SCBS	USGS[1]	<1	<10	<100	<5	<1	<10	<0.1	<5	<10	<10	<10	<20	<0.1
06ST01	USGS[1]	<5	25	<200	<5	8.8	<10	108	<5	<10	<10	<10	<20	0.95
06ST02	USGS[1]	<5	27	<200	<5	8.9	<10	109	<5	<10	<10	<10	<20	1.14
06ST03	USGS[1]	<5	46	<200	<5	28	<10	74.5	<5	<10	<10	<10	<20	1.1
06ST04	USGS[1]	<5	45	<200	<5	12	<10	101	<5	<10	<10	<10	<20	1.17
06ST05	USGS[1]	<5	48	<200	<5	12	<10	102	<5	<10	<10	<10	<20	1.22
06ST06	USGS[1]	<5	47	<200	<5	12	<10	103	<5	<10	<10	<10	33	1.26
06ST07	USGS[1]	<5	53	<200	<5	12	<10	106	<5	<10	<10	<10	407	1.36
06ST08	USGS[1]	<5	61	<200	<5	11	<10	106	<5	<10	<10	<10	32	1.36
06ST09	USGS[1]	<5	26	<200	<5	19	<10	70.4	<5	<10	<10	<10	92	1.18
06ST10	USGS[1]	<5	48	<200	<5	13	<10	99.9	<5	<10	<10	<10	<20	1.34
06ST11	USGS[1]	<5	46	<200	<5	14	<10	97.1	<5	<10	<10	<10	<20	1.27
06ST12	USGS[1]	<5	44	<200	<5	15	<10	96.1	<5	<10	<10	<10	<20	1.28
06ST13	USGS[1]	<5	56	<200	5.7	25	<10	42.9	<5	<10	<10	<10	<20	0.85
06ST14	USGS[1]	<5	52	<200	<5	14	<10	57.2	<5	<10	<10	<10	141	0.77
06ST15	USGS[1]	<5	59	<200	<5	20	<10	46	<5	<10	<10	<10	56	0.77
06ST16	USGS[1]	<5	48	<200	<5	11	<10	30.7	<5	<10	<10	<10	101	0.32
06ST17	USGS[1]	<5	52	<200	<5	10	<10	53.6	<5	<10	<10	<10	160	0.7
06ST17D	USGS[1]	<5	51	<200	<5	10	<10	53.4	<5	<10	<10	<10	161	0.67
06ST18	USGS[1]	<5	64	<200	<5	15	<10	40	<5	<10	<10	<10	<20	0.88
06STBS	USGS[1]	<5	<20	<200	<5	<1	<10	<0.1	<5	<10	<10	<10	<20	<0.1

[1] Briggs, P.H., 2001. The determination of twenty-seven elements in aqueous samples by inductively coupled plasma-atomic emission spectrometry. Chapter F, US Geological Survey Open File Report 02-223-F.

Table A.7 *Continued*

Sample ID	Li µg/L	Mg mg/L	Mn µg/L	Mo µg/L	Na mg/L	Ni µg/L	P mg/L	Pb µg/L	Sb µg/L	SiO2 mg/L	Sr µg/L	Ti µg/L	V µg/L	Zn µg/L
05SC01	1	11.2	28	<20	0.83	<10	<0.1	<50	<50	6.2	86	<50	<10	<10
05SC02	5.6	52.6	11400	<20	0.5	543	<0.1	<50	54	15	284	<50	<10	1640
05SC03	2.2	31.9	812	<20	0.52	30	<0.1	<50	430	6.5	161	<50	<10	46
05SC04	1	11.8	92.5	<20	0.97	<10	<0.1	<50	228	6.4	89	<50	<10	18
05SC05	1.6	30.2	168	<20	0.85	<10	<0.1	<50	224	6.2	139	<50	<10	<10
05SC06	1.7	27.7	345	<20	0.69	12	<0.1	<50	743	6.3	148	<50	<10	15
05SC07	1.4	27.2	311	<20	0.67	10	<0.1	<50	744	6.2	158	<50	<10	<10
05SC08	1.4	24.6	144	<20	0.72	<10	<0.1	<50	513	6.9	160	<50	<10	13
05SC09	1.3	24.8	73.1	<20	0.8	<10	<0.1	<50	351	7.2	158	<50	<10	<10
05SC10	1.5	26.1	24	<20	0.96	<10	<0.1	<50	335	7	175	<50	<10	12
05SC11	1.6	18.2	5	<20	1.4	<10	<0.1	<50	156	8.9	173	<50	<10	<10
05SC12	17	245	16200	<20	4.9	137	<0.1	<50	<50	17.8	1820	<50	<10	48200
05SC13	2.1	19.1	15	<20	1.4	<10	<0.1	<50	78	9.2	190	<50	<10	18
05SC14A	14	69.1	719	<20	23.5	<10	<0.1	<50	<50	13.3	2960	<50	<10	<10
05SC14B	15	70.5	746	<20	25.1	<10	<0.1	<50	<50	13.6	3040	<50	<10	<10
05SC15	2.3	21	57	<20	2.6	<10	<0.1	<50	58	8.9	326	<50	<10	19
05SC16	36	187	1030	<20	139	<10	<0.1	<50	<50	24	9880	<50	<10	70
05SC17	2.7	24.8	59.9	<20	4	<10	<0.1	<50	56	9.8	457	<50	<10	20
05SC18	3.2	26.1	50.6	<20	3.6	<10	<0.1	<50	51	9.2	442	<50	<10	13
05SC19	2.7	23	42	<20	3.6	<10	<0.1	<50	50	8.1	417	<50	<10	11
05SC20	2.9	26.2	44	<20	3.9	<10	<0.1	<50	61	9.5	483	<50	<10	11
05SC21	3.1	12.2	<5	<20	2.9	<10	<0.1	<50	<50	10	228	<50	<10	<10
05SCBS	<1	<0.1	<5	<20	<0.1	<10	<0.1	<50	<50	<0.1	<1	<50	<10	<10
06ST01	12	51.4	<10	<20	0.86	<10	<0.5	<50	<50	5.4	432	<50	<10	<20
06ST02	13	56.5	<10	<20	0.99	<10	<0.5	<50	<50	5.2	442	<50	<10	<20
06ST03	6.3	54	<10	<20	0.85	<10	<0.5	<50	<50	6.9	280	<50	<10	<20
06ST04	13	57.9	<10	<20	0.94	<10	<0.5	<50	<50	5.5	399	<50	<10	<20
06ST05	14	63.9	<10	<20	1.02	<10	<0.5	<50	<50	5.6	406	<50	<10	<20
06ST06	13	71.3	39	<20	1.08	<10	<0.5	<50	139	5.5	418	<50	<10	<20
06ST07	14	76.5	151	<20	1.19	<10	<0.5	<50	160	5.6	432	<50	<10	<20
06ST08	15	77.9	40	<20	1.33	<10	<0.5	<50	244	5.4	452	<50	<10	<20
06ST09	<5	27.5	123	<20	1.08	<10	<0.5	<50	<50	4.3	406	<50	<10	<20
06ST10	15	70.4	22	<20	1.44	<10	<0.5	<50	194	5.2	455	<50	<10	<20
06ST11	14	66.5	12	<20	1.4	<10	<0.5	<50	162	5.1	449	<50	<10	<20
06ST12	13	65.2	<10	<20	1.46	<10	<0.5	<50	155	5.1	447	<50	<10	<20
06ST13	<5	19	14	<20	5.15	<10	<0.5	<50	<50	6.6	230	<50	<10	<20
06ST14	<5	34.7	41	<20	0.89	<10	<0.5	<50	69	4.5	263	<50	<10	<20
06ST15	<5	23.4	22	<20	3.66	<10	<0.5	<50	<50	5.7	230	<50	<10	<20
06ST16	7.8	11.8	<10	<20	0.92	<10	<0.5	<50	<50	4.5	146	<50	<10	<20
06ST17	<5	31.6	43	<20	0.78	<10	<0.5	<50	66	4.3	244	<50	<10	<20
06ST17D	<5	31.5	44	<20	0.75	<10	<0.5	<50	76	4.3	241	<50	<10	<20
06ST18	<5	14.9	19	<20	1.25	<10	<0.5	<50	<50	5.3	219	<50	<10	<20
06STBS	<5	<0.1	<10	<20	<0.1	<10	<0.5	<50	<50	<0.1	<1	<50	<10	<20

Table A.8 Elemental composition of filtered (0.20 µm) water samples by ICP-MS

Sample ID	Lab	Ag µg/L	Al µg/L	As µg/L	Ba µg/L	Be µg/L	Cd µg/L	Ce µg/L	Co µg/L	Cr µg/L	Cu µg/L	Dy µg/L	Er µg/L	Eu µg/L	Fe µg/L
06ST01	UAF	1.29E-02	3.711	1.05	6.35	1.31E-02	1.64E-02	2.04E-02	2.31E-01	2.05E-02	1.178	9.08E-03	5.91E-03	<0.01	20.40
06ST03	UAF	<0.01	10.38	0.50	20.71	<0.01	5.38E-02	6.04E-02	2.93E-01	1.25E-01	2.102	2.60E-02	1.03E-02	<0.01	21.93
06ST05	UAF	<0.01	4.839	0.90	9.36	<0.01	1.67E-02	3.04E-02	3.58E-01	<0.01	1.659	1.04E-02	<0.01	<0.01	16.16
06ST07	UAF	<0.01	4.3130	10.42	8.48	<0.01	2.50E-02	3.00E-02	1.56E+00	<0.01	1.443	<0.01	<0.01	<0.01	358.40
06ST10	UAF	<0.01	3.72	2.05	8.27	<0.01	1.03E-02	1.81E-02	3.82E-01	<0.01	1.577	<0.01	<0.01	<0.01	24.68
06ST11	UAF	<0.01	4.101	1.06	11.87	<0.01	9.43E-03	2.17E-02	1.25E-01	<0.01	2.260	<0.01	<0.01	<0.01	18.53
06ST14	UAF	<0.01	29.86	1.07	10.42	<0.01	1.02E-02	2.12E-01	5.65E-01	1.28E-01	2.319	3.30E-02	2.20E-02	<0.01	119.30
06ST16	UAF	<0.01	32.19	0.65	9.13	<0.01	4.30E-03	2.08E-01	2.25E-01	1.82E-01	1.700	3.08E-02	2.47E-02	<0.01	90.00
06ST17	UAF	<0.01	27.77	2.00	7.90	<0.01	1.60E-02	2.12E-01	5.69E-01	1.17E-01	3.417	3.54E-02	2.28E-02	<0.01	140.20
06ST17D	UAF	<0.01	28.1	2.00	8.23	<0.01	1.58E-02	2.23E-01	5.72E-01	1.19E-01	3.381	3.72E-02	2.46E-02	<0.01	146.70
06ST18	UAF	<0.01	48.81	0.31	12.20	<0.01	2.06E-02	5.83E-01	8.05E-01	<0.01	1.545	4.61E-02	2.61E-02	<0.01	12.78
07SC01	UAF	<0.01	3.704	4.33	3.48	<0.01	1.34E-02	2.10E-02	1.56E-01	1.86E-02	1.785	<0.01	7.53E-03	<0.01	74.10
07SC02	UAF	<0.01	0.3306	0.08	0.03	<0.01	<0.01	<0.01	<0.01	<0.01	0.157	<0.01	1.17E-03	<0.01	6.26
07SC03	UAF	<0.01	13.46	16.42	16.25	4.09E-02	1.53E-01	4.99E-02	2.24E+01	1.07E-02	0.634	<0.01	<0.01	<0.01	5257.33
07SC04	UAF	<0.01	10.09	14.10	4.84	<0.01	3.18E-02	4.54E-02	1.62E+00	2.30E-02	2.098	<0.01	<0.01	<0.01	1091.00
07SC05	UAF	<0.01	7.405	34.38	6.67	1.26E-02	3.54E-02	6.26E-02	3.57E+00	3.69E-02	1.260	1.22E-02	<0.01	<0.01	1265.00
07SC06	UAF	<0.01	4.573	9.59	7.39	<0.01	3.26E-02	2.16E-02	2.90E+00	5.22E-02	1.153	<0.01	<0.01	<0.01	485.40
07SC07	UAF	<0.01	5.162	4.76	5.71	<0.01	2.12E-02	1.83E-02	1.85E-01	5.07E-02	1.353	<0.01	<0.01	<0.01	84.49
07SC08	UAF	8.28E-02	50.73	4.88	18.28	3.21E-02	2.13E-01	4.55E-01	7.96E-01	2.08E-01	3.911	7.76E-02	5.33E-02	<0.01	836.20
07SC09	UAF	5.63E-02	5.832	3.58	13.96	2.53E-02	7.02E-02	9.79E-02	3.58E-01	7.15E-02	0.904	5.35E-02	4.43E-02	<0.01	628.20
07EK01	UAF	<0.01	2.621	0.63	14.92	<0.01	1.24E-02	<0.01	9.68E-02	6.92E-02	0.577	<0.01	<0.01	<0.01	6.28
07MC01	UAF	<0.01	2.172	2.43	18.41	<0.01	1.78E-02	<0.01	1.69E-01	6.87E-02	0.670	<0.01	<0.01	<0.01	100.80
07MC02	UAF	<0.01	3.74	3.58	13.25	<0.01	4.54E-02	<0.01	1.91E-01	1.91E-02	1.057	<0.01	<0.01	<0.01	10.79
07FR01	UAF	<0.01	10.75	3.41	23.18	<0.01	2.26E-01	1.80E-02	2.19E-01	6.42E-02	2.004	<0.01	<0.01	<0.01	17.61
07TG01B	UAF	<0.01	0.4003	0.29	0.05	<0.01	<0.01	<0.01	<0.01	<0.01	0.063	<0.01	<0.01	<0.01	11.76

" - " = not determined

Table A.8 *Continued*

Sample ID	Gd µg/L	Ho µg/L	K mg/L	La µg/L	Lu µg/L	Mg mg/L	Mn µg/L	Na mg/L	Nb µg/L	Nd µg/L	P mg/L	Pb µg/L	Pr µg/L	Sb µg/L
06ST01	<0.01	<0.01	1.049	2.69E-02	1.62E-02	46.32	2.47	0.81	-	2.46E-02	<0.01	3.95E-02	1.04E-02	1.96
06ST03	2.81E-02	<0.01	1.056	1.02E-01	<0.01	48.33	3.28	0.79	-	1.03E-01	<0.01	5.16E-02	2.02E-02	20.52
06ST05	<0.01	<0.01	1.136	4.03E-02	<0.01	56.41	3.62	0.94	-	3.31E-02	<0.01	5.46E-02	<0.01	36.50
06ST07	<0.01	<0.01	1.343	4.19E-02	<0.01	61.28	155.40	1.15	-	3.32E-02	<0.01	1.56E-02	<0.01	180.73
06ST10	<0.01	<0.01	1.213	3.25E-02	<0.01	58.64	24.10	1.26	-	1.80E-02	<0.01	2.11E-02	<0.01	178.10
06ST11	<0.01	<0.01	1.409	3.61E-02	<0.01	63.11	13.32	1.53	-	2.32E-02	<0.01	4.18E-02	<0.01	177.40
06ST14	3.71E-02	<0.01	0.723	1.42E-01	<0.01	32.22	41.71	0.88	-	1.51E-01	<0.01	6.68E-02	3.97E-02	82.59
06ST16	4.04E-02	<0.01	0.327	1.73E-01	<0.01	11.28	10.43	0.99	-	1.65E-01	<0.01	3.59E-02	4.30E-02	11.70
06ST17	3.17E-02	<0.01	0.689	1.55E-01	<0.01	30.70	44.90	0.78	-	1.56E-01	<0.01	6.14E-02	3.54E-02	83.10
06ST17D	3.12E-02	<0.01	0.677	1.59E-01	<0.01	30.15	44.76	0.77	-	1.55E-01	<0.01	6.39E-02	3.78E-02	86.60
06ST18	5.90E-02	<0.01	0.907	4.41E-01	<0.01	14.56	18.53	1.38	-	3.24E-01	<0.01	1.66E-02	8.76E-02	1.38
07SC01	<0.01	<0.01	0.994	2.38E-02	<0.01	12.87	14.68	1.30	3.95E-01	-	<0.01	3.43E-01	<0.01	54.28
07SC02	<0.01	<0.01	0.007	<0.01	<0.01	0.01	0.10	0.02	<0.01	-	<0.01	4.03E-01	<0.01	0.32
07SC03	<0.01	<0.01	0.603	5.65E-02	<0.01	33.12	1690.00	0.95	1.49E-02	-	<0.01	3.16E-01	<0.01	27.59
07SC04	<0.01	<0.01	0.380	6.96E-02	<0.01	16.52	136.30	1.35	2.70E-02	-	<0.01	3.58E-01	<0.01	471.10
07SC05	<0.01	<0.01	0.350	9.78E-02	<0.01	24.61	336.20	1.05	2.94E-02	-	<0.01	3.48E-01	<0.01	694.80
07SC06	<0.01	<0.01	0.414	7.08E-02	<0.01	27.81	334.20	1.05	1.16E-02	-	<0.01	3.37E-01	<0.01	708.90
07SC07	<0.01	<0.01	0.427	4.12E-02	<0.01	24.78	15.69	1.07	1.40E-02	-	<0.01	3.05E-01	<0.01	316.50
07SC08	7.59E-02	1.63E-02	1.668	2.57E-01	<0.01	67.94	242.80	37.75	2.75E-01	-	<0.01	3.87E-01	6.60E-02	4.20
07SC09	3.63E-02	1.35E-02	0.887	7.65E-02	<0.01	31.42	107.40	7.23	8.37E-02	-	<0.01	3.18E-01	1.71E-02	71.05
07EK01	<0.01	<0.01	0.591	1.05E-02	<0.01	9.21	2.77	4.44	1.47E-02	-	<0.01	3.41E-01	<0.01	0.69
07MC01	<0.01	<0.01	0.744	<0.01	<0.01	12.79	27.66	4.55	<0.01	-	<0.01	3.14E-01	<0.01	4.01
07MC02	<0.01	<0.01	0.968	1.44E-02	<0.01	39.70	2.10	1.78	1.35E-02	-	<0.01	3.81E-01	<0.01	8.33
07FR01	<0.01	<0.01	1.949	2.38E-02	<0.01	34.46	0.38	1.56	2.30E-02	-	<0.01	4.15E-01	<0.01	1.58
07TG01B	<0.01	<0.01	0.012	<0.01	<0.01	0.03	0.11	0.01	<0.01	-	<0.01	2.94E-01	<0.01	0.33

Table A.8 *Continued*

Sample ID	Sc µg/L	Se µg/L	Sm µg/L	Sr µg/L	Tb µg/L	Th µg/L	Ti µg/L	U µg/L	V µg/L	Y µg/L	Yb µg/L	Zn µg/L
06ST01	6.72E-01	2.85E-01	1.90E-02	491.2	1.61E-02	2.37E-02	6.24E-01	5.627	7.72E-02	5.11E-02	<0.01	1.432
06ST03	7.15E-01	4.33E-01	2.58E-02	273.6	<0.01	3.10E-02	3.85E+00	3.199	6.24E-02	1.90E-01	1.94E-02	3.598
06ST05	7.03E-01	3.14E-01	<0.01	400.8	<0.01	1.34E-02	5.66E+00	7.807	4.63E-02	1.03E-01	<0.01	1.609
06ST07	6.65E-01	2.95E-01	<0.01	424.7	<0.01	1.44E-02	6.64E+00	7.724	5.21E-02	1.08E-01	<0.01	5.484
06ST10	6.03E-01	1.29E-01	<0.01	460.2	<0.01	<0.01	6.54E+00	6.377	4.15E-02	6.64E-02	<0.01	2.043
06ST11	6.23E-01	1.95E-01	<0.01	471.3	<0.01	<0.01	5.67E+00	6.356	5.26E-02	7.58E-02	<0.01	1.673
06ST14	5.84E-01	2.36E-01	3.16E-02	263.2	<0.01	4.99E-02	2.80E+00	3.176	1.51E-01	2.07E-01	2.35E-02	1.370
06ST16	5.41E-01	1.53E-01	3.94E-02	141.6	<0.01	6.54E-02	8.84E-01	1.210	9.98E-02	2.02E-01	2.79E-02	1.818
06ST17	5.51E-01	2.41E-01	3.55E-02	251.3	<0.01	5.32E-02	2.81E+00	2.720	1.09E-01	2.43E-01	2.36E-02	1.796
06ST17D	5.58E-01	2.59E-01	3.80E-02	255.3	<0.01	5.36E-02	2.80E+00	2.711	1.05E-01	2.53E-01	2.46E-02	1.777
06ST18	5.71E-01	3.51E-02	5.38E-02	231.2	<0.01	<0.01	7.23E-01	1.710	5.52E-02	2.71E-01	2.12E-02	1.429
07SC01	9.11E-01	1.21E-01	<0.01	91.9	<0.01	<0.01	5.34E-01	0.313	4.62E-02	4.47E-02	<0.01	8.526
07SC02	<0.01	<0.01	<0.01	0.7	<0.01	<0.01	<0.01	0.001	1.80E-02	<0.01	<0.01	1.519
07SC03	1.30E+00	<0.01	<0.01	204.3	<0.01	<0.01	7.13E-01	0.051	2.35E-02	1.85E-01	<0.01	82.963
07SC04	9.97E-01	<0.01	<0.01	103.4	<0.01	9.91E-03	6.21E-01	0.317	6.68E-02	7.93E-02	<0.01	26.040
07SC05	1.01E+00	<0.01	<0.01	139.2	<0.01	1.46E-02	5.53E-01	0.468	3.19E-02	1.28E-01	<0.01	53.320
07SC06	1.02E+00	<0.01	<0.01	176.8	<0.01	<0.01	5.61E-01	0.372	3.37E-02	5.89E-02	<0.01	91.620
07SC07	9.72E-01	<0.01	<0.01	164.6	<0.01	<0.01	5.95E-01	0.689	3.33E-02	4.05E-02	<0.01	28.070
07SC08	1.82E+00	8.29E+01	6.65E-02	3152.0	1.24E-02	1.36E-01	1.12E+00	0.597	8.45E-02	6.35E-01	5.69E-02	13.740
07SC09	1.64E+00	1.00E+01	2.51E-02	732.1	<0.01	<0.01	9.01E-01	1.875	9.46E-02	5.92E-01	4.17E-02	32.920
07EK01	1.59E+00	8.08E-01	<0.01	234.8	<0.01	<0.01	8.98E-01	0.699	2.19E-01	3.89E-02	<0.01	1.823
07MC01	1.55E+00	1.54E+00	<0.01	312.4	<0.01	<0.01	8.77E-01	1.038	1.77E-01	3.85E-02	<0.01	2.289
07MC02	1.16E+00	9.53E-01	<0.01	470.7	<0.01	<0.01	6.84E-01	4.687	4.09E-02	4.22E-02	<0.01	5.111
07FR01	1.14E+00	7.63E-01	<0.01	465.5	<0.01	<0.01	7.59E-01	3.114	7.81E-02	5.43E-02	<0.01	16.370
07TG01B	<0.01	<0.01	<0.01	0.3	<0.01	<0.01	<0.01	0.003	1.17E-02	<0.01	<0.01	2.070

Table A.9 Elemental composition of unfiltered water samples by ICP-MS

Sample ID	Lab	Ag µg/L	Al µg/L	As µg/L	Ba µg/L	Be µg/L	Bi µg/L	Ca mg/L	Cd µg/L	Ce µg/L	Co µg/L	Cr µg/L	Cs µg/L	Cu µg/L	Dy µg/L	Er µg/L	Eu µg/L	Fe µg/L
06ST01	USGS[1]	<3	12.7	1	8.82	<0.05	< 0.2	103	<0.02	0.13	0.06	<1	< 0.02	1.8	0.01	0.01	0.005	<50
06ST02	USGS[1]	<3	16.5	2	8.5	<0.05	< 0.2	105	<0.02	0.14	0.07	<1	< 0.02	3.4	0.01	0.01	< 0.005	76
06ST03	USGS[1]	<3	214	<1	27.5	<0.05	< 0.2	74.2	0.09	0.82	0.38	<1	0.02	3.2	0.075	0.05	0.02	625
06ST04	USGS[1]	<3	26.5	1	11.8	<0.05	< 0.2	98.1	<0.02	0.11	0.06	<1	< 0.02	2	0.02	0.01	< 0.005	54
06ST05	USGS[1]	<3	180	2	13.3	<0.05	< 0.2	101	0.04	0.71	0.4	<1	0.03	2.8	0.063	0.04	0.02	545
06ST06	USGS[1]	<3	70.7	2	12.2	<0.05	< 0.2	105	0.03	0.29	0.68	<1	< 0.02	3	0.04	0.02	0.008	243
06ST07	USGS[1]	<3	25.1	11.5	11.5	<0.05	< 0.2	109	0.03	0.1	1.6	<1	< 0.02	2.4	0.02	0.01	< 0.005	525
06ST08	USGS[1]	<3	12.6	4.2	11.5	<0.05	< 0.2	110	<0.02	0.05	0.4	<1	< 0.02	2.5	0.005	0.007	< 0.005	67
06ST09	USGS[1]	<3	23.2	<1	18.3	<0.05	< 0.2	74.3	<0.02	0.17	0.47	<1	< 0.02	3.3	0.03	0.01	0.007	254
06ST10	USGS[1]	<3	92.6	3.2	13.8	<0.05	< 0.2	107	0.02	0.36	0.33	<1	< 0.02	3	0.02	0.02	0.009	363
06ST11	USGS[1]	<3	16.1	2	15.5	<0.05	< 0.2	108	<0.02	0.07	0.12	<1	< 0.02	2.8	0.01	0.009	< 0.005	55
06ST12	USGS[1]	<3	9.7	1	15.1	<0.05	< 0.2	104	<0.02	0.05	0.08	<1	< 0.02	2.9	0.008	0.008	< 0.005	<50
06ST13	USGS[1]	<3	522	<1	26	<0.05	< 0.2	44.9	0.07	5.44	1.1	<1	0.04	3.5	0.38	0.18	0.1	1040
06ST14	USGS[1]	<3	1250	3.2	24.6	<0.05	< 0.2	64.7	0.08	3.55	2.1	2.1	0.05	7.4	0.28	0.15	0.078	3650
06ST15	USGS[1]	<3	840	1	27.1	<0.05	< 0.2	56	0.07	4.99	1.51	1.4	0.04	4.6	0.35	0.17	0.094	1980
06ST16	USGS[1]	<3	135	<1	12.6	<0.05	< 0.2	35.4	<0.02	0.6	0.3	<1	< 0.02	11.2	0.065	0.04	0.02	417
06ST17	USGS[1]	<3	334	2	13.4	<0.05	< 0.2	65.2	0.03	1.05	0.76	1	< 0.02	31.4	0.089	0.04	0.02	1360
06ST17D	USGS[1]	<3	348	3	13	<0.05	< 0.2	64.8	0.03	1.1	0.86	1	< 0.02	4.4	0.089	0.051	0.03	1220
06ST18	USGS[1]	<3	271	<1	16.7	<0.05	< 0.2	49.6	0.05	4.21	0.89	<1	< 0.02	3.3	0.28	0.14	0.077	372
06STBS	USGS[1]	<3	<2	<1	<0.2	<0.05	< 0.2	<0.2	<0.02	< 0.01	<0.02	<1	< 0.02	<0.5	< 0.005	< 0.005	< 0.005	<50

[1] Lamothe, P.J., Meier, A.L., Wilson, S.A., 2002. The determination of forty-four elements in aqueous samples by inductively coupled plasma-mass spectrometry. Chapter H, US Geological Survey Open File Report 02-223-H.

Table A.9 *Continued*

Sample ID	Ga µg/L	Gd µg/L	Ho µg/L	K mg/L	La µg/L	Li µg/L	Mg mg/L	Mn µg/L	Na mg/L	Nb µg/L	Nd µg/L	Ni µg/L	P mg/L	Pb µg/L	Pr µg/L	Rb µg/L	Sb µg/L
06ST01	< 0.05	0.02	< 0.005	0.86	0.09	7.4	44.6	5.7	0.75	< 0.2	0.07	1.6	< 0.01	0.06	0.02	0.88	2.02
06ST02	< 0.05	0.02	< 0.005	0.98	0.09	7.5	47.8	5.1	0.83	< 0.2	0.08	1.9	< 0.01	0.2	0.02	0.99	10.6
06ST03	0.07	0.09	0.02	0.95	0.51	6.5	47.3	24.6	0.74	< 0.2	0.47	10.1	0.02	0.81	0.12	1.46	18.7
06ST04	< 0.05	0.02	< 0.005	1.08	0.09	7.9	50.7	3.9	0.88	< 0.2	0.09	3	< 0.01	0.1	0.02	1.1	15.8
06ST05	0.06	0.078	0.01	1.13	0.42	8.8	57.7	28.7	0.94	< 0.2	0.39	4.9	< 0.01	0.69	0.09	1.24	35.1
06ST06	< 0.05	0.04	0.008	1.2	0.19	9	65.1	46.5	1.02	< 0.2	0.17	7.7	< 0.01	0.3	0.04	1.23	175
06ST07	< 0.05	0.01	< 0.005	1.33	0.09	9.3	70.3	154	1.14	< 0.2	0.07	13.3	< 0.01	0.09	0.02	1.3	187
06ST08	< 0.05	0.008	< 0.005	1.38	0.05	10.1	73	41.5	1.3	< 0.2	0.04	8.9	< 0.01	<0.05	< 0.01	1.21	258
06ST09	< 0.05	0.02	0.006	1.18	0.12	4.4	26.7	126	1.11	< 0.2	0.12	5.5	< 0.01	0.2	0.03	0.63	4.02
06ST10	< 0.05	0.03	0.006	1.41	0.21	9.3	70.2	35.6	1.48	< 0.2	0.19	6.3	< 0.01	0.4	0.05	1.08	218
06ST11	< 0.05	0.01	< 0.005	1.46	0.06	9	70.2	14.9	1.52	0.72	0.05	4.4	< 0.01	0.08	0.01	0.95	196
06ST12	< 0.05	0.009	< 0.005	1.37	0.05	8.4	66.2	7.7	1.5	0.26	0.03	4.3	< 0.01	0.05	< 0.01	0.91	173
06ST13	0.1	0.49	0.065	0.88	2.98	4.4	19	41.8	5.68	< 0.2	2.8	4.7	0.02	0.85	0.73	0.77	1.31
06ST14	0.35	0.35	0.055	0.86	1.82	5.8	36.7	133	0.99	< 0.2	1.72	9.3	0.06	3.8	0.44	0.96	65.2
06ST15	0.22	0.49	0.061	0.96	2.69	4.9	27.1	73	4.59	< 0.2	2.51	6.6	0.04	1.8	0.66	0.89	24.7
06ST16	< 0.05	0.074	0.01	0.44	0.37	2.3	13.2	23	1.13	< 0.2	0.36	2.8	0.02	0.5	0.09	0.21	11
06ST17	0.1	0.11	0.02	0.84	0.58	5.2	36.5	72.3	0.92	< 0.2	0.56	6.9	0.02	1.9	0.14	0.64	77.5
06ST17D	0.09	0.11	0.02	0.83	0.6	5.3	36.1	74.7	0.92	< 0.2	0.59	7	0.06	1	0.14	0.64	75.8
06ST18	0.06	0.4	0.053	1.1	2.36	3	17.9	30	1.68	< 0.2	2.24	4.5	< 0.01	0.2	0.58	0.96	1.31
06STBS	< 0.05	< 0.005	< 0.005	<0.03	< 0.01	< 0.1	<0.01	<0.2	<0.01	< 0.2	< 0.01	<0.4	< 0.01	<0.05	< 0.01	< 0.01	<0.3

Table A.9 *Continued*

Sample ID	Sc µg/L	SiO2 mg/L	Sm µg/L	SO4 mg/L	Sr µg/L	Ta µg/L	Tb µg/L	Th µg/L	Ti µg/L	Tm µg/L	U µg/L	V µg/L	W µg/L	Y µg/L	Yb µg/L	Zn µg/L	Zr µg/L
06ST01	< 0.6	4.5	0.02	312	424	0.05	< 0.005	< 0.2	4.6	< 0.005	4.81	<0.5	< 0.5	0.09	0.008	1.4	< 0.2
06ST02	< 0.6	4.4	0.02	332	427	< 0.02	< 0.005	< 0.2	5.4	< 0.005	7.59	<0.5	< 0.5	0.1	0.009	1.6	< 0.2
06ST03	0.7	6	0.08	269	277	< 0.02	0.01	< 0.2	5	0.006	3.45	<0.5	< 0.5	0.45	0.04	7.3	< 0.2
06ST04	< 0.6	4.6	0.01	322	400	< 0.02	< 0.005	< 0.2	4.8	< 0.005	7.18	<0.5	< 0.5	0.11	0.01	2	< 0.2
06ST05	0.6	5	0.07	347	405	< 0.02	0.01	< 0.2	5.7	0.006	7.72	<0.5	< 0.5	0.37	0.03	4.8	< 0.2
06ST06	0.7	5	0.04	409	426	< 0.02	0.005	< 0.2	6.8	< 0.005	7.84	<0.5	< 0.5	0.2	0.02	4.7	< 0.2
06ST07	0.7	5	0.02	435	433	< 0.02	< 0.005	< 0.2	6.8	< 0.005	7.56	<0.5	< 0.5	0.12	0.01	6.6	< 0.2
06ST08	0.7	4.8	< 0.01	453	462	< 0.02	< 0.005	< 0.2	6.9	< 0.005	7.41	<0.5	< 0.5	0.07	0.006	3.4	< 0.2
06ST09	0.6	4.1	0.02	132	415	< 0.02	< 0.005	< 0.2	2.1	< 0.005	2.76	<0.5	< 0.5	0.17	0.01	1.5	0.3
06ST10	0.7	5.2	0.04	416	476	< 0.02	0.005	< 0.2	6.6	< 0.005	7.05	<0.5	< 0.5	0.15	0.02	3.6	< 0.2
06ST11	0.7	5.2	< 0.01	409	480	0.05	< 0.005	< 0.2	5.9	< 0.005	6.62	<0.5	0.91	0.08	0.006	2.2	< 0.2
06ST12	0.7	4.8	< 0.01	392	458	< 0.02	< 0.005	< 0.2	5.5	< 0.005	6.15	<0.5	< 0.5	0.08	0.009	2.1	< 0.2
06ST13	1	7.1	0.5	95	221	< 0.02	0.07	< 0.2	5.2	0.02	1.29	0.9	< 0.5	1.74	0.13	8.9	< 0.2
06ST14	1.2	7.5	0.34	217	271	< 0.02	0.05	0.29	11.2	0.02	3.03	2.7	< 0.5	1.3	0.12	16.1	0.57
06ST15	1.2	8	0.46	144	250	< 0.02	0.066	< 0.2	7.7	0.02	1.95	1.6	< 0.5	1.67	0.14	11.8	0.3
06ST16	0.8	5.2	0.07	52	143	< 0.02	0.01	< 0.2	2	< 0.005	1.06	<0.5	< 0.5	0.35	0.04	3.4	0.2
06ST17	0.8	5.6	0.09	206	260	< 0.02	0.02	< 0.2	6	0.006	2.67	0.9	< 0.5	0.45	0.04	9.8	0.4
06ST17D	0.9	5.8	0.1	208	261	< 0.02	0.02	< 0.2	6	0.006	2.7	0.8	< 0.5	0.48	0.05	5.6	0.4
06ST18	0.9	6.2	0.38	106	244	< 0.02	0.057	< 0.2	2.6	0.02	1.67	<0.5	< 0.5	1.38	0.1	5.6	< 0.2
06STBS	< 0.6	< 0.2	< 0.01	3	< 0.5	< 0.02	< 0.005	< 0.2	< 0.5	< 0.005	< 0.1	<0.5	< 0.5	< 0.01	< 0.005	<0.5	< 0.2

Table A.10 Elemental composition of unfiltered water samples by ICP-AES

Sample ID	Lab	Ag µg/L	Al µg/L	As µg/L	Ba µg/L	Be µg/L	Ca mg/L	Cd µg/L	Co µg/L	Cr µg/L	Cu µg/L	Fe µg/L	K mg/L	Li µg/L
06ST01	USGS[1]	<5	<20	<200	8.7	<10	107	<5	<10	<10	<10	69	0.91	8
06ST02	USGS[1]	<5	<20	<200	8.9	<10	109	<5	<10	<10	<10	100	1.09	8.3
06ST03	USGS[1]	<5	241	<200	30	<10	73.8	<5	<10	<10	<10	646	1	6.7
06ST04	USGS[1]	<5	36	<200	12	<10	100	<5	<10	<10	<10	77	1.1	8.1
06ST05	USGS[1]	<5	211	<200	14	<10	101	<5	<10	<10	<10	571	1.18	8.9
06ST06	USGS[1]	<5	77	<200	13	<10	104	<5	<10	<10	<10	258	1.24	9.5
06ST07	USGS[1]	<5	24	<200	12	<10	105	<5	<10	<10	<10	547	1.33	9
06ST08	USGS[1]	<5	<20	<200	12	<10	109	<5	<10	<10	<10	90	1.41	10
06ST09	USGS[1]	<5	44	<200	19	<10	71.5	<5	<10	<10	<10	282	1.1	<5
06ST10	USGS[1]	<5	145	<200	15	<10	105	<5	<10	<10	<10	381	1.43	9.8
06ST11	USGS[1]	<5	<20	<200	16	<10	103	<5	<10	<10	<10	74	1.34	9.4
06ST12	USGS[1]	<5	<20	<200	16	<10	102	<5	<10	<10	<10	34	1.33	9.3
06ST13	USGS[1]	<5	566	<200	31	<10	43.7	<5	<10	<10	<10	1060	0.87	5.5
06ST14	USGS[1]	<5	1280	<200	29	<10	60.5	<5	<10	<10	<10	3600	0.81	5.8
06ST15	USGS[1]	<5	729	<200	30	<10	49.8	<5	<10	<10	<10	1880	0.84	5.9
06ST16	USGS[1]	<5	120	<200	14	<10	33.1	<5	<10	<10	<10	414	0.39	<5
06ST17	USGS[1]	<5	311	<200	14	<10	57.7	<5	<10	<10	28	1250	0.73	5.1
06ST17D	USGS[1]	<5	330	<200	14	<10	58.1	<5	<10	<10	<10	1020	0.69	5.5
06ST18	USGS[1]	<5	271	<200	18	<10	44.2	<5	<10	<10	<10	356	0.94	<5
06STBS	USGS[1]	<5	<20	<200	<1	<10	<0.1	<5	<10	<10	<10	<20	<0.1	<5

Sample ID	Lab	Mg mg/L	Mn µg/L	Mo µg/L	Na µg/L	Ni µg/L	P mg/L	Pb µg/L	Sb µg/L	SiO2 mg/L	Sr µg/L	Ti µg/L	V µg/L	Zn µg/L
06ST01	USGS[1]	51	<10	<20	0.82	<10	<0.5	<50	<50	5.3	317	429	<50	<10
06ST02	USGS[1]	56.4	<10	<20	0.96	<10	<0.5	<50	<50	5.2	326	443	<50	<10
06ST03	USGS[1]	53.3	26	<20	0.83	10	<0.5	<50	<50	7.3	269	280	<50	<10
06ST04	USGS[1]	58	<10	<20	0.98	<10	<0.5	<50	<50	5.5	321	407	<50	<10
06ST05	USGS[1]	63.8	31	<20	1.06	<10	<0.5	<50	<50	5.9	344	414	<50	<10
06ST06	USGS[1]	72.3	49	<20	1.13	<10	<0.5	<50	147	5.7	383	431	<50	<10
06ST07	USGS[1]	76.6	156	<20	1.24	11	<0.5	<50	156	5.6	399	439	<50	<10
06ST08	USGS[1]	81	44	<20	1.44	<10	<0.5	<50	248	5.6	425	483	<50	<10
06ST09	USGS[1]	28.3	130	<20	1.15	<10	<0.5	<50	<50	4.6	125	426	<50	<10
06ST10	USGS[1]	74.2	37	<20	1.54	<10	<0.5	<50	192	5.9	383	492	<50	<10
06ST11	USGS[1]	70.6	15	<20	1.52	<10	<0.5	<50	170	5.6	367	491	<50	<10
06ST12	USGS[1]	69.2	<10	<20	1.59	<10	<0.5	<50	156	5.5	360	487	<50	<10
06ST13	USGS[1]	19.5	45	<20	5.63	<10	<0.5	<50	<50	8.2	94.4	241	<50	<10
06ST14	USGS[1]	36.6	130	<20	0.97	<10	<0.5	<50	<50	8	181	287	<50	<10
06ST15	USGS[1]	25.4	72	<20	4.09	<10	<0.5	<50	<50	7.9	124	259	<50	<10
06ST16	USGS[1]	12.7	23	<20	1.02	<10	<0.5	<50	<50	5.2	43.7	162	<50	<10
06ST17	USGS[1]	33.9	70	<20	0.85	<10	<0.5	<50	54	5.5	169	272	<50	<10
06ST17D	USGS[1]	34.2	73	<20	0.83	<10	<0.5	<50	53	5.5	170	274	<50	<10
06ST18	USGS[1]	16.5	29	<20	1.5	<10	<0.5	<50	<50	6.3	87.7	252	<50	<10
06STBS	USGS[1]	<0.1	<10	<20	<0.1	<10	<0.5	<50	<50	<0.1	< 1	<1	<50	<10

[1] Briggs, P.H., 2001. The determination of twenty-seven elements in aqueous samples by inductively coupled plasma-atomic emission spectrometry. Chapter F, US Geological Survey Open File Report 02-223-F.

Table A.11 Major and minor anion composition of water samples by IC

Sample ID	Lab	Cl^- mg/L	F^- mg/L	NO_3^- mg/L	SO_4^{2-} mg/L	NO_2^- mg/L	Br^- mg/L	PO_4^{3-} mg/L	$CaCO_3$ mg/L
05SC01	USGS	1.2	0.1	0.23	28	-	-	-	73.06
05SC02	USGS	25	1.8	<.08	2004	-	-	-	0
05SC03	USGS	22	<.08	<.08	171	-	-	-	97.97
05SC04	USGS	1.1	0.11	0.2	34	-	-	-	71.22
05SC05	USGS	2.4	0.19	<.08	89	-	-	-	114.1
05SC06	USGS	3.4	0.3	<.08	93	-	-	-	103.5
05SC07	USGS	3.4	0.24	<.08	99	-	-	-	105.3
05SC08	USGS	2.2	0.18	0.6	85	-	-	-	90.74
05SC09	USGS[1]	2.3	0.17	0.7	89	-	-	-	85.35
05SC10	USGS[1]	2.2	0.2	0.8	90	-	-	-	93.23
05SC11	USGS[1]	2.3	0.2	1	57	-	-	-	103.7
05SC12	USGS[1]	55	<.08	<.08	2115	-	-	-	90.73
05SC13	USGS[1]	2.3	0.2	1.1	73	-	-	-	101.3
05SC14A	USGS[1]	65	<.08	<.08	224	-	-	-	0
05SC14B	USGS[1]	100	<.08	<.08	233	-	-	-	0
05SC15	USGS[1]	5.3	0.23	1.4	88	-	-	-	138.1
05SC16	USGS[1]	485	<.08	<.08	203	-	-	-	0
05SC17	USGS[1]	8.4	0.23	1.5	93	-	-	-	148.2
05SC18	USGS[1]	8.4	0.24	1.5	104	-	-	-	147.9
05SC19	USGS[1]	8.4	0.23	1.4	106	-	-	-	149.9
05SC20	USGS[1]	8.6	0.24	1.5	110	-	-	-	150.7
05SC21	USGS[1]	3	0.2	0.8	62	-	-	-	77.94
06ST01	USGS[1]	6	0.5	3	331	-	-	-	140.9
06ST02	USGS[1]	6	0.5	3	342	-	-	-	153.9
06ST03	USGS[1]	3.7	0.35	2	290	-	-	-	143.5
06ST04	USGS[1]	6	0.44	2.8	336	-	-	-	156.8
06ST05	USGS[1]	7.6	<.08	3	354	-	-	-	151.3
06ST06	USGS[1]	6	<.08	3	404	-	-	-	173.9
06ST07	USGS[1]	5	0.4	3	429	-	-	-	176.3
06ST08	USGS[1]	6	0.44	3	448	-	-	-	192.3
06ST09	USGS[1]	3.77	<.08	1.6	117	-	-	-	154.7
06ST10	USGS[1]	6.2	<.08	3	390	-	-	-	156.9
06ST11	USGS[1]	6	<.08	2.7	368	-	-	-	155.7
06ST12	USGS[1]	6.4	<.08	2.9	362	-	-	-	180
06ST13	USGS[1]	2.6	0.2	1.4	88	-	-	-	94.52
06ST14	USGS[1]	3.5	0.3	1.8	175	-	-	-	99.36
06ST15	USGS[1]	2.6	0.2	1.3	118	-	-	-	98.02
06ST16	USGS[1]	<.08	0.1	0.7	40	-	-	-	77.83
06ST17	USGS[1]	2.4	0.2	1.3	167	-	-	-	94.98
06ST18	USGS[1]	2.4	0.2	1.3	80	-	-	-	87.11
07SC01	UAF	<0.23	<0.09	<0.39	32.5	<0.34	<0.51	<1.23	63.1
07SC03	UAF	0.30	<0.09	<0.39	144.4	<0.34	<0.51	<1.23	124.85
07SC04	UAF	<0.23	<0.09	<0.39	<0.55	<0.34	<0.51	<1.23	134.0
07SC05	UAF	<0.23	<0.09	<0.39	91.2	<0.34	<0.51	<1.23	93.8
07SC06	UAF	<0.23	<0.09	<0.39	97.4	<0.34	<0.51	<1.23	102.7
07SC07	UAF	<0.23	<0.09	<0.39	73.1	<0.34	<0.51	<1.23	88.0
07SC08	UAF	113.68	<0.09	0.77	65.9	<0.34	0.79	<1.23	326.65
07SC09	UAF	7.71	<0.09	<0.39	29.0	<0.34	<0.51	<1.23	288.2
07EK01	UAF	1.27	<0.09	0.56	171.5	<0.34	<0.51	<1.23	137.1
07MC01	UAF	1.61	<0.09	<0.39	42.7	<0.34	<0.51	<1.23	79.0
07MC02	UAF	2.62	<0.09	0.39	56.3	<0.34	<0.51	<1.23	94.5
07FR01	UAF	1.04	<0.09	1.74	150.5	<0.34	<0.51	<1.23	159.9

" - " = not determined

[1] Theodorakos, P.M., d'Angelo, W.M., Ficklin, W.H., 2002. Fluoride, chloride, nitrate, and sulfate in aqueous solution utilizing AutoSuppression chemically suppressed ion chromatography. Chapter V, US Geological Survey Open File Report 02-223-V.

Table A.12 Major and minor cation composition of water samples by IC

Sample ID	Lab	Ca^{2+} mg/L	K^{+} mg/L	Mg mg/L	Na mg/L	NH_4^{+} mg/L
07SC01	UAF	20.87	0.09	10.42	0.80	0.003
07SC02	UAF	<0.05	<0.008	<0.015	<0.025	<0.0008
07SC03	UAF	119	0.87	60.05	1.27	0.798
07SC04	UAF	27.43	0.12	15.86	0.76	0.009
07SC05	UAF	47.02	0.27	29.05	0.93	0.162
07SC06	UAF	54.47	0.32	33.31	0.87	0.092
07SC07	UAF	47.43	0.37	29.66	0.97	0.131
07SC08	UAF	1033	8.42	543	288	0.862
07SC09	UAF	269	1.70	87.48	24.07	0.418
07EK01	UAF	280	2.26	130	4.06	0.074
07MC01	UAF	32.44	0.46	7.85	3.68	0.002
07MC02	UAF	41.30	0.62	10.87	3.71	0.007
07FR01	UAF	236	4.58	84.69	2.90	0.060
07TG01B	UAF	<0.05	<0.008	<0.015	<0.025	<0.0008

Table A.13 Major and minor element composition of (<63 μm) streambed sediment samples by ICP-MS

Sample ID	Lab	Ag mg/kg	Al mg/kg	As mg/kg	Ba mg/kg	Be mg/kg	Bi mg/kg	Ca mg/kg	Cd mg/kg	Ce mg/kg	Co mg/kg	Cr mg/kg
05SC01	USGS[1]	<2	106000	1900	1200	2.2	0.1	6590	0.77	124	27.2	122
05SC02	USGS[1]	<2	51000	2370	381	1.2	0.08	2070	0.24	53.2	10.9	63
05SC03	USGS[1]	<2	13100	855	196	0.89	< 0.06	5660	0.46	24.2	13.4	14.2
05SC04	USGS[1]	<2	125000	3080	1390	2.8	0.2	5130	0.88	109	27.8	135
05SC05	USGS[1]	<2	103000	3980	1050	2.3	0.38	5720	0.72	121	39.8	113
05SC06	USGS[1]	<2	94500	3820	1000	2.6	0.24	6870	0.68	102	35	100
05SC07	USGS[1]	<2	88900	3380	947	2.7	0.27	9780	0.89	77.2	39.6	95
05SC08	USGS[1]	<2	89000	2640	925	2.4	0.33	10400	2.2	89.9	47.7	106
05SC09	USGS[1]	<2	84600	2330	877	2.3	0.19	8440	2.6	98.9	44.5	101
05SC10	USGS[1]	<2	94700	2650	947	2.5	0.38	7170	2.6	112	44.6	111
05SC11	USGS[1]	<2	93400	2300	924	2.2	0.42	8650	2.4	105	42.8	108
05SC12	USGS[1]	<2	6810	10100	97.4	4.7	< 0.06	12200	284	49.5	37.2	4.9
05SC13	USGS[1]	<2	95900	2000	918	2.5	0.32	10700	9.8	115	35.5	115
05SC14A	USGS[1]	<2	1180	272	375	8.3	< 0.06	57400	0.78	139	0.58	4.3
05SC14B	USGS[1]	<2	84500	875	677	4.4	1.02	25900	9.1	242	12.5	116
05SC15	USGS[1]	<2	51600	1920	489	3.4	0.23	11100	2	170	19.8	63.4
05SC16	USGS[1]	<2	62600	435	640	2.2	0.4	23400	1.2	88.2	13.7	89.9
05SC17	USGS[1]	<2	65700	1640	732	3.3	0.35	12100	3.1	155	31.5	86.9
05SC18	USGS[1]	<2	71800	1190	828	3.6	0.48	15300	3.8	132	35.5	97.6
05SC19	USGS[1]	<2	72400	1220	806	3.6	0.22	17800	5.3	139	42.5	121
05SC20	USGS[1]	<2	74200	1380	832	3.5	0.4	18100	6.2	145	45.2	115
05SC21	USGS[1]	<2	83000	107	871	2	0.27	11600	0.94	63	16.2	73.4
06ST01	USGS[1]	0.746	112000	214	1460	3	0.48	9960	0.41	145	33.4	132
06ST02	USGS[1]	0.702	114000	208	1440	3	0.48	27200	0.53	131	33.9	129
06ST03	USGS[1]	0.244	138000	25.5	1550	3.5	0.29	6630	0.99	193	23.7	147
06ST04	USGS[1]	0.336	142000	55.7	1560	3.7	0.34	9320	0.8	144	25.9	151
06ST05	USGS[1]	0.326	137000	83.9	1530	3.6	0.32	9270	0.81	150	26.6	152
06ST06	USGS[1]	0.443	128000	336	1540	3.1	0.31	10700	0.85	126	37.8	137
06ST07	USGS[1]	0.428	140000	692	1550	3.4	0.35	9990	0.91	118	39.8	152
06ST08	USGS[1]	0.288	138000	173	1430	3.5	0.32	10100	0.57	112	31.3	161
06ST09	USGS[1]	0.167	127000	25.8	1350	3.1	0.36	9080	0.32	103	24.6	126
06ST10	USGS[1]	0.24	123000	49.9	1430	3.2	0.38	9400	0.32	124	27.4	131
06ST11	USGS[1]	0.157	120000	43.8	1310	3	0.34	11100	0.33	123	25	119
06ST12	USGS[1]	0.153	90000	41.4	1170	2.6	0.33	10400	0.3	142	20.8	94.4
06ST13	USGS[1]	0.213	66400	15	910	1.5	0.2	18300	0.7	82.9	22	123
06ST14	USGS[1]	0.164	82000	48.2	1080	2.3	0.37	11700	0.28	156	22.5	87.2
06ST15	USGS[1]	0.198	81000	31.2	1160	2.1	0.27	11800	0.51	123	22.5	113
06ST16	USGS[1]	0.215	111000	39.7	1510	3.2	0.48	7470	0.43	158	22.2	124
06ST18	USGS[1]	0.195	96500	21.5	1170	3	0.32	10800	0.75	167	25.5	106

[1] Briggs, P.H., Meier, A.L., 2002. The determination of forty-two elements in geological materials by inductively coupled plasma-mass spectrometry. Chapter I, US Geological Survey Open File Report 02-223-I.

Table A.13 *Continued*

Sample ID	Cs mg/kg	Cu mg/kg	Fe mg/kg	Ga mg/kg	K mg/kg	La mg/kg	Li mg/kg	Mg mg/kg	Mn mg/kg	Mo mg/kg	Na mg/kg	Nb mg/kg
05SC01	6.3	74	95700	23.9	36400	66	51.8	8440	4440	0.43	4000	18
05SC02	4	22.9	253000	13.2	22000	28.1	12.4	3870	447	0.1	1100	0.9
05SC03	0.84	25.6	406000	3.3	5070	14.2	2	1460	550	< 0.05	332	< 0.1
05SC04	7.7	109	90400	27.8	48300	55.4	36.5	7900	2210	0.45	2910	19
05SC05	6.2	66	118000	22.8	39500	60.4	31.6	7290	3500	0.52	2570	16
05SC06	5.4	57.2	153000	20.9	38000	51.5	27.6	7340	2790	0.41	2310	13
05SC07	5	56.6	159000	19.6	35400	42.4	26.3	8920	2980	0.42	2340	14
05SC08	5.9	46.3	110000	19.8	32100	45.8	40.3	10200	5160	0.46	3490	16
05SC09	6.1	59	115000	18.5	28400	50.2	45.7	8340	5180	0.43	3870	15
05SC10	6.7	57	117000	20	31700	57.2	49.6	8380	4610	0.54	4120	16
05SC11	6.4	55.2	108000	19.8	29900	53.4	51	9180	4300	0.79	4760	16
05SC12	0.37	22.4	397000	1.4	1520	128	1.7	3030	3490	0.31	244	< 0.1
05SC13	6.3	46.8	108000	20.2	29400	59.8	54	11000	3600	0.8	5970	17
05SC14A	0.06	3.2	431000	1.2	378	69.9	< 0.3	1770	189	0.2	500	0.74
05SC14B	6.6	1070	78900	19.4	25900	124	56.2	12900	363	2.2	6040	18
05SC15	3.3	955	212000	10.8	13900	130	27.9	5030	1630	1.6	3660	8.3
05SC16	6.2	79.5	75700	15.6	20600	45	38.8	14200	1000	0.77	9190	14
05SC17	4.8	1010	126000	15	18600	128	35.4	7020	2820	0.85	4380	14
05SC18	5.3	917	125000	16.9	21800	111	38.1	10000	3490	0.86	4530	13
05SC19	4.9	1380	118000	17.1	20700	122	35.5	12700	4000	0.45	4700	16
05SC20	5.2	1280	115000	17.4	20700	123	37.2	11900	4360	0.88	5670	18
05SC21	4.2	33.8	42800	18.3	17900	35	46.2	9890	900	0.76	9900	19
06ST01	10.6	42.1	61900	28.1	39700	77.3	55	8520	2680	1.4	4040	26
06ST02	11.9	47.5	61800	27.2	38300	70.1	55.1	10400	2980	1.5	3850	23
06ST03	8.1	42.9	65200	31.8	38300	106	69.4	16300	1080	2.9	8400	14
06ST04	9.2	48.5	67600	32	40500	80.5	71.5	16100	1310	3	7400	15
06ST05	8.9	47.3	67100	30.7	40000	80.9	68	16300	1330	2.8	7960	15
06ST06	8.8	45.6	67800	28.8	36300	69.8	61	15600	2340	2.5	7920	12
06ST07	9.4	53.2	108000	29.9	39600	64.6	65.4	16100	2350	2.8	6760	12
06ST08	8.2	49.8	76700	31.5	41100	59.3	62.2	16600	1830	2.2	7300	12
06ST09	6	44.8	59000	27	35800	54.6	56.9	10400	1200	2.5	7680	17
06ST10	6	46.8	60600	27	35300	66.5	55.1	11500	1180	2.1	7920	18
06ST11	5.4	42.4	59600	24.9	33100	66.4	52.4	12100	1120	2	8950	16
06ST12	4.6	40.6	51500	22.7	24700	78.8	45.3	9130	920	1.9	7280	18
06ST13	3	66.5	50400	16	13600	43.6	31.8	10800	911	1.1	9350	17
06ST14	3.9	41.8	53400	20.4	21700	83.3	42	9090	1010	1.7	8800	20
06ST15	4.2	57.4	51800	20.5	20700	66.9	37.6	10600	876	1.2	8170	20
06ST16	7.3	42.5	56600	28	32500	84.8	60.2	8880	1230	1.4	7480	20
06ST18	5.3	46.9	49400	23.7	28100	97.2	44.7	9740	934	1.4	8400	17

Table A.13 *Continued*

Sample ID	Ni mg/kg	P mg/kg	Pb mg/kg	Rb mg/kg	Sb mg/kg	Sc mg/kg	Sr mg/kg	Th mg/kg	Ti mg/kg	Tl mg/kg	U mg/kg	V mg/kg	Y mg/kg	Zn mg/kg
05SC01	59.2	1080	48.1	170	968	16.4	172	22	2760	1.57	5.87	95.8	17.9	203
05SC02	23.6	580	60.8	97.7	1040	8.4	83.3	18.2	1030	1.14	2.86	57.1	7.5	92.2
05SC03	28.8	139	14	23.3	116	3	51.5	3.44	171	0.27	3.64	8.1	14.5	146
05SC04	49.4	787	130	222	4990	19.3	184	26.2	2480	2.19	6.46	103	20.3	236
05SC05	55.3	879	154	179	7230	15.8	170	24.6	2470	1.94	8.91	86.3	19.9	209
05SC06	55.9	690	110	169	7020	15	157	19.8	2030	1.68	7.71	77.8	24.8	264
05SC07	68.5	643	89.1	154	6330	14.2	170	18.8	2100	1.6	6.24	72.9	25	382
05SC08	89.8	860	84.6	148	3890	14.5	180	19.3	2660	1.49	5.49	82.4	19.2	473
05SC09	121	852	67	135	3070	14	170	18	2880	1.24	4.67	81	21.6	632
05SC10	104	854	88.8	148	3260	15.6	170	20.1	2820	1.45	5.49	87.4	23.4	609
05SC11	90.6	1060	87.1	139	2680	15.8	173	20.3	3050	1.34	6.06	90.9	22.7	479
05SC12	34.5	61.6	65.2	6.6	223	1.5	156	1.03	96.7	<0.08	124	4.2	222	40100
05SC13	75.2	1080	70.4	139	1800	16.4	185	19.1	3170	1.16	8.53	98.7	28.2	1780
05SC14A	1.8	210	2.2	1.2	14.4	18.8	842	5.57	< 40	<0.08	6.32	36.4	547	98.1
05SC14B	40.4	1750	176	108	1530	23.4	293	42.3	3500	1.21	3.78	133	262	690
05SC15	37.1	831	43.1	59.6	1220	13	174	12.4	1770	0.58	20.6	67.6	174	306
05SC16	37.4	1320	50.2	94.2	189	14.6	830	16.8	2430	0.82	2.3	80.3	30.2	258
05SC17	61	953	52.1	85.9	1300	14.9	209	16.4	2430	0.88	6.09	80.2	112	582
05SC18	78.3	919	60.2	97.3	972	16.9	220	16.1	2280	0.91	4.84	89.9	99.7	719
05SC19	95.8	1030	67	90.9	1060	17.3	228	13.6	2960	0.82	4.17	95	103	1040
05SC20	102	1130	90.7	92.1	1170	17.6	232	15.5	3360	0.92	4.4	96.6	93.1	1190
05SC21	35.7	1050	39	74.4	24.6	15.6	298	11.1	5240	0.67	2.9	105	25.6	223
06ST01	46.5	870	33.7	205	90.7	20	155	27.8	4290	1.58	4.46	130	22.9	150
06ST02	53.4	1060	34.8	199	97.1	20.3	175	27.6	3480	1.52	5.17	130	26.5	167
06ST03	80.3	1120	36.7	191	59.8	22.4	198	28.8	3150	1.27	4.79	167	25.1	231
06ST04	71.5	1040	38.6	199	78.6	23.2	209	27	3170	1.32	4.83	168	27.2	224
06ST05	71.3	1100	37.9	194	305	22.2	200	26.7	3160	1.32	4.88	170	25.1	216
06ST06	89.9	1130	36.1	178	1240	20.8	194	23.2	2790	1.25	4.98	162	22.5	232
06ST07	99.9	940	39.2	185	1020	22.1	207	23.9	2580	1.28	6.34	172	26.2	256
06ST08	80.5	895	39.2	194	296	24.8	195	21.7	2660	1.24	4.29	182	21	232
06ST09	51.3	930	35.8	169	20.5	19.7	196	23.5	3530	1.19	4.4	140	19.7	174
06ST10	55.4	1040	40.3	165	94.2	20.1	189	25.6	3580	1.15	4.61	137	21.3	179
06ST11	55.5	1040	35.1	150	78.6	18.6	188	24.9	3680	1.05	4.52	130	22.5	172
06ST12	45	1020	33.3	139	87	15.1	184	25.3	3430	0.96	4.63	100	22	147
06ST13	57.8	1170	15	61.5	8.7	16.6	212	10.3	6000	0.49	2.77	152	30.4	152
06ST14	45.4	1490	35.7	118	110	13.8	186	27	4330	0.84	4.97	91.8	26.7	140
06ST15	53.5	1170	23.6	105	69.5	16.6	179	18.8	4980	0.76	3.78	133	28	149
06ST16	44.2	780	35.2	174	71.1	19.5	195	26.2	3260	1.15	4.17	131	22.5	161
06ST18	56.5	797	27.7	144	6.6	16.7	181	21.8	3410	0.93	4.51	117	43.8	173

Table A.14 Carbon and sulfur composition of (<63 μm) streambed sediment samples by combustion and coulometric tritration

Sample ID	Lab	Total C [1] %	Carbon as CO_2 [2] %	Carbon as CO_3^{2-} [2] %	Total S [3] %
05SC01	USGS	2.95	-	-	0.13
05SC02	USGS	1.22	-	-	3.68
05SC03	USGS	2.76	-	-	0.36
05SC04	USGS	2.23	-	-	0.27
05SC05	USGS	2.42	-	-	0.27
05SC06	USGS	2.58	-	-	0.37
05SC07	USGS	INS	-	-	0.6
05SC08	USGS	INS	-	-	0.51
05SC09	USGS	2.74	-	-	0.25
05SC10	USGS	2.4	-	-	0.2
05SC11	USGS	2.91	-	-	0.2
05SC12	USGS	1.19	-	-	1.06
05SC13	USGS	3.09	-	-	0.26
05SC14A	USGS	3.09	-	-	0.36
05SC14B	USGS	3.05	-	-	1.22
05SC15	USGS	4.21	-	-	0.37
05SC16	USGS	4.32	-	-	0.3
05SC17	USGS	3.54	-	-	0.21
05SC18	USGS	3.43	-	-	0.23
05SC19	USGS	3.82	-	-	0.31
05SC20	USGS	3.52	-	-	0.25
05SC21	USGS	1.29	-	-	0.08
06ST01	USGS	3.10	0.54	0.15	0.35
06ST02	USGS	4.43	2.14	0.58	0.51
06ST03	USGS	2.66	0.36	0.10	0.07
06ST04	USGS	3.44	0.53	0.15	0.25
06ST05	USGS	3.10	0.53	0.15	0.18
06ST06	USGS	2.81	0.58	0.16	0.34
06ST07	USGS	3.93	0.80	0.22	0.25
06ST08	USGS	2.78	0.84	0.23	0.32
06ST09	USGS	1.50	1.45	0.40	0.12
06ST10	USGS	1.57	1.69	0.46	0.18
06ST11	USGS	1.75	1.65	0.45	0.23
06ST12	USGS	1.63	1.91	0.52	0.18
06ST13	USGS	1.17	1.60	0.44	0.07
06ST14	USGS	1.51	2.33	0.64	0.27
06ST15	USGS	1.34	1.61	0.44	0.06
06ST16	USGS	2.86	0.56	0.15	0.07
06ST18	USGS	1.74	1.18	0.32	0.09

" - " = not determined

[1] Brown, Z.A., Curry, K.J., 2002. Total carbon by combustion. Chapter R, US Geological Survey Open File Report 02-223-R.

[2] Brown, Z.A., Papp, C., Brandt, E., Aruscavage, P., 2002. Caronate carbon by coulometric titration. Chapter S, US Geological Survey Open File Report 02-223-S.

[3] Brown, Z.A., Curry, K.J., 2001. Total sulfur by combustion. Chapter Q, US Geological Survey Open File Report 02-223-Q.